Exhibit 579

Unnatural evolutionary processes of SARS-CoV-2 variants and possibility of deliberate natural selection

https://zenodo.org/records/8361577

Unnatural evolutionary processes of SARS-CoV-2 variants and possibility of deliberate natural selection

Atsushi Tanaka[1,2,*] †, Takayuki Miyazawa[2,3,*] †

[1]Division of Research Animal Laboratory and Translational Medicine, Research and Development Center Osaka Medical and Pharmaceutical University, Takatsuki, Osaka 569-8686, Japan

[2]Laboratory of Virus-Host Coevolution, Institute for Life and Medical Sciences, Kyoto University, Sakyo-ku, Kyoto 606-8507, Japan

[3)] Resilience Research Unit, Kyoto University, Katsura, Nishikyo-ku, Kyoto 615-8540, Japan

*** Correspondence:**
Atsushi Tanaka*****
atsushi.tanaka@ompu.ac.jp

Takayuki Miyazawa*****
takavet@infront.kyoto-u.ac.jp

Keywords: SARS-CoV-2, evolution, Omicron BA.1, Omicron BA.2, SARS-CoV-2 Omicron, Puerto Rico.

Abstract

Over the past three years, severe acute respiratory syndrome coronavirus 2 (SARS-CoV-2) has repeatedly caused pandemics, generating various mutated variants ranging from Alpha to Omicron. In this study, we aimed to clarify the evolutionary processes leading to the formation of SARS-CoV-2 Omicron variants, focusing on Omicron variants with many amino acid mutations in the spike protein among SARS-CoV-2 isolates. To determine the order of mutations leading to the formation of the SARS-CoV-2 Omicron variants, we compared the sequences of 129 Omicron BA.1-related, 141 BA.1.1-related, and 122 BA.2-related isolates, and attempted to clarify the evolutionary processes of SARS-CoV-2 Omicron variants, including the order of mutations leading to their formation and the occurrence of homologous recombination. As a result, we concluded that the formation of a part of Omicron isolates BA.1, BA.1.1, and BA.2 was not the product of genome evolution, as is commonly observed in nature, such as the accumulation of mutations and homologous recombinations. Furthermore, the study of 35 recombinant isolates of Omicron variants BA.1 and BA.2 confirmed that Omicron variants were already present in 2020. The analysis showed that Omicron variants were formed by an entirely new mechanism that cannot be explained by previous biology, and knowing how the SARS-CoV-2 variants were formed prompts a reconsideration of the SARS-CoV-2 pandemic.

1 Introduction

COVID-19, the coronavirus disease 2019, caused by severe acute respiratory syndrome coronavirus 2 (SARS-CoV-2), was first reported in December 2019 in Wuhan, China (1). This emerging infectious disease was unprecedentedly fast, spreading worldwide, leading the World Health Organization (WHO) to declare a global pandemic of COVID-19 on March 11, 2020 (https://www.who.int/). SARS-CoV-2, belonging to betacoronavirus subgroup B, has a single-stranded positive-sense RNA genome that codes for ten genes, ultimately producing 26 proteins according to an annotation of NCBI Reference Sequence: NC_045512.2. Its genome size varies from 29.8 to 29.9 kb. It consists of four structural proteins: spike (S), envelope (E), membrane (M), and nucleocapsid (N) proteins (2, 3). In the structural proteins, the S protein as the surface glycoprotein is the largest protein, being approximately 180 kDa, and consisting of two subunits, S1 and S2. It mediates membrane fusion and ultimately facilitates virus entry. The receptor-binding domain (RBD) (amino

acid residues 319‑541) of the S1 subunit interacts with angiotensin‑converting enzyme 2 (ACE2), binding to its peptidase domain (4, 5).

Over the three years from 2019 to 2022, SARS-CoV-2 was re-accelerated by new variants that emerged over several months in various geographical regions and disseminated throughout the world, to induce the pandemic repeatedly.

In the early stage of the first pandemic, the most impactful mutation of SARS-CoV-2 was the non-synonymous mutation D614G in the S protein. This mutation, which was not present in the ancestral lineage that caused the Wuhan outbreak, quickly became dominant worldwide (6). Soon after, the variant of concern, B.1.1.7 : 20I (Alpha, V1), the lineage B.1.1.7 (clade 501.YV1), or Alpha, characterized by 17 unique mutations containing ten amino acid differences in the S protein, was first detected in southeastern England in late September 2020 (7) and expanded rapidly across the United Kingdom to become predominant during early 2021, spreading to most European countries with similar success. By November 2021, local transmission of this lineage had been reported in 175 countries (8). Shortly after, the emergence of variant strains of SARS-CoV-2 Alpha, variants B.1.351 : 20H (Beta, V2), was identified in October 2020, which was first detected in the Eastern Cape province of South Africa from specimens collected in early August. This Beta variant spread within South Africa and was considered to have displaced the other SARS-CoV-2 lineages circulating there (9). Then, the variant P.1: 20J (Gamma, V3) was identified in Brazil in December 2020, thought to have evolved in Brazil. Health officials in Japan first reported it publicly on January 10, 2021, after identifying the Gamma variant in four Brazilian travelers at Haneda Airport in Tokyo, Japan (10).
At about the same time, the Delta variant (Pango lineage designation B.1.617.2), which was first detected in India in February 2021, and the Mu variant, also known as lineage B.1.621 first detected in Colombia in January 2021, were reported (11, 12). While the lambda variant (Pango lineage designation C.37), was detected in Peru in August 2020, but designated in June 15, 2021 by WHO (13, 14).

Almost one year later, regarding these emergences of variants of concern, Omicron (phylogenetic assignment of named global outbreak (Pango) lineage designation B.1.1.529; BA.1, Nextstrain clade 21K) was a variant of SARS-CoV-2 first reported to WHO by the Network for Genomics Surveillance in South Africa on November 24, 2021 (15, 16) with more than 50 amino acids changes when compared with the first reported strain Wuhan-Hu-H1 (NCBI Reference Sequence: NC_045512.2.), and 39 of these amino acids difference were observed in the S protein. This variant was first detected in Botswana and became the predominant circulating variant worldwide (17).

In the United States, the San Francisco Department of Public Health confirmed that a case of COVID-19 among individuals in California was caused by Omicron variant BA.1, carried by a traveler who returned from South Africa on November 22, 2021 (https://www.cdc.gov/media/releases/2021/s1201-Omicron-variant.html). Then, the first Omicron sub-lineage BA.1 expanded rapidly and replaced the Delta variant (18).

Less than two weeks later, the Omicron variant BA.1, the new Omicron variant, BA.2 lineage, showing 31 amino acids changes in the S protein when compared with the Wuhan-Hu-H1, was initially identified in Denmark on December 5, 2021 (19). On February 22, 2022, WHO mentioned the Omicron sublineage BA.2 (https://www.who.int/news/item/22-02-2022-statement-on-Omicron-sublineage-ba.2), whereby the Omicron variant of concern was currently the dominant variant circulating globally, replacing the Delta variant (Pango lineage designation B.1.617.2) (https://www.who.int/docs/default-source/coronaviruse/2022-01-07-global-technical-brief-and-priority-action-on-Omicron---corr2.pdf?sfvrsn=918b09d_20), accounting for nearly all sequences reported to GISAID. Then, as of March 16, 2023, WHO stated that the Omicron variants accounted for over 98% of the publicly available viral sequences after February 2022 (https://www.who.int/news/item/16-03-2023-statement-on-the-update-of-who-s-working-definitions-and-tracking-system-for-SARS-CoV-2-variants-of-concern-and-variants-of-interest).

Omicron variants BA.1 and BA.2 were suggested to have expanded and diverged around October to December 2021, respectively. These mutants were estimated to have diverged from a common ancestor around February to March 2021 (20). Since Omicron variants BA.1 and BA.2 share a common 14-amino acid mutation in the S

protein, the common ancestor of Omicron variants BA.1 and BA.2 may have already acquired the 14-amino acid mutation in the S protein region around February to March 2021; however, no common ancestral strain has been found in the international databases, and the strains may have acquired their mutations through different pathways.

In this study, we attempted to clarify the evolutionary processes of the Omicron variant, which has two-times more amino acid mutations in the S protein than other variants, by examining the rank order of introduced amino acid mutations in the S protein.

2 Results

Each variant is considered to have arisen through an independent evolutionary pathway from isolates with the D614G mutation in the S protein. Concerning the genetic variation in the S protein of these variants, most of the mutations were non-synonymous (Fig. 1). There were no synonymous mutations in the Alpha, Beta, Gamma, Delta, or Mu variants, but only one each in the Lambda and Omicron variants. Among these variants, the Omicron variant (BA.1 lineage), which shows the greatest accumulation of mutations in the S protein, is primarily non-synonymous in the S protein and has only one synonymous mutation, at c25000u. The synonymous/non-synonymous ratio is abnormal, considering how human coronaviruses have mutated (See Supplemental Figure 1).

At first, we considered the existence of the isolate of SARS-CoV-2, whose amino acid sequence in the S protein contains the Omicron-BA.1-type mutation subsets, but one mutation position was not mutated and comprised the original Wuhan-type amino acid sequence. We designated these isolates as BA.1-01. Each amino acid sequence of the S protein region was named BA.1-0.1_S: amino acids of the Omicron-BA.1 type (Oaa) and Wuhan type (Waa) and its position number (XXX) (Ex., BA.1-0.1_S:OaaXXXWaa), as described in Methods. Then, the putative isolates bearing BA.1-0.1_S:OaaXXXWaa were searched for using the BLAST program based on their amino acid sequences. In this search, we obtained the isolates whose identities showed 100% matches with the query amino acid sequence except for SARS-CoV-2_human_USA_NY-PV55373_2022(GenBank: ON246090.1), whose identity was 99.92%.

Surprisingly, we found that Omicron BA.1-0.1 isolates were detected at all mutation sites except N501Y (Fig. 2A). In the BA.1 lineage of the Omicron variant, there are Omicron isolates (BA.1.1) with the R346K mutation seen in the Mu(m) variant (termed B.1.621), *i.e.*, BA.1_S can be defined as BA.1.1_S:K346R. We also performed a BLAST search for isolates with amino acid sequences of BA.1-0.1.1_S:OaaXXXWaa, as described in Methods. As a result, Omicron BA.1.1-subset-0.1 isolates were detected at all mutation sites except S373P (Fig. 2B). Similar to the BA.1 lineage of the Omicron variant, in the BA.2 lineage of the Omicron variant, isolates of BA.2-0.1 were found at all mutant sites except T478K and P681H in the S protein (Supplemental Figure 2). The presence of these isolates refutes the establishment of Omicron strains through a continuous evolutionary process by accumulating mutations. So, we could not determine which mutation occurred first or last to form the Omicron variants. As shown in Fig. 2B, over half of the BA.1.1-0.1 isolates have the synonymous mutation c21595u detected in the S protein. However, this does not help explain the order in which the c21595u mutation arose. Curiously, in BA.1 strain isolates, this c21595u mutation was only detected in SARS-CoV-2_human_USA_ID-CDC-LC0481844_2022 (GenBank: OM409228.1) and SARS-CoV-2_human_USA_MI-CDC- ASC210597972_2022 (GenBank: OM396816.1). These isolates commonly lack the G339D mutation. This synonymous mutation is in a mutation-prone hotspot location. Still, if the same mutation occurred independently in different isolates, it is highly unnatural for the proportion of c21595u occurrences to be significantly biased in the Omicron variants BA.1.1-0.1.

It has been reported that two different variants were infected in a single cell while establishing various SARS-CoV-2 variants, causing homologous recombination in the process of viral RNA synthesis, resulting in multiple variants. On considering that homologous recombination caused the isolates shown in Fig. 2, some of the breakpoints at which strand changes occur by homologous recombination are too short (1nt, 2nt, 3nt, etc.) (Fig. 3 and Supplemental Figure 3). Therefore, it is unreasonable to employ homologous recombination as the basis for establishing these isolates. Also, most of these isolates were found in the USA between 2021 and 2022;

however, considering that the most prevalent variant in the USA in August 2021 was the Delta variant, it is most unlikely that it did not cause mutations such as T478K and D614G, which were already prevalent. It is inconceivable that the oldest variants (such as T478K and D614G), which were no longer prevalent, were sufficiently present to cause superinfection and be involved in homologous recombination. Also, most of these isolates were isolated in the USA between 2021 and 2022. Still, given that the isolates primarily prevalent in the USA in August 2021 were Delta variants, it is unlikely that an older type of variant without the T478K or D614G mutation was present to cause superinfection and be involved in homologous recombination. This consideration is supported by the fact that all of these BA.1-0.1 and BA.1.1-0.1 isolates retained the sequence of the BA.1 lineage in all regions except the S protein (Fig. 4). In addition, the fact that all of these BA.1-0.1 and BA.1.1-0.1 strains retained the sequence of Omicron strain BA.1 except for the S protein also makes it unreasonable to consider that these isolates arose by homologous recombination with an older type of mutant without the T478K or D614G mutations (Fig. 4).

Furthermore, some of the BA.1 and BA.1-0.1 isolates have mutation subsets (synonymous: u10135c, ORF3: L106F, N: D343G) up- and downstream of the S gene, and the u10135c and L106F (ORF3) mutations correspond perfectly. Therefore, it is considered that homologous recombination between the BA.1 variant and variants without these mutations did not occur during the mutants' formation processes (Fig. 4). The synonymous mutation c2470u occurred in BA.1.1 compared with BA.1, and this c2470u mutation was retained by most, excluding a few of the BA.1.1-0.1 isolates (SARS-CoV-2_human_USA_IL-CDC-ASC210695497_2022 : GenBank: OM770362.1; SARS-CoV-2_human_USA_NY-CDC-LC0450936_2021: GenBank: OM228453.1）. The synonymous mutation c2470u has also only been observed in a minimal number of BA.1-0.1 isolates （ SARS-CoV-2_human_USA_OR-CDC-LC0470830_2022: GenBank: OM367679.1; SARS-CoV-2_human_USA_ID-CDC-LC0481844_2022: GenBank: OM409228.1; SARS-CoV-2_human_USA_MI-CDC-ASC210597972_2022: GenBank:OM396816.1; SARS-CoV-2_human_USA_WI-CDC-LC0494047_2022: GenBank: OM500517.1）. These results suggest that the establishment of BA.1-0.1 and BA.1.1-0.1 isolates occurred independently. On the other hand, if reversion mutations caused each of these isolates with one amino acid different to the Wuhan-type, these isolates could be detected by examining an astronomical number of isolates. However, these virus strains were detected in the number of sequenced whole genomes (a limited number), rather than in astronomical numbers examined. The fact that most of these mutations occurred without synonymous mutations (Fig. 2) suggests that none of them arose as a result of trial-and-error random mutations in nature. Few synonymous mutations are detected in some BA.1-0.1, BA.1.1-0.1, and BA.2-0.1 isolates (Fig. 2 and Supplemental Figure 2), as seen in other viruses (Supplemental Figure 1). The c25000u is the only synonymous mutation that did not occur until BA.1, BA.1.1, BA.2, BA.1-0.1 BA.1.1-0.1, and BA.2-0.1 isolates were formed and was not observed in previous variants such as alpha, beta, gamma, delta, etc. Nevertheless, it is curious to find the occurrence of mutants with synonymous mutations such as c22120u, c24034u, c23635u, c24448u, c21811u, a23884g, c22987u, c23609a, c23413u, c23896u, c22879u, u24097a, c23893u, c24442u, u24847c, c24382u, c22264u, c22879u, c22480u, u21976c, c22480u, g24577a, and u23101c in BA.1.1, BA.1-0.1, and BA.1.1-0.1 isolates (Fig. 2 Synonymous Others), and a22948g, c23635u, c21859u, c22945u, c23701u, c22987u, a24433g, c23347u, u24640c, a24619g, c24865u, a23989g, u23047c, u24346c, c21811u, c21952u, a22753u, c23635u, c24023u, c24382u, and c22572u in BA.2-0.1 isolates (Supplemental Figure 2 Synonymous Others) after the formation of mutants with these subsets.

Although the only bias in our isolates collection, was only selection of isolates whose identities showed 100% matches with the query amino acid sequence in the BLAST search, these curious tendencies were observed is very interesting.

If two different viral variants infect a single cell simultaneously in the process of establishing various SARS-CoV-2 variants, and if homologous recombination occurs during viral RNA synthesis between the Omicron variant BA.1 lineage and BA.2 lineage, it is expected that there are variants caused by homologous recombination between the BA.1 and BA.2 lineages.

Therefore, we also performed BLAST searches for isolates with mutant amino acid subsets of both the Omicron variant BA.1 and BA.2 strains. We detected recombinant isolates of Omicron BA.1 and BA.2 lineages.

Surprisingly, the recombinant Omicron BA.1 and BA.2 lineages, SARS-CoV-2/human/PRI/PR-PR-UPRRP-582/2020 (GenBank: ON928946.1), were already present in Puerto Rico in 2020. Omicron (B.1.1.529) is a variant of SARS-CoV-2 first reported to WHO by the Network for Genomics Surveillance in South Africa on November 24, 2021 (15, 16). It was first detected in Botswana and spread to become the predominant variant in circulation worldwide (17). Following the appearance of the original B.1.1.529 variant, several subvariants of Omicron emerged, including BA.1, BA.2, BA.3, BA.4, and BA.5 (21). After October 2022, two subvariants of BA.5 called BQ.1 and BQ.1.1 emerged.

The question then arose about why a recombinant strain, SARS-CoV-2/human/PRI/PR-UPRRP-582/2020 (GenBank: ON928946.1), already existed in 2020. We searched for SARS-CoV-2 isolates prevalent in Puerto Rico using the keywords "PRI", "PR-UPRRP", and "2020" in the NCBI search; nucleotide (https://www.ncbi.nlm.nih.gov/). Consequently, we found 29 Omicron-associated sequences in the 127 hits obtained (Fig. 5B). These results suggest that the SARS-CoV-2 variants bearing the amino acid sequences of the S protein are identical to Omicron BA.1 and Omicron BA.2 variants, which were already prevalent in Puerto Rico in 2020, with 15 isolates showing the complete Omicron BA.1+ R346K_mut-subset (BA1.1) , and 14 isolates showing a synonymous substitution of c21595u. Four isolates had an amino acid sequence of the S protein that perfectly matched that of Omicron BA2 (BA.2_S), four isolates were Omicron BA.2-0.1 (BA.2-S:K440N) and four isolates were Omicron BA.2-0.1 (BA.2-S:K440N)+F79S, BA.2-0.1 (BA.2-S:K440N)+Q613H, BA.2-0.1 (BA.2-S:K440N)+212S+D215E and BA.2-0.1 (BA.2-S:K440N)+212S (Fig. 5B).

3 Discussion

Several hypotheses have been proposed in which the original SARS-CoV-2 virus resulted from an accidental laboratory spill. With recent developments in biotechnology, many viruses, including coronaviruses, have been artificially synthesized and used in various experiments (22-24). The artificial generation of mutant viruses in laboratories and study of viral phenotypes by introducing mutations is called "reverse genetics", being a common technique in virology. It has been claimed that SARS-CoV-2 must have been artificially generated because of the unnatural presence of a codon (CGG) encoding a contiguous arginine at the furin cleavage site of SARS-CoV-2. This claim has been refuted based on the following facts: 1) there is no logical reason for a genetically engineered virus to utilize such a suboptimal furin cleavage site; 2) The only previous study on artificial insertion of furin cleavage sites at the S1/S2 boundary of the S protein of SARS-CoV-1 using the pseudotype virus experimental system utilized the optimal "RRSRR" sequence, which is different from the furin cleavage site's sequence present in SARS-CoV-2; 3) There is no evidence of previous studies at the Wuhan Institute of Virology that artificially inserted a complete furin cleavage site in coronaviruses; 4) Unnatural CGG codons adjacent to arginine at the furin cleavage site are rare in coronaviruses but are observed at a particular frequency in SARS-CoV-1, SARS-CoV-2, and other human coronaviruses. However, these are only declarations and are not logical. No one has offered an explanation why a naturally occurring virus would utilize a suboptimal furin cleavage site. There has been no mention of the technical possibility of inserting this furin cleavage site or a CGG codon artificially. The insertion of a polybasic furin cleavage site into the S protein makes it impossible to conclude whether SARS-CoV-2 is a naturally occurring or an artificial virus.

Despite the accumulation of many mutations in the S protein of Omicron mutants, most of the mutations are non-synonymous, with only one synonymous mutation of c25000u, which is highly unnatural, leading to the hypothesis that the Omicron mutants were artificially synthesized. The following results presented in this study may support the hypothesis that the Omicron variants were artificially synthesized rather than naturally occurring: 1) the presence of Omicron variant-associated isolates with one mutation site being the Wuhan-type; 2) the almost complete absence of synonymous mutations in the S protein in these isolates; 3) the Omicron variant, which should have been first reported to WHO from South Africa on November 24, 2021, was already endemic in Puerto Rico in 2020, and there were isolates that were recombinants between Omicron strains BA1 and BA2. In addition, the Omicron mutant-related isolates (BA.1-0.1, BA.1.1-0.1, and BA.2-0.1 isolates) with a Wuhan-type mutation at one of the mutation sites were established. Some had synonymous mutations after

establishing the Omicron mutant-related isolates (Fig. 2 and Supplemental Figure 2 Synonymous Others). It is reasonable to assume that viruses with the reversion amino acid mutations caused by non-synonymous mutations in the S protein were artificially synthesized and then acquired further synonymous mutations in the natural environment.

Assuming that artificially synthesized mutants with only non-synonymous mutations are spread globally, this would explain how mutants with non-synonymous mutations without previous synonymous mutations develop synonymous mutations under natural circumstances. Considering the current epidemic situation of SARS-CoV-2, it is unlikely that these viruses arose spontaneously. Based on our efforts to explain the formation of the SARS-CoV-2 isolates, they were formed by a completely new mechanism that cannot be explained by previous biology.

One idea, the hypothesis that these viruses were artificially generated, is more reasonable than proposing a novel mutation acquisition mechanism. However, is there any reason to artificially create these mutants, which are unlikely to have occurred naturally, given the current SARS-CoV-2 epidemic?

It is known that the pathogenicity, host specificity, cell tropism, and immunogenicity of numerous viruses can be altered by mutation of a single (or several) amino acid(s) of a viral protein on the viral envelope (envelope protein, HA protein, spike protein, etc.). A single-amino-acid substitution in the HA protein of the 2009 pandemic A (H1N1) influenza viruses changed their replication and pathogenicity (25). In the Chikungunya virus, single amino acid changes in the E2 glycoprotein influenced glycosaminoglycan utilization for target-cell binding (26), and a single amino acid change in the E1 glycoprotein affected mosquito vector specificity and epidemic potential (27). In previous coronaviruses such as MERS-CoV and SARS-CoV-1, point mutations have been demonstrated to confer resistance to neutralizing antibodies (28-30).

Consider that the SARS-CoV-2 Omicron variant and its one-amino-acid reversion mutants were artificially and systematically generated. In that case, we should suspect that the other variants (Alpha to Delta) were also artificially generated viruses. Indeed, the lack of findings to date that many of the various mutations seen, especially in the early variants, are indeed associated with increased viral infection (31) supports the hypothesis that each variant was artificially synthesized to identify the amino acids of the S protein responsible for infectivity and pathogenicity. The possibility that the set of mutants was artificially generated to identify amino acids of the S protein involved in the infectivity and virulence is supported.

Reverse genetics experiments are an essential part of virus research, and it is inimical to virus research to consider that artificially synthesized viruses were deliberately spread throughout the world. However, now that reverse genetics has become common in virus research, we believe it is not scientific to discuss the mutation process of SARS-CoV-2 without excluding the possibility of artificially synthesized viruses.

Finally, we would like to add that while artificially synthesized viruses may have spread, we are not criticizing reverse genetics technology, as such technology has led to marked advances in virology. In addition, our analysis employed databases with a limited number of viral sequences, and we cannot deny the possibility that unreliable data may have been registered due to technical problems in sequencing or some other issues. Furthermore, we do not conclude that these viruses were artificially synthesized and distributed based on malicious intent. This study aims to point out that SARS-CoV-2 has undergone unthinkable mutations based on conventional coronavirus mutation mechanisms, and we hope that the possibility of artificial creation is included in serious discussions on the formation of SARS-CoV-2 variants.

Nonetheless, the analysis we have shown here concludes that the Omicron variants were formed by a completely new mechanism that cannot be explained by previous biology. The process of how SARS-CoV-2 mutations occurred should prompt a reconsideration of the SARS-CoV-2 pandemic. If the SARS-CoV-2 epidemic strain is an artificially mutated virus and if the corona disaster (corona hoopla) was a well-designed global experiment in human inoculation and a social experiment, then the design of this experiment and the nature of the virus used make it likely that this experiment (corona hoopla) is a preliminary experiment.

4 Methods

4.1 Data acquisition

The SARS-CoV-2 RNA genome, genes, and proteins according to an annotation of SARS-CoV-2 Wuhan-Hu-H1 (COVID-19/Wuhan-Hu-1CHN/2019/First Isolate) NCBI Reference Sequence: NC_045512.2 were used as references for the definition of mutations, and provided a basis for the numbering of nucleotides and amino acids of each protein. Genome data of SARS-CoV-2 isolates described in this article were obtained from the NCBI Nucleotide database (https://www.ncbi.nlm.nih.gov/) on 25/11/2022 to 17/03/2023.

4.2 Query of representative SARS-CoV-2 variant genome

Amino acid sequences of spike protein of SARS-CoV-2 variants（Alpha:B.1.1.7, Beta:B.1.351, Gamma:P1, Delta:B.1.617.2.63, Lambda:C.37, Mu:B.1.621, Omicron:BA.1, BA.1.1, and BA.2）were obtained from an Internet site, Stanford Coronavirus Antiviral & Resistance Database (https://covdb.stanford.edu/) or Covariant (https://covariants.org/), and used as a query sequence for an NCBI protein BLAST search (blastp: protein-protein BLAST, https://blast.ncbi.nlm.nih.gov/Blast.cgi?PROGRAM=blastp&PAGE_TYPE=BlastSearch&LINK_LOC=blasthome). Then, the whole genome sequence of each isolate bearing the query spike sequence was derived from the BLAST search result, identified with query amino acid sequences of 100%. The nucleotide sequences of the detected SARS-CoV-2 genome were as follows: GenBank Accession No.: GenBank: MW423686.2; MW430966.1; MW430967.1; MW422256.1; MW598419.1; MW667552.1; MW667553.1; MW721502.1; MW721504.1; MW520923.1; MW642248.1; MW642249.1; MW642250.1; MZ182066.1; MZ155303.1; MZ155230.1; MZ170364.1; MZ179869.1; MW666666.1; MW696612.1; MW699217.1; MW644498.1; MZ727706.1; MZ620161.1; MZ637380.1; MZ637401.1; MZ780550.1; OL672836.1; OL677199.1; OP769083.1; OL764360.1; OL815447.1; ON762438.1; OL849989.1; OL897126.1; OL896945.1; OL896936.1; OL896931.1; OM233931.1; OM072551.1; OM072822.1; OM296922.1.

4.3 Query of SARS-CoV-2 Omicron variant genome bearing an S protein amino acid sequence in which one of the Omicron-type nucleotide mutation subsets was not mutated and retains the original SARS-CoV-2 Wuhan-Hu-H1-type arrangement.

For each of the Omicron variants, BA.1, BA.1.1, and BA.2, the isolate series bearing an S protein amino acid sequence in which one of the Omicron-type nucleotide mutation subsets is not mutated and retains the original SARS-CoV-2 Wuhan-Hu-H1-type arrangement were named BA.1-0.1, BA.1.1-0.1 and BA.2-0.1, respectively. In addition, in this article, we named the amino acid sequences of spike protein of BA.1, BA.1.1, and BA.2 as BA.1_S, BA.1.1_S, and BA.2_S, respectively, and then the series of amino acid sequences of spike protein of BA.1-0.1, BA.1.1-0.1, and BA.2-0.1 were named, respectively, as follows: Omicron BA.1-0.1 spike series (BA.1-0.1_Ss) were named as BA.1_S:V67A; BA.1_S:69H_70V; BA.1_S:I95T; BA.1_S:D142G_143V_144Y_145Y; BA.1_S:I211N_212L; BA.1_S:ΔEPE; BA.1_S:D339G; BA.1_S:L371S; BA.1_S:P373S; BA.1_S:F375S; BA.1_S:N417K; BA.1_S:K440N; BA.1_S:S446G; BA.1_S:N477S; BA.1_S:K478T; BA.1_S:A484E; BA.1_S:R493Q; BA.1_S:S496G; BA.1_S:R498Q; BA.1_S:Y501N; BA.1_S:H505Y; BA.1_S:K547T; BA.1_S:G614D; BA.1_S:Y655H; BA.1_S:K679N; BA.1_S:H681P; BA.1_S:K764N; BA.1_S:Y796D; BA.1_S:K856N; BA.1_S:H954Q; BA.1_S:K969N and BA.1_S:F981L / Omicron BA.1.1-0.1 spike series (BA.1.1-0.1_Ss) were named as BA.1.1_S:V67A; BA.1.1_S:69H_70V; BA.1.1_S:I95T; BA.1.1_S:D142G_143V_144Y_145Y; BA.1.1_S:I211N_212L; BA.1.1_S:ΔEPE; BA.1.1_S:D339G; BA.1.1_S:L371S; BA.1.1_S:P373S; BA.1.1_S:F375S; BA.1.1_S:N417K; BA.1.1_S:K440N; BA.1.1_S:S446G; BA.1.1_S:N477S; BA.1.1_S:K478T; BA.1.1_S:A484E; BA.1.1_S:R493Q; BA.1.1_S:S496G; BA.1.1_S:R498Q; BA.1.1_S:Y501N; BA.1.1_S:H505Y; BA.1.1_S:K547T; BA.1.1_S:G614D; BA.1.1_S:Y655H; BA.1.1_S:K679N; BA.1.1_S:H681P; BA.1.1_S:K764N; BA.1.1_S:Y796D; BA.1.1_S:K856N; BA.1.1_S:H954Q; BA.1.1_S:K969N; BA.1.1_S:F981L / Omicron BA.2-0.1 spike series (BA.2-0.1_Ss) were named as BA.2_S:I19T;

BA.2_S:24L_25P_26P_S27A; BA.2_S:D142G; BA.2_S:V213G; BA.2_S:D339G; BA.2_S:F371S; BA.2_S:P373S; BA.2_S:F375S; BA.2_S:A376T; BA.2_S:N405D; BA.2_S:S408R; BA.2_S:N417K; BA.2_S:K440N; BA.2_S:N477S; BA.2_S:K478T; BA.2_S:A484E; BA.2_S:R493Q; BA.2_S:R498Q; BA.2_S:Y501N; BA.2_S:H505Y; BA.2_S:G614D; BA.2_S:Y655H; BA.2_S:K679N; BA.2_S:H681P; BA.2_S:K764N; BA.2_S:Y796D; BA.2_S:H954Q; BA.2_S:K969N, and these constructs are shown in Figs. 2, 4 and supplemental Figure 1. These amino acids sequences of spike protein of SARS-CoV-2 Omicron variants, BA.1-0.1, BA.1.1-0.1, and BA.2-0.1, were used as query sequences for an NCBI protein BLAST search. Then, the whole genome sequences of BA.1-0.1, BA.1.1-0.1, and BA.2-0.1 isolates bearing the query spike sequence were derived from the BLAST search results, identified with a query amino acid sequence of 100%. The nucleotide sequences of the detected SARS-CoV-2 genome were as follows: GenBank Accession No.: OM117411.1; OP797378.1; OM789835.1; OP928789.1; OP928803.1; OP929381.1; OP929396.1; OP929417.1; OM173977.1; OM518459.1; OM566981.1; ON019560.1; OM097227.1; OM096937.1; OM099902.1; OM117114.1; OM096685.1; OM354436.1; OM646886.1; OM472901.1; OM364511.1; OM131858.1; OL815451.1; OL896986.1; OL897116.1; OL897118.1; OL896964.1; OM367679.1; OM343778.1; OM409228.1; OM396816.1; OM134162.1; OM075886.1; OM123427.1; OM122677.1; OM121681.1; OM224850.1; ON246090.1; OM931599.1; OM864873.1; OM906519.1; OM906587.1; OM464776.1; OM015999.1; OM015958.1; OM015597.1; OM016329.1; OL898806.1; OL898861.1; OM016937.1; OM016186.1; OM036549.1; OM051171.1; OM126493.1; OM079115.1; OM099199.1; OM134489.1; OM098796.1; ON618279.1; ON618009.1; OM627701.1; OM356511.1; OM295457.1; ON700063.1; OM033824.1; ON368355.1; OM084700.1; ON208126.1; OM566593.1; OM945690.2; ON030252.1; ON019844.1; OM890075.1; ON020044.1; OM833954.1; ON376082.1; OM084604.1; OP795273.1; ON066609.1; OM352882.1; OM290510.1; OM369978.1; OM199342.1; OM011974.1; OM090274.1; OM043984.1; OM121683.1; OM121624.1; OM175506.1; OM360429.1; OM360221.1; OM358058.1; OM500517.1; OM135027.1; OM742858.1; OM521685.1; OM896558.1; ON694155.1; OM686755.1; OM484260.1; OM332056.1; OM156397.1; OM079447.1; OM134645.1; OM173298.1; OM123082.1; OM116023.1; OM652943.1; OL994299.1; OL994920.1; OM122027.1; OM121015.1; OL898817.1; OM527504.1; OM225320.1; OM931491.1; OM931575.1; OM931587.1; OM034409.1; OM036283.1; OL996129.1; OM035680.1; OM096996.1; ON065532.1; OM968098.1; OM816604.1; ON235452.1; ON334146.1; OP024162.1; OP209732.1; OM354578.1; OM099080.1; OM297301.1; OM297438.1; OM365368.1; OM449159.1; OM078863.1; OM096959.1; OM117155.1; OM133880.1; OM077358.1; OM372005.1; OM770362.1; OM897488.1; OM918459.1; OM918478.1; OL897115.1; OL897114.1; OL986779.1; OL986696.1; OL987046.1; ON831866.1; OM864099.1; OM863888.1; OP745925.1; ON831672.1; OM043643.1; OM176192.1; OM226685.1; OM343689.1; OM295527.1; OM894975.1; OM846676.1; OM822024.1; OM846844.1; OM906550.1; OM015933.1; OM016323.1; OM016331.1; OM035685.1; OM022498.1; OM156115.1; OM036875.1; OM099560.1; OM199246.1; OM067048.1; OM079299.1; OM099911.1; OM116588.1; OM097010.1; OM173300.1; OM805961.1; OM983266.1; OM983325.1; ON618010.1; OM084691.1; ON021265.1; ON039239.1; ON056981.1; ON144127.1; OM770527.1; OM156164.1; OM155119.1; OM199353.1; OM084630.1; OM084605.1; OM084621.1; OM359369.1; OM411574.1; OM584789.1; OM720486.1; OM429777.1; ON047062.1; ON065416.1; OP415118.1; OM954373.1; ON042406.1; OM335528.1; OM332335.1; OM353626.1; OM332813.1; OM197398.1; OM226919.1; OM228399.1; OM225859.1; OM271353.1; OM159454.1; OM224473.1; OM358278.1; OM361030.1; OM412141.1; OM496298.1; OM044048.1; OM121864.1; OM224477.1; OM227379.1; OM228453.1; OM622156.1; OM906370.1; OM970683.1; ON117965.1; OM198667.1; OM357800.1; OM357161.1; OM335230.1; OM261124.1; OM077578.1; OM497172.1; OM625194.1; OM907131.1; ON047464.1; OM911851.1; OM042846.1; OM155337.1; OM097339.1; OM116805.1; OM134409.1; OM686782.1; OM695863.1; OM724725.1; OM174366.1; OM822132.1; OM822106.1; OM822105.1; OM822485.1; OM135143.1; OM125829.1; OM098855.1; OM156118.1; OM155114.1; OM863926.1; OP359104.1; ON209298.1; ON232806.1; ON421981.1; ON811217.1; OM698275.1; ON052769.1; ON060006.1; ON060007.1; ON060009.1; OM843171.1; OM843276.1; OM843550.1; OM843316.1; OM843340.1; ON049267.1; ON450720.1; ON250163.1; ON256603.1; ON480422.1; OM888844.1; OM890089.1; ON009425.2; ON082904.1; OM901275.1; OM877094.2; OM877095.2; OM877096.2; OM877097.2; ON378542.1; ON389858.1; ON389889.1; ON390359.1; OM936703.1; ON352711.1; ON378000.1; ON177702.1; ON205494.1; ON378633.1; ON617689.1;

ON619375.1; OM567618.1; OM659585.1; OM770913.1; OM781641.1; OM533441.1; OM533458.1; OM570235.1; OM570252.1; OM570249.1; OM283361.1; OM283362.1; OM283320.1; OM283343.1; ON618014.1; ON618018.1; ON618019.1; ON618363.1; ON311615.1; ON383919.1; OP579158.1; OP054411.1; ON633107.1; ON414693.1; ON422887.1; OP364296.1; OP629673.1; ON363097.1; OP633561.1; ON458445.1; ON592247.1; ON549687.1; ON067040.1; ON321116.1; ON199452.1; ON200331.1; OM861064.1; OM969592.1; ON019120.1; ON221861.1; OM861619.1; ON091288.1; ON151370.1; ON233850.1; ON236456.1; ON296711.1; ON535443.1; ON624524.1; ON377450.1; ON397268.1; ON239032.1; ON373649.1; ON481637.1; ON701163.1; ON312677.1; ON349263.1; ON377487.1; ON377609.1; OM638574.1; OM911616.1; OM988767.1; ON019770.1; OM988769.1; ON468158.1; ON608924.1; ON604965.1; ON535763.1; ON378227.1; ON378238.1; ON728470.1.

4.4 Query of recombinant SARS-CoV-2 Omicron variant between BA.1 and BA.2 genome

Deduced recombinant spike protein between Omicron variants, BA.1 and BA.2 shown as BA.1_S:T19I_L24-_P25-_P26-_A27S_V213G_S371F_T376A_D405N_R408S was used as a query sequence for an NCBI protein BLAST search. The whole genome sequence of BA.1 and BA.2 recombinant-Omicron isolates showed some of the specific amino acid mutations observed in variant BA.1 and BA.2 in the S protein. The nucleotide sequences of the detected SARS-CoV-2 genome were as follows: GenBank Accession No.: OM360636.1; OM410816.1; OM429902.1; OM497964.1; OM565587.1; OM628132.1; ON549899.1; ON449685.1; ON176765.1; OM628094.1; ON099844.1; OM942313.1; ON395480.1; ON171854.1; ON172005.1; ON076710.1; ON928946.1; OM932113.1; OM942438.1; OM989528.1; OM499181.1; ON414822.1; OM878325.1; ON103067.1; ON103153.1; ON419036.1; ON928719.1; ON337887.1; ON420444.1; ON146520.1; OM469541.1; OM904085.1; ON254531.1; OM881098.1; ON373310.1.

4.5 Query of SARS-CoV-2 Omicron variant genome detected in Puerto Rico in 2020

Nucleotide sequences were searched using the keywords PRI PR-UPRRP 2020 (Search details: PRI[All Fields] AND (PR[All Fields] AND UPRRP[All Fields]) AND 2020[All Fields]). The search results were all SARS-CoV-2 isolate genome sequences. Among these sequences, SARS-CoV-2 Omicron variant-related sequences were picked up as follows: GenBank Accession No.: ON928761.1; ON928660.1; ON928794.1; ON928762.1; ON928848.1; ON928741.1; ON928918.1; ON928680.1; ON928975.1; ON928949.1; ON928673.1; ON928865.1; ON928716.1; ON928663.1; ON928779.1; ON928896.1; ON928946.1; ON928912.1; ON928704.1; ON928873.1; ON928813.1; ON928898.1; ON928765.1; ON928912.1; ON928883.1; ON928957.1; ON928880.1; ON928699.1; ON928724.1; ON928941.1.

Genomes were aligned using SnapGene software or GENETYX software. Numbering of nucleotides and amino acids of each protein was determined using Wuhan-Hu-1 (NC_045512.2; COVID-19/Wuhan-Hu-1CHN/2019/First Isolate) as a reference strain for the definition of mutations.

5. References

1. F. Wu, S. Zhao, B. Yu, Y. M. Chen, W. Wang, Z. G. Song, Y. Hu, Z. W. Tao, J. H. Tian, Y. Y. Pei, M. L. Yuan, Y. L. Zhang, F. H. Dai, Y. Liu, Q. M. Wang, J. J. Zheng, L. Xu, E. C. Holmes and Y. Z. Zhang: A new coronavirus associated with human respiratory disease in China. *Nature*, 579(7798), 265-269 (2020) doi:10.1038/s41586-020-2008-3
2. R. A. Khailany, M. Safdar and M. Ozaslan: Genomic characterization of a novel SARS-CoV-2. *Gene Rep*, 19, 100682 (2020) doi:10.1016/j.genrep.2020.100682
3. Y. M. Bar-On, A. Flamholz, R. Phillips and R. Milo: SARS-CoV-2 (COVID-19) by the numbers. *Elife*, 9 (2020) doi:10.7554/eLife.57309
4. J. Lan, J. Ge, J. Yu, S. Shan, H. Zhou, S. Fan, Q. Zhang, X. Shi, Q. Wang, L. Zhang and X. Wang: Structure of the SARS-CoV-2 spike receptor-binding domain bound to the ACE2 receptor. *Nature*, 581(7807), 215-220 (2020) doi:10.1038/s41586-020-2180-5
5. D. Wrapp, N. Wang, K. S. Corbett, J. A. Goldsmith, C. L. Hsieh, O. Abiona, B. S. Graham and J. S. McLellan: Cryo-EM structure of the 2019-nCoV spike in the prefusion conformation. *Science*, 367(6483), 1260-1263 (2020) doi:10.1126/science.abb2507
6. B. Korber, W. M. Fischer, S. Gnanakaran, H. Yoon, J. Theiler, W. Abfalterer, N. Hengartner, E. E. Giorgi, T. Bhattacharya, B. Foley, K. M. Hastie, M. D. Parker, D. G. Partridge, C. M. Evans, T. M. Freeman, T. I. de Silva, C.-G. G. Sheffield, C. McDanal, L. G. Perez, H. Tang, A. Moon-Walker, S. P. Whelan, C. C. LaBranche, E. O. Saphire and D. C. Montefiori: Tracking Changes in SARS-CoV-2 Spike: Evidence that D614G Increases Infectivity of the COVID-19 Virus. *Cell*, 182(4), 812-827 e19 (2020) doi:10.1016/j.cell.2020.06.043
7. A. Carrazco-Montalvo, A. Bruno, D. de Mora, M. Olmedo, J. Garces, M. Paez, M. Regato-Arrata, M. Gonzalez, J. Romero, O. Mestanza, B. Freire-Paspuel, A. Gaviria, S. A. Orlando, M. A. Garcia-Bereguiain and L. Patino: First Report of SARS-CoV-2 Lineage B.1.1.7 (Alpha Variant) in Ecuador, January 2021. *Infect Drug Resist*, 14, 5183-5188 (2021) doi:10.2147/IDR.S319439
8. S. Zarate, B. Taboada, J. E. Munoz-Medina, P. Isa, A. Sanchez-Flores, C. Boukadida, A. Herrera-Estrella, N. Selem Mojica, M. Rosales-Rivera, B. Gomez-Gil, A. G. Salas-Lais, C. E. Santacruz-Tinoco, H. Montoya-Fuentes, J. E. Alvarado-Yaah, G. M. Molina-Salinas, G. E. Espinoza-Ayala, J. A. Enciso-Moreno, R. M. Gutierrez-Rios, A. Loza, J. Moreno-Contreras, R. Garcia-Lopez, X. Rivera-Gutierrez, A. Comas-Garcia, R. M. Wong-Chew, M. E. Jimenez-Corona, R. M. Del Angel, J. A. Vazquez-Perez, M. Matias-Florentino, M. Perez-Garcia, S. Avila-Rios, H. G. Castelan-Sanchez, L. Delaye, L. P. Martinez-Castilla, M. Escalera-Zamudio, S. Lopez and C. F. Arias: The Alpha Variant (B.1.1.7) of SARS-CoV-2 Failed to Become Dominant in Mexico. *Microbiol Spectr*, 10(2), e0224021 (2022) doi:10.1128/spectrum.02240-21
9. H. Tegally, E. Wilkinson, M. Giovanetti, A. Iranzadeh, V. Fonseca, J. Giandhari, D. Doolabh, S. Pillay, E. J. San, N. Msomi, K. Mlisana, A. von Gottberg, S. Walaza, M. Allam, A. Ismail, T. Mohale, A. J. Glass, S. Engelbrecht, G. Van Zyl, W. Preiser, F. Petruccione, A. Sigal, D. Hardie, G. Marais, N.-y. Hsiao, S. Korsman, M.-A. Davies, L. Tyers, I. Mudau, D. York, C. Maslo, D. Goedhals, S. Abrahams, O. Laguda-Akingba, A. Alisoltani-Dehkordi, A. Godzik, C. K. Wibmer, B. T. Sewell, J. Lourenço, L. C. J. Alcantara, S. L. Kosakovsky Pond, S. Weaver, D. Martin, R. J. Lessells, J. N. Bhiman, C. Williamson and T. de Oliveira: Detection of a SARS-CoV-2 variant of concern in South Africa. *Nature*, 592(7854), 438-443 (2021) doi:10.1038/s41586-021-03402-9
10. T. Fujino, H. Nomoto, S. Kutsuna, M. Ujiie, T. Suzuki, R. Sato, T. Fujimoto, M. Kuroda, T. Wakita and N. Ohmagari: Novel SARS-CoV-2 Variant in Travelers from Brazil to Japan. *Emerg Infect Dis*, 27(4), 1243-5 (2021) doi:10.3201/eid2704.210138
11. M. Joshi, M. Kumar, V. Srivastava, D. Kumar, D. S. Rathore, R. Pandit, D. W. Graham and C. G. Joshi: Genetic sequencing detected the SARS-CoV-2 delta variant in wastewater a month prior to the first COVID-19 case in Ahmedabad (India). *Environ Pollut*, 310, 119757 (2022) doi:10.1016/j.envpol.2022.119757
12. K. Laiton-Donato, C. Franco-Munoz, D. A. Alvarez-Diaz, H. A. Ruiz-Moreno, J. A. Usme-Ciro, D. A. Prada, J. Reales-Gonzalez, S. Corchuelo, M. T. Herrera-Sepulveda, J. Naizaque, G. Santamaria, J. Rivera, P. Rojas, J. H. Ortiz, A. Cardona, D. Malo, F. Prieto-Alvarado, F. R. Gomez, M. Wiesner, M. L. O. Martinez and M. Mercado-Reyes: Characterization of the emerging B.1.621 variant of interest of SARS-CoV-2. *Infect Genet Evol*, 95, 105038 (2021) doi:10.1016/j.meegid.2021.105038

13. P. L. Wink, F. C. Z. Volpato, F. L. Monteiro, J. B. Willig, A. P. Zavascki, A. L. Barth and A. F. Martins: First identification of SARS-CoV-2 lambda (C.37) variant in Southern Brazil. *Infect Control Hosp Epidemiol*, 43(12), 1996-1997 (2022) doi:10.1017/ice.2021.390
14. COVID-19 Weekly Epidemiological Update Edition 44, published 15 June 2021. *World Health Organization* (2021)
15. J. Quarleri, V. Galvan and M. V. Delpino: Omicron variant of the SARS-CoV-2: a quest to define the consequences of its high mutational load. *Geroscience*, 44(1), 53-56 (2022) doi:10.1007/s11357-021-00500-4
16. A. Gowrisankar, T. M. C. Priyanka and S. Banerjee: Omicron: a mysterious variant of concern. *Eur Phys J Plus*, 137(1), 100 (2022) doi:10.1140/epjp/s13360-021-02321-y
17. A. Vitiello, F. Ferrara, A. M. Auti, M. Di Domenico and M. Boccellino: Advances in the Omicron variant development. *J Intern Med*, 292(1), 81-90 (2022) doi:10.1111/joim.13478
18. Y. Fan, X. Li, L. Zhang, S. Wan, L. Zhang and F. Zhou: SARS-CoV-2 Omicron variant: recent progress and future perspectives. *Signal Transduct Target Ther*, 7(1), 141 (2022) doi:10.1038/s41392-022-00997-x
19. J. Fonager, M. Bennedbaek, P. Bager, J. Wohlfahrt, K. M. Ellegaard, A. C. Ingham, S. M. Edslev, M. Stegger, R. N. Sieber, R. Lassauniere, A. Fomsgaard, T. Lillebaek, C. W. Svarrer, F. T. Moller, C. H. Moller, R. Legarth, T. V. Sydenham, K. Steinke, S. J. Paulsen, J. A. S. Castruita, U. V. Schneider, C. H. Schouw, X. C. Nielsen, M. Overvad, R. T. Nielsen, R. L. Marvig, M. S. Pedersen, L. Nielsen, L. L. Nilsson, J. Bybjerg-Grauholm, I. H. Tarpgaard, T. S. Ebsen, J. U. H. Lam, V. Gunalan and M. Rasmussen: Molecular epidemiology of the SARS-CoV-2 variant Omicron BA.2 sub-lineage in Denmark, 29 November 2021 to 2 January 2022. *Euro Surveill*, 27(10) (2022) doi:10.2807/1560-7917.ES.2022.27.10.2200181
20. L. B. Shrestha, C. Foster, W. Rawlinson, N. Tedla and R. A. Bull: Evolution of the SARS-CoV-2 omicron variants BA.1 to BA.5: Implications for immune escape and transmission. *Rev Med Virol*, 32(5), e2381 (2022) doi:10.1002/rmv.2381
21. L. Yao, K. L. Zhu, X. L. Jiang, X. J. Wang, B. D. Zhan, H. X. Gao, X. Y. Geng, L. J. Duan, E. H. Dai and M. J. Ma: Omicron subvariants escape antibodies elicited by vaccination and BA.2.2 infection. *Lancet Infect Dis*, 22(8), 1116-1117 (2022) doi:10.1016/S1473-3099(22)00410-8
22. S. Torii, C. Ono, R. Suzuki, Y. Morioka, I. Anzai, Y. Fauzyah, Y. Maeda, W. Kamitani, T. Fukuhara and Y. Matsuura: Establishment of a reverse genetics system for SARS-CoV-2 using circular polymerase extension reaction. *Cell Rep*, 35(3), 109014 (2021) doi:10.1016/j.celrep.2021.109014
23. T. Y. Taha, I. P. Chen, J. M. Hayashi, T. Tabata, K. Walcott, G. R. Kimmerly, A. M. Syed, A. Ciling, R. K. Suryawanshi, H. S. Martin, B. H. Bach, C. L. Tsou, M. Montano, M. M. Khalid, B. K. Sreekumar, G. Renuka Kumar, S. Wyman, J. A. Doudna and M. Ott: Rapid assembly of SARS-CoV-2 genomes reveals attenuation of the Omicron BA.1 variant through NSP6. *Nat Commun*, 14(1), 2308 (2023) doi:10.1038/s41467-023-37787-0
24. W. Wang, X. Peng, Y. Jin, J. A. Pan and D. Guo: Reverse genetics systems for SARS-CoV-2. *J Med Virol*, 94(7), 3017-3031 (2022) doi:10.1002/jmv.27738
25. L. Xu, L. Bao, Q. Lv, W. Deng, Y. Ma, F. Li, L. Zhan, H. Zhu, C. Ma and C. Qin: A single-amino-acid substitution in the HA protein changes the replication and pathogenicity of the 2009 pandemic A (H1N1) influenza viruses in vitro and in vivo. *Virol J*, 7, 325 (2010) doi:10.1186/1743-422X-7-325
26. L. A. Silva, S. Khomandiak, A. W. Ashbrook, R. Weller, M. T. Heise, T. E. Morrison and T. S. Dermody: A single-amino-acid polymorphism in Chikungunya virus E2 glycoprotein influences glycosaminoglycan utilization. *J Virol*, 88(5), 2385-97 (2014) doi:10.1128/JVI.03116-13
27. K. A. Tsetsarkin, D. L. Vanlandingham, C. E. McGee and S. Higgs: A single mutation in chikungunya virus affects vector specificity and epidemic potential. *PLoS Pathog*, 3(12), e201 (2007) doi:10.1371/journal.ppat.0030201
28. X. C. Tang, S. S. Agnihothram, Y. Jiao, J. Stanhope, R. L. Graham, E. C. Peterson, Y. Avnir, A. S. Tallarico, J. Sheehan, Q. Zhu, R. S. Baric and W. A. Marasco: Identification of human neutralizing antibodies against MERS-CoV and their role in virus adaptive evolution. *Proc Natl Acad Sci U S A*, 111(19), E2018-26 (2014) doi:10.1073/pnas.1402074111
29. J. Sui, D. R. Aird, A. Tamin, A. Murakami, M. Yan, A. Yammanuru, H. Jing, B. Kan, X. Liu, Q. Zhu, Q. A. Yuan, G. P. Adams, W. J. Bellini, J. Xu, L. J. Anderson and W. A. Marasco: Broadening of neutralization activity to directly block a dominant antibody-driven SARS-coronavirus evolution pathway. *PLoS Pathog*, 4(11), e1000197 (2008) doi:10.1371/journal.ppat.1000197

30. J. ter Meulen, E. N. van den Brink, L. L. Poon, W. E. Marissen, C. S. Leung, F. Cox, C. Y. Cheung, A. Q. Bakker, J. A. Bogaards, E. van Deventer, W. Preiser, H. W. Doerr, V. T. Chow, J. de Kruif, J. S. Peiris and J. Goudsmit: Human monoclonal antibody combination against SARS coronavirus: synergy and coverage of escape mutants. *PLoS Med*, 3(7), e237 (2006) doi:10.1371/journal.pmed.0030237
31. L. van Dorp, D. Richard, C. C. S. Tan, L. P. Shaw, M. Acman and F. Balloux: No evidence for increased transmissibility from recurrent mutations in SARS-CoV-2. *Nat Commun*, 11(1), 5986 (2020) doi:10.1038/s41467-020-19818-2

Conflict of Interest

The authors declare that the research was conducted in the absence of any commercial or financial relationships that could be construed as a potential conflict of interest.

Figure legends

Fig. 1. Mutation subsets of S protein of SARS-CoV-2 variants.

Sequences of S protein of SARS-CoV-2 variants（variants of concern, VOCs: Alpha:B.1.1.7, Beta:B.1.351, Gamma:P1, Delta:B.1.617.2.63, and Omicron:BA.1; BA.2 and variants of interest, VOIs: Lambda:C.37, Mu:B.1.621) are compared with the SARS-CoV-2 Wuhan-Hu-H1 reference sequence, and different amino acids (amino acid change, deletion, and insertion) and synonymous changes of nucleotides are shown. Non-synonymous changes are shown by amino acid changes (capital letters), and synonymous changes are shown by nucleotide changes (small letters). Amino acids different from Wuhan-Hu-H1 found in each variant: Alpha: B.1.1.7, Beta: B.1.351, Gamma: P1, Delta: B.1.617.2.63, Lambda: C.37, Mu: B.1.621, and Omicron: BA.1, BA.2 are highlighted with red, orange, green, yellow, aquamarine, lime, deep sky blue, and blue violet, respectively. Amino acid changes common to Omicron: BA.1 and BA.2 are shown in purple.

Fig. 2. Mutations of S proteins of SARS-CoV-2 Omicron isolates.

(A) Different amino acids and synonymous changes of nucleotides in **S** proteins of SARS-CoV-2 Omicron BA.1, BA.1.1 isolates, and BA.1-0.1s compared with SARS-CoV-2 Wuhan-Hu-H1. Nucleotide deletions and insertions were "deletion^{1}" (deletion: nt 21,766-21,771), "deletion^{2}" (deletion: nt 21,987-21,995), "deletion^{3}" (deletion: nt 22,194-22,196), and "insertion^{4}" (insertion between 22,206-22,196), and introduced amino acid changes were H69-_V70-, G142D_V143-_Y144-_Y145-, N211I_L212-, and 215ins.EPE, respectively. (B) Different amino acids and synonymous nucleotide changes in S proteins of SARS-CoV-2 Omicron BA.1.1-0.1 isolates. Amino acids different from Wuhan-Hu-H1 found in each variant: Alpha: B.1.1.7, Beta: B.1.351, Gamma: P1, Delta: B.1.617.2.63, Mu: B.1.621, and Omicron: BA.1, BA.2 are highlighted with red, orange, green, yellow, lime, deep sky blue, and blue violet, respectively. Amino acid changes common to Omicron:BA.1 and BA.2 are highlighted with purple.

Fig. 3. Estimated homologous recombination breakpoints of the SARS-CoV-2 S gene of Omicron BA.1-0.1 or BA.1.1-0.1.

Sequence alignment of amino acids and their coding nucleotides (nt.21,746-21,787; nt.22,658-22,702; nt.22,976-23,011, and nt.23,582-23,620) containing the mutation point of the SARS-CoV-2 S gene of the Omicron BA.1 variant compared with SARS-CoV-2 Wuhan-Hu-H1. Changed nucleotides and amino acids of Omicron BA.1 are shown in red letters. Estimated homologous recombination breakpoints of the SARS-CoV-2 S gene of Omicron BA.1-0.1 or BA.1.1-0.1 are shown by asterisks.

Fig. 4. Representative mutations of SARS-CoV-2 Omicron isolates other than S protein.

(A) Representative amino acids and synonymous changes of nucleotides of SARS-CoV-2 Omicron BA.1, BA.1.1 isolates, and BA.1-0.1 compared with SARS-CoV-2 Wuhan-Hu-H1. **(B)** Representative amino acids and synonymous changes of nucleotides of SARS-CoV-2 Omicron BA.1.1-0.1 compared with SARS-CoV-2 Wuhan-Hu-H1. Amino acids different from Wuhan-Hu-H1 found in each variant: Alpha: B.1.1.7, Lambda: C.37, Mu: B.1.621, and Omicron: BA.1 are highlighted with red, aquamarine, deep sky blue, and blue violet, respectively.

Amino acid changes common to Omicron: BA.1 and BA.2 are shown in purple. Synonymous nucleotide changes: c2470u observed in Omicron:BA.1.1 mainly shown with blue. Synonymous and non-synonymous changes: u10135c of nsp5, L106F in ORF3, and D343G in N protein subset observed in ~40% of Omicron;

BA.1-0.1 are highlighted with emerald-green. Undetermined nucleotides or amino acids are shown as UD or X, respectively.

Fig. 5. Mutations of S proteins of SARS-CoV-2 Omicron BA.1-BA.2 recombinant isolates and SARS-CoV-2 Omicron BA.1 and BA.2 isolates detected in Puerto Rico in 2020.

(A) Different amino acids and synonymous change of nucleotides in S proteins of SARS-CoV-2 Omicron BA.1-BA.2 recombinant isolates compared with SARS-CoV-2 Wuhan-Hu-H1. Nucleotide deletions, "deletion^{5}" (deletion: nt 21,633-21,641), introduced the amino acids changes L24-_P25-_P26-_A27S. **(B)** Different amino acids and synonymous change of nucleotides in S proteins of SARS-CoV-2 Omicron BA.1.1 and Omicron BA.1-BA.2 recombinant isolate, highlighted with magenta (GenBank: ON928946.1), Omicron BA.2, and Omicron 2-0.1(K440N), detected in Puerto Rico in 2020. Amino acids different from Wuhan-Hu-H1 found in each variant: Alpha: B.1.1.7, Beta: B.1.351, Gamma: P1, Delta: B.1.617.2.63, Mu: B.1.621, and Omicron: BA.1, BA.2 are highlighted with red, orange, green, yellow, lime, deep sky blue, and blue-violet, respectively. Amino acid changes common to Omicron: BA.1 and BA.2 are highlighted with purple.

Supplemental Figure 1

Human coronavirus 229E strains detected in Seattle, USA, in 2015 and 2019.

Alignment of nucleotide **(A)** and amino acid **(B)** sequences of the S protein of Human coronavirus 229E strains, HCoV_229E/Seattle/USA/SC3112/2015 (GenBank: KY983587.1), and CoV_229E/Seattle/USA/SC0865/2019 (GenBank: MN306046.1). The number of nucleotide substitutions observed between them was 32, amino acid substitutions numbered 18 between them, and the synonymous (14: 32-18)–non-synonymous mutation (18) rate between them was 1.285

Supplemental Figure 2

Different amino acids and synonymous changes of nucleotides in S proteins of SARS-CoV-2 Omicron BA.2 isolates and BA.2-0.1s compared with SARS-CoV-2 Wuhan-Hu-H1.

Nucleotide deletions, "deletion^{5}" (deletion: nt 21,633-21,641), introduced the amino acid changes L24-_P25-_P26-_A27S. Amino acids different from Wuhan-Hu-H1 found in each variant: Alpha: B.1.1.7, Beta: B.1.351, Gamma: P1, Delta: B.1.617.2.63, Mu: B.1.621, and Omicron: BA.1, BA.2 are highlighted with red, orange, green, yellow, lime, deep sky blue, and blue-violet, respectively. Amino acid changes common to Omicron: BA.1 and BA.2 are highlighted with purple.

Supplemental Figure 3

Estimated homologous recombination breakpoints of the SARS-CoV-2 S gene of the Omicron BA.2-0.1 or BA.1-BA.2 recombinant.

(A) Sequence alignment of the amino acids and coding nucleotides (nt. 22,658-22,702) containing the mutation point of the SARS-CoV-2 S gene of Omicron BA.2 variants compared with SARS-CoV-2 Wuhan-Hu-H1. **(B)** Sequence alignment of the amino acids and coding nucleotides (nt. 22,178-22,222) containing the mutation point of the SARS-CoV-2 S gene of Omicron BA,1, BA.2 variant and BA.1-BA.2 recombinant isolate compared with SARS-CoV-2 Wuhan-Hu-H1. Changed nucleotides and amino acids of Omicron variants BA.1, BA.2, and

615 BA.1-BA.2 recombinant isolates compared with SARS-CoV-2 Wuhan-Hu-H1 sequences are shown in red
616 letters. Asterisks show an estimated homologous recombination breakpoint of the SARS-CoV-2 S gene of
617 Omicron BA.2-0.1.

Fig. 1

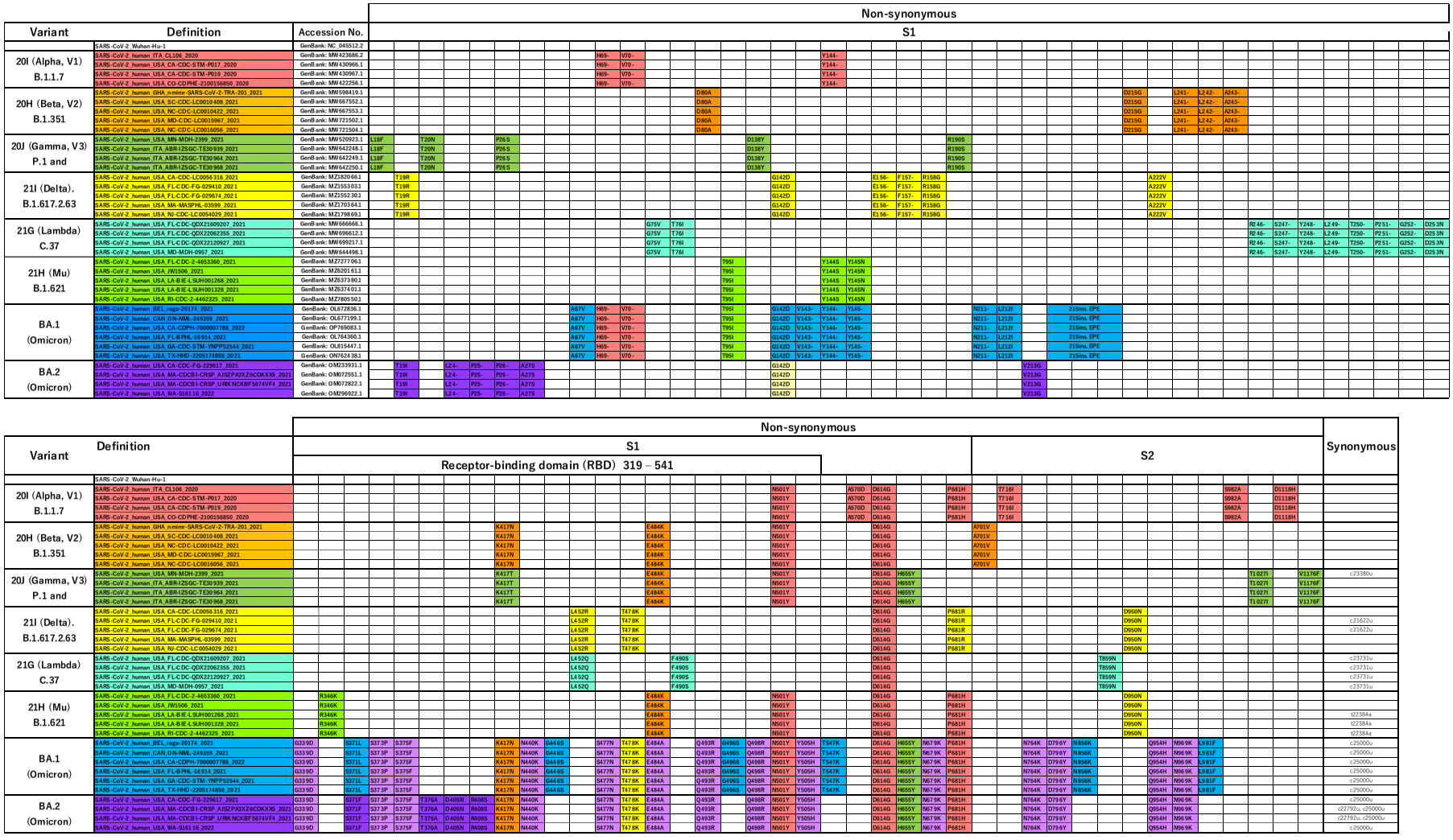

| Variant | Definition | Accession No. | Non-synonymous | | |

Fig. 2 A

Variant	Definition	GenBank Accession No.	Non-synonymous: deletion[1] A67V	deletion[1] H69-	deletion[1] V70-	deletion[2] T95I	deletion[2] G142D	deletion[2] V143-	deletion[2] Y144-	deletion[2] Y145-	deletion[3] N211I	deletion[3] L212-	insertion[4] 215ins_EPE	G339D	R346K	S371L	S373P	S375F	K417N	N440K	G446S	S477N	T478K	E484A	Q493R	G496S	Q498R	N501Y	Y505H	T547K	D614G	H655Y	N679K	P681H	N764K	D796Y	N856K	Q954H	N969K	L981F	Others	Synonymous: c21595u	c25000u	Others
	SARS-CoV-2_Wuhan-Hu-1	NC_045512.2																																									
BA.1	SARS-CoV-2_human_BEL_rega-20174_20.21	Sin-eBank: OL672836.1	A67V	H69-	V70-	T95I	G142D	V143-	Y144-	Y145-	N211I	L212-	215ins_EPE	G339D		S371L	S373P	S375F	K417N	N440K	G446S	S477N	T478K	E484A	Q493R	G496S	Q498R	N501Y	Y505H	T547K	D614G	H655Y	N679K	P681H	N764K	D796Y	N856K	Q954H	N969K	L981F		c21595u	c25000u	
	SARS-CoV-2_human_USA_GA-CDC-STM-YNPS2544_20.21	Sin-eBank: OL815447.1	A67V	H69-	V70-	T95I	G142D	V143-	Y144-	Y145-	N211I	L212-	215ins_EPE	G339D		S371L	S373P	S375F	K417N	N440K	G446S	S477N	T478K	E484A	Q493R	G496S	Q498R	N501Y	Y505H	T547K	D614G	H655Y	N679K	P681H	N764K	D796Y	N856K	Q954H	N969K	L981F		c21595u	c25000u	
	SARS-CoV-2_human_USA_FL-BPHL-L6914_2021	Sin-eBank: OL764360.1	A67V	H69-	V70-	T95I	G142D	V143-	Y144-	Y145-	N211I	L212-	215ins_EPE	G339D		S371L	S373P	S375F	K417N	N440K	G446S	S477N	T478K	E484A	Q493R	G496S	Q498R	N501Y	Y505H	T547K	D614G	H655Y	N679K	P681H	N764K	D796Y	N856K	Q954H	N969K	L981F			c25000u	
	SARS-CoV-2_human_CAN_ON-NML-2-49359_2021	Sin-eBank: OL677109.1	A67V	H69-	V70-	T95I	G142D	V143-	Y144-	Y145-	N211I	L212-	215ins_EPE	G339D		S371L	S373P	S375F	K417N	N440K	G446S	S477N	T478K	E484A	Q493R	G496S	Q498R	N501Y	Y505H	T547K	D614G	H655Y	N679K	P681H	N764K	D796Y	N856K	Q954H	N969K	L981F			c25000u	
	SARS-CoV-2_human_USA_CA-CDPH-700000739I_20.22	Sin-eBank: OP709181.1	A67V	H69-	V70-	T95I	G142D	V143-	Y144-	Y145-	N211I	L212-	215ins_EPE	G339D		S371L	S373P	S375F	K417N	N440K	G446S	S477N	T478K	E484A	Q493R	G496S	Q498R	N501Y	Y505H	T547K	D614G	H655Y	N679K	P681H	N764K	D796Y	N856K	Q954H	N969K	L981F			c25000u	
	SARS-CoV-2_human_USA_TX-HHD-220151748R_20.21	Sin-eBank: ON742438.1	A67V	H69-	V70-	T95I	G142D	V143-	Y144-	Y145-	N211I	L212-	215ins_EPE	G339D		S371L	S373P	S375F	K417N	N440K	G446S	S477N	T478K	E484A	Q493R	G496S	Q498R	N501Y	Y505H	T547K	D614G	H655Y	N679K	P681H	N764K	D796Y	N856K	Q954H	N969K	L981F			c25000u	
BA.1.1	SARS-CoV-2_human_USA_COR-21-434106_20.21.seq	Sin-eBank: OL869869.1	A67V	H69-	V70-	T95I	G142D	V143-	Y144-	Y145-	N211I	L212-	215ins_EPE	G339D	R346K	S371L	S373P	S375F	K417N	N440K	G446S	S477N	T478K	E484A	Q493R	G496S	Q498R	N501Y	Y505H	T547K	D614G	H655Y	N679K	P681H	N764K	D796Y	N856K	Q954H	N969K	L981F			c25000u	c22120u
	SARS-CoV-2_human_USA_TX-CDC-QDX31492 531_2021_seq	Sin-eBank: OL897126.1	A67V	H69-	V70-	T95I	G142D	V143-	Y144-	Y145-	N211I	L212-	215ins_EPE	G339D	R346K	S371L	S373P	S375F	K417N	N440K	G446S	S477N	T478K	E484A	Q493R	G496S	Q498R	N501Y	Y505H	T547K	D614G	H655Y	N679K	P681H	N764K	D796Y	N856K	Q954H	N969K	L981F			c25000u	
	SARS-CoV-2_human_USA_MO-CDC-LC00 7004_2021_seq	Sin-eBank: OL899045.1	A67V	H69-	V70-	T95I	G142D	V143-	Y144-	Y145-	N211I	L212-	215ins_EPE	G339D	R346K	S371L	S373P	S375F	K417N	N440K	G446S	S477N	T478K	E484A	Q493R	G496S	Q498R	N501Y	Y505H	T547K	D614G	H655Y	N679K	P681H	N764K	D796Y	N856K	Q954H	N969K	L981F			c25000u	
	SARS-CoV-2_human_USA_GA-CDC-STM-CVB3036BC_2021.seq	Sin-eBank: OL899036.1	A67V	H69-	V70-	T95I	G142D	V143-	Y144-	Y145-	N211I	L212-	215ins_EPE	G339D	R346K	S371L	S373P	S375F	K417N	N440K	G446S	S477N	T478K	E484A	Q493R	G496S	Q498R	N501Y	Y505H	T547K	D614G	H655Y	N679K	P681H	N764K	D796Y	N856K	Q954H	N969K	L981F			c25000u	
	SARS-CoV-2_human_USA_TX-CDC-HCSC592_2021.seq	Sin-eBank: OL899031.1	A67V	H69-	V70-	T95I	G142D	V143-	Y144-	Y145-	N211I	L212-	215ins_EPE	G339D	R346K	S371L	S373P	S375F	K417N	N440K	G446S	S477N	T478K	E484A	Q493R	G496S	Q498R	N501Y	Y505H	T547K	D614G	H655Y	N679K	P681H	N764K	D796Y	N856K	Q954H	N969K	L981F			c25000u	
	SARS-CoV-2_human_USA_MT-CDC-ASC21059 6 46_2021	Sin-eBank: OM117411.1		H69-	V70-	T95I	G142D	V143-	Y144-	Y145-	N211I	L212-	215ins_EPE	G339D		S371L	S373P	S375F	K417N	N440K	G446S	S477N	T478K	E484A	Q493R	G496S	Q498R	N501Y	Y505H	T547K	D614G	H655Y	N679K	P681H	N764K	D796Y	N856K	Q954H	N969K	L981F			c25000u	
	SARS-CoV-2_human_USA_FL-BPHL-L4188_2022	Sin-eBank: OP7973 78.1		H69-	V70-	T95I	G142D	V143-	Y144-	Y145-	N211I	L212-	215ins_EPE	G339D		S371L	S373P	S375F	K417N	N440K	G446S	S477N	T478K	E484A	Q493R	G496S	Q498R	N501Y	Y505H	T547K	D614G	H655Y	N679K	P681H	N764K	D796Y	N856K	Q954H	N969K	L981F			c25000u	
	SARS-CoV-2_human_USA_WI-CDC-LC053769 66_2022	Sin-eBank: OM7 89835.1		H69-	V70-	T95I	G142D	V143-	Y144-	Y145-	N211I	L212-	215ins_EPE	G339D		S371L	S373P	S375F	K417N	N440K	G446S	S477N	T478K	E484A	Q493R	G496S	Q498R	N501Y	Y505H	T547K	D614G	H655Y	N679K	P681H	N764K	D796Y	N856K	Q954H	N969K	L981F			c25000u	
	SARS-CoV-2_Hoagland_USA_TB-0-90009935_20.21	Sin-eBank: OP9287 89.1	A67V																																							
	SARS-CoV-2_Hoagland_USA_TB-0-90009936_20.21	Sin-eBank: OP9288 03.1	A67V			T95I	G142D	V143-	Y144-	Y145-	N211I	L212-	215ins_EPE	G339D		S371L	S373P	S375F	K417N	N440K	G446S	S477N	T478K	E484A	Q493R	G496S	Q498R	N501Y	Y505H	T547K	D614G	H655Y	N679K	P681H	N764K	D796Y	N856K	Q954H	N969K	L981F			c25000u	
	SARS-CoV-2_Hoagland_USA_TB-0-90009940_20.21	Sin-eBank: OP9289 17.1	A67V			T95I	G142D	V143-	Y144-	Y145-	N211I	L212-	215ins_EPE	G339D		S371L	S373P	S375F	K417N	N440K	G446S	S477N	T478K	E484A	Q493R	G496S	Q498R	N501Y	Y505H	T547K	D614G	H655Y	N679K	P681H	N764K	D796Y	N856K	Q954H	N969K	L981F			c25000u	
	SARS-CoV-2_Hoagland_USA_TB-0-90009142_20.21	Sin-eBank: OP9293 96.1	A67V			T95I	G142D	V143-	Y144-	Y145-	N211I	L212-	215ins_EPE	G339D		S371L	S373P	S375F	K417N	N440K	G446S	S477N	T478K	E484A	Q493R	G496S	Q498R	N501Y	Y505H	T547K	D614G	H655Y	N679K	P681H	N764K	D796Y	N856K	Q954H	N969K	L981F			c25000u	
	SARS-CoV-2_Hoagland_USA_TB-0-90009187_20.22	Sin-eBank: OP9294 17.1	A67V			T95I	G142D	V143-	Y144-	Y145-	N211I	L212-	215ins_EPE	G339D		S371L	S373P	S375F	K417N	N440K	G446S	S477N	T478K	E484A	Q493R	G496S	Q498R	N501Y	Y505H	T547K	D614G	H655Y	N679K	P681H	N764K	D796Y	N856K	Q954H	N969K	L981F			c25000u	
	SARS-CoV-2_human_USA_MO-CDC-ASC2103 98706_2021	Sin-eBank: OM117417.1	A67V	H69-	V70-		G142D	V143-	Y144-	Y145-	N211I	L212-	215ins_EPE	G339D		S371L	S373P	S375F	K417N	N440K	G446S	S477N	T478K	E484A	Q493R	G496S	Q498R	N501Y	Y505H	T547K	D614G	H655Y	N679K	P681H	N764K	D796Y	N856K	Q954H	N969K	L981F			c25000u	
	SARS-CoV-2_human_USA_CA-CDC-ASC2103 93579_2022	Sin-eBank: OM5 18459.1	A67V	H69-	V70-		G142D	V143-	Y144-	Y145-	N211I	L212-	215ins_EPE	G339D		S371L	S373P	S375F	K417N	N440K	G446S	S477N	T478K	E484A	Q493R	G496S	Q498R	N501Y	Y505H	T547K	D614G	H655Y	N679K	P681H	N764K	D796Y	N856K	Q954H	N969K	L981F			c25000u	
	SARS-CoV-2_human_USA_MO-CDC-ASC2103 94733_202 2	Sin-eBank: OM5 66981.1	A67V	H69-	V70-		G142D	V143-	Y144-	Y145-	N211I	L212-	215ins_EPE	G339D		S371L	S373P	S375F	K417N	N440K	G446S	S477N	T478K	E484A	Q493R	G496S	Q498R	N501Y	Y505H	T547K	D614G	H655Y	N679K	P681H	N764K	D796Y	N856K	Q954H	N969K	L981F		c21603du	c25000u	c21603du
	SARS-CoV-2_human_USA_PA-CDC-ASC2 10737971 2_022	Sin-eBank: OM119560.1	A67V	H69-	V70-		G142D	V143-	Y144-	Y145-	N211I	L212-	215ins_EPE	G339D		S371L	S373P	S375F	K417N	N440K	G446S	S477N	T478K	E484A	Q493R	G496S	Q498R	N501Y	Y505H	T547K	D614G	H655Y	N679K	P681H	N764K	D796Y	N856K	Q954H	N969K	L981F			c25000u	
	SARS-CoV-2_human_USA_TN-CDC-ASC2102 9204_2021	Sin-eBank: OM0 972271	A67V	H69-	V70-	T95I					N211I	L212-	215ins_EPE	G339D		S371L	S373P	S375F	K417N	N440K	G446S	S477N	T478K	E484A	Q493R	G496S	Q498R	N501Y	Y505H	T547K	D614G	H655Y	N679K	P681H	N764K	D796Y	N856K	Q954H	N969K	L981F			c25000u	
	SARS-CoV-2_human_USA_TX-CDC-ASC2 10639391 2_021	Sin-eBank: OM0 96037.1	A67V	H69-	V70-	T95I					N211I	L212-	215ins_EPE	G339D		S371L	S373P	S375F	K417N	N440K	G446S	S477N	T478K	E484A	Q493R	G496S	Q498R	N501Y	Y505H	T547K	D614G	H655Y	N679K	P681H	N764K	D796Y	N856K	Q954H	N969K	L981F			c25000u	
	SARS-CoV-2_human_USA_TX-CDC-ASC2 10631567 2_021	Sin-eBank: OM0 99902.1	A67V	H69-	V70-	T95I					N211I	L212-	215ins_EPE	G339D		S371L	S373P	S375F	K417N	N440K	G446S	S477N	T478K	E484A	Q493R	G496S	Q498R	N501Y	Y505H	T547K	D614G	H655Y	N679K	P681H	N764K	D796Y	N856K	Q954H	N969K	L981F			c25000u	
	SARS-CoV-2_human_USA_IL-CDC-IDCC2101 61962_202 1	Sin-eBank: OM1 17114.1	A67V	H69-	V70-	T95I					N211I	L212-	215ins_EPE	G339D		S371L	S373P	S375F	K417N	N440K	G446S	S477N	T478K	E484A	Q493R	G496S	Q498R	N501Y	Y505H	T547K	D614G	H655Y	N679K	P681H	N764K	D796Y	N856K	Q954H	N969K	L981F			c25000u	
	SARS-CoV-2_human_USA_OH-CDC-ASC21 0635565_2021	Sin-eBank: OM0 96688.1	A67V	H69-	V70-	T95I					N211I	L212-	215ins_EPE	G339D		S371L	S373P	S375F	K417N	N440K	G446S	S477N	T478K	E484A	Q493R	G496S	Q498R	N501Y	Y505H	T547K	D614G	H655Y	N679K	P681H	N764K	D796Y	N856K	Q954H	N969K	L981F			c25000u	
	SARS-CoV-2_human_USA_CA-CDC-STM-SZ-CDW9HQF_202 2	Sin-eBank: OM3 54186.1	A67V	H69-	V70-	T95I	G142D	V143-	Y144-	Y145-				G339D		S371L	S373P	S375F	K417N	N440K	G446S	S477N	T478K	E484A	Q493R	G496S	Q498R	N501Y	Y505H	T547K	D614G	H655Y	N679K	P681H	N764K	D796Y	N856K	Q954H	N969K	L981F			c25000u	
	SARS-CoV-2_human_USA_OR-UW-2-2010866 094_2022	Sin-eBank: OM6 46886.1	A67V	H69-	V70-	T95I	G142D	V143-	Y144-	Y145-			215ins_EPE	G339D		S371L	S373P	S375F	K417N	N440K	G446S	S477N	T478K	E484A	Q493R	G496S	Q498R	N501Y	Y505H	T547K	D614G	H655Y	N679K	P681H	N764K	D796Y	N856K	Q954H	N969K	L981F			c25000u	
	SARS-CoV-2_human_USA_KY-CDC-LC0167 8_2022	Sin-eBank: OM5 61778.1	A67V	H69-	V70-	T95I	G142D	V143-	Y144-	Y145-			215ins_EPE	G339D		S371L	S373P	S375F	K417N	N440K	G446S	S477N	T478K	E484A	Q493R	G496S	Q498R	N501Y	Y505H	T547K	D614G	H655Y	N679K	P681H	N764K	D796Y	N856K	Q954H	N969K	L981F			c25000u	
	SARS-CoV-2_human_USA_FL-CDC-ASC2100 3798_2022	Sin-eBank: OM3 64511.1	A67V	H69-	V70-	T95I	G142D	V143-	Y144-	Y145-			215ins_EPE	G339D		S371L	S373P	S375F	K417N	N440K	G446S	S477N	T478K	E484A	Q493R	G496S	Q498R	N501Y	Y505H	T547K	D614G	H655Y	N679K	P681H	N764K	D796Y	N856K	Q954H	N969K	L981F			c25000u	
	SARS-CoV-2_human_USA_WA-CDC-UW 11211761 830_2021	Sin-eBank: OM1 31898.1	A67V	H69-	V70-	T95I	G142D	V143-	Y144-	Y145-			215ins_EPE	G339D		S371L	S373P	S375F	K417N	N440K	G446S	S477N	T478K	E484A	Q493R	G496S	Q498R	N501Y	Y505H	T547K	D614G	H655Y	N679K	P681H	N764K	D796Y	N856K	Q954H	N969K	L981F			c25000u	
	SARS-CoV-2_human_USA_CA-CDC-FG-L80106_2021	Sin-eBank: OL815581.1	A67V	H69-	V70-	T95I	G142D	V143-	Y144-	Y145-	N211I	L212-		G339D		S371L	S373P	S375F	K417N	N440K	G446S	S477N	T478K	E484A	Q493R	G496S	Q498R	N501Y	Y505H	T547K	D614G	H655Y	N679K	P681H	N764K	D796Y	N856K	Q954H	N969K	L981F			c25000u	
	SARS-CoV-2_human_USA_CA-CDC-FG-L86264_2021	Sin-eBank: OL896986.1	A67V	H69-	V70-	T95I	G142D	V143-	Y144-	Y145-	N211I	L212-		G339D		S371L	S373P	S375F	K417N	N440K	G446S	S477N	T478K	E484A	Q493R	G496S	Q498R	N501Y	Y505H	T547K	D614G	H655Y	N679K	P681H	N764K	D796Y	N856K	Q954H	N969K	L981F			c25000u	
	SARS-CoV-2_human_USA_CA-CDC-FG-L87097_2021	Sin-eBank: OL897116.1	A67V	H69-	V70-	T95I	G142D	V143-	Y144-	Y145-	N211I	L212-		G339D		S371L	S373P	S375F	K417N	N440K	G446S	S477N	T478K	E484A	Q493R	G496S	Q498R	N501Y	Y505H	T547K	D614G	H655Y	N679K	P681H	N764K	D796Y	N856K	Q954H	N969K	L981F			c25000u	
	SARS-CoV-2_human_USA_CA-CDC-FG-L87115_2021	Sin-eBank: OL897119.1	A67V	H69-	V70-	T95I	G142D	V143-	Y144-	Y145-	N211I	L212-		G339D		S371L	S373P	S375F	K417N	N440K	G446S	S477N	T478K	E484A	Q493R	G496S	Q498R	N501Y	Y505H	T547K	D614G	H655Y	N679K	P681H	N764K	D796Y	N856K	Q954H	N969K	L981F			c25000u	
	SARS-CoV-2_human_USA_NY-CDC-FG-L89188_2021	Sin-eBank: OL896964.1	A67V	H69-	V70-	T95I	G142D	V143-	Y144-	Y145-	N211I	L212-		G339D		S371L	S373P	S375F	K417N	N440K	G446S	S477N	T478K	E484A	Q493R	G496S	Q498R	N501Y	Y505H	T547K	D614G	H655Y	N679K	P681H	N764K	D796Y	N856K	Q954H	N969K	L981F			c25000u	
	SARS-CoV-2_human_USA_OR-CDC-LC0470 83 2_022	Sin-eBank: OM3 67976.1	A67V	H69-	V70-	T95I	G142D	V143-	Y144-	Y145-	N211I	L212-	215ins_EPE																														
	SARS-CoV-2_human_USA_CA-LC047 5895_2022	Sin-eBank: OM5 61779.1	A67V	H69-	V70-	T95I	G142D	V143-	Y144-	Y145-	N211I	L212-	215ins_EPE	G339D		S371L	S373P	S375F	K417N	N440K	G446S	S477N	T478K	E484A	Q493R	G496S	Q498R	N501Y	Y505H	T547K	D614G	H655Y	N679K	P681H	N764K	D796Y	N856K	Q954H	N969K	L981F			c25000u	
	SARS-CoV-2_human_USA_ID-CDC-LC0481 844_2022	Sin-eBank: OM4 09228.1	A67V	H69-	V70-	T95I	G142D	V143-	Y144-	Y145-	N211I	L212-	215ins_EPE			S371L	S373P	S375F	K417N	N440K	G446S	S477N	T478K	E484A	Q493R	G496S	Q498R	N501Y	Y505H	T547K	D614G	H655Y	N679K	P681H	N764K	D796Y	N856K	Q954H	N969K	L981F		c21595u	c25000u	
	SARS-CoV-2_human_USA_MI-CDC-ASC21093 7972_2022	Sin-eBank: OM3 98816.1	A67V	H69-	V70-	T95I	G142D	V143-	Y144-	Y145-	N211I	L212-	215ins_EPE			S371L	S373P	S375F	K417N	N440K	G446S	S477N	T478K	E484A	Q493R	G496S	Q498R	N501Y	Y505H	T547K	D614G	H655Y	N679K	P681H	N764K	D796Y	N856K	Q954H	N969K	L981F		c21595u	c25000u	
	SARS-CoV-2_human_USA_KY-CDC-ASC21061 3441_2021	Sin-eBank: OM0 96688.1	A67V	H69-	V70-	T95I	G142D	V143-	Y144-	Y145-	N211I	L212-	215ins_EPE																														
	SARS-CoV-2_human_USA_CA-CDC-LC0463 29 2_021	Sin-eBank: OM0 75886.1	A67V	H69-	V70-	T95I	G142D	V143-	Y144-	Y145-	N211I	L212-	215ins_EPE	G339D			S373P	S375F	K417N	N440K	G446S	S477N	T478K	E484A	Q493R	G496S	Q498R	N501Y	Y505H	T547K	D614G	H655Y	N679K	P681H	N764K	D796Y	N856K	Q954H	N969K	L981F			c25000u	
	SARS-CoV-2_human_USA_CA-CDC-LC0463 31 2_021	Sin-eBank: OM0 75892.1	A67V	H69-	V70-	T95I	G142D	V143-	Y144-	Y145-	N211I	L212-	215ins_EPE	G339D			S373P	S375F	K417N	N440K	G446S	S477N	T478K	E484A	Q493R	G496S	Q498R	N501Y	Y505H	T547K	D614G	H655Y	N679K	P681H	N764K	D796Y	N856K	Q954H	N969K	L981F			c25000u	
	SARS-CoV-2_human_USA_DC-CDC-LC04 40324_2021	Sin-eBank: OM1 22677.1	A67V	H69-	V70-	T95I	G142D	V143-	Y144-	Y145-	N211I	L212-	215ins_EPE	G339D			S373P	S375F	K417N	N440K	G446S	S477N	T478K	E484A	Q493R	G496S	Q498R	N501Y	Y505H	T547K	D614G	H655Y	N679K	P681H	N764K	D796Y	N856K	Q954H	N969K	L981F			c25000u	
	SARS-CoV-2_human_USA_NY-CDC-LC0440381 5_2021	Sin-eBank: OM1 21681.1	A67V	H69-	V70-	T95I	G142D	V143-	Y144-	Y145-	N211I	L212-	215ins_EPE	G339D			S373P	S375F	K417N	N440K	G446S	S477N	T478K	E484A	Q493R	G496S	Q498R	N501Y	Y505H	T547K	D614G	H655Y	N679K	P681H	N764K	D796Y	N856K	Q954H	N969K	L981F			c25000u	
	SARS-CoV-2_human_USA_CA-CDC-LC0463 34 2_021	Sin-eBank: OM2 24892.1	A67V	H69-	V70-	T95I	G142D	V143-	Y144-	Y145-	N211I	L212-	215ins_EPE	G339D			S373P	S375F	K417N	N440K	G446S	S477N	T478K	E484A	Q493R	G496S	Q498R	N501Y	Y505H	T547K	D614G	H655Y	N679K	P681H	N764K	D796Y	N856K	Q954H	N969K	L981F			c25000u	
	SARS-CoV-2_human_USA_NY-PV67373_2022	Sin-eBank: ON2 46090.1	A67V	H69-	V70-	T95I	G142D	V143-	Y144-	Y145-	N211I	L212-	215ins_EPE	G339D		S371L		S375F	K417N	N440K	G446S	S477N	T478K	E484A	Q493R	G496S	Q498R	N501Y	Y505H	T547K	D614G	H655Y	N679K	P681H	N764K	D796Y	N856K	Q954H	N969K	L981F	Q309X			
	SARS-CoV-2_human_USA_CO-CDC-MMB1435 3060_2022	Sin-eBank: OM9 31599.1	A67V	H69-	V70-	T95I	G142D	V143-	Y144-	Y145-	N211I	L212-	215ins_EPE	G339D		S371L	S373P		K417N	N440K	G446S	S477N	T478K	E484A	Q493R	G496S	Q498R	N501Y	Y505H	T547K	D614G	H655Y	N679K	P681H	N764K	D796Y	N856K	Q954H	N969K	L981F			c25000u	
	SARS-CoV-2_human_USA_PA-CDC-MMB1436 0214_2022	Sin-eBank: OM9 94973.1	A67V	H69-	V70-	T95I	G142D	V143-	Y144-	Y145-	N211I	L212-	215ins_EPE	G339D		S371L	S373P		K417N	N440K	G446S	S477N	T478K	E484A	Q493R	G496S	Q498R	N501Y	Y505H	T547K	D614G	H655Y	N679K	P681H	N764K	D796Y	N856K	Q954H	N969K	L981F			c25000u	
	SARS-CoV-2_human_USA_NC-CDC-MMB1418 5004_2022	Sin-eBank: OM9 09519.1	A67V	H69-	V70-	T95I	G142D	V143-	Y144-	Y145-	N211I	L212-	215ins_EPE	G339D		S371L	S373P		K417N	N440K	G446S	S477N	T478K	E484A	Q493R	G496S	Q498R	N501Y	Y505H	T547K	D614G	H655Y	N679K	P681H	N764K	D796Y	N856K	Q954H	N969K	L981F			c25000u	
	SARS-CoV-2_human_USA_CO-CDC-MMB1423 0000_2022	Sin-eBank: OM9 06587.1	A67V	H69-	V70-	T95I	G142D	V143-	Y144-	Y145-	N211I	L212-	215ins_EPE	G339D		S371L	S373P		K417N	N440K	G446S	S477N	T478K	E484A	Q493R	G496S	Q498R	N501Y	Y505H	T547K	D614G	H655Y	N679K	P681H	N764K	D796Y	N856K	Q954H	N969K	L981F			c25000u	
	SARS-CoV-2_human_USA_FL-CDC-STM-SPHP19843_20.22	Sin-eBank: OM4 64770.1	A67V	H69-	V70-	T95I	G142D	V143-	Y144-	Y145-	N211I	L212-	215ins_EPE	G339D		S371L	S373P		K417N	N440K	G446S	S477N	T478K	E484A	Q493R	G496S	Q498R	N501Y	Y505H	T547K	D614G	H655Y	N679K	P681H	N764K	D796Y	N856K	Q954H	N969K	L981F			c25000u	
	SARS-CoV-2_human_USA_IL-CDC-IDCC2103 4027_202 1	Sin-eBank: OM0 159991	A67V	H69-	V70-	T95I	G142D	V143-	Y144-	Y145-	N211I	L212-	215ins_EPE	G339D		S371L	S373P	S375F		N440K	G446S	S477N	T478K	E484A	Q493R	G496S	Q498R	N501Y	Y505H	T547K	D614G	H655Y	N679K	P681H	N764K	D796Y	N856K	Q954H	N969K	L981F			c25000u	
	SARS-CoV-2_human_USA_IL-CDC-IDCC2103 4081_202 1	Sin-eBank: OM0 159561	A67V	H69-	V70-	T95I	G142D	V143-	Y144-	Y145-	N211I	L212-	215ins_EPE	G339D		S371L	S373P	S375F		N440K	G446S	S477N	T478K	E484A	Q493R	G496S	Q498R	N501Y	Y505H	T547K	D614G	H655Y	N679K	P681H	N764K	D796Y	N856K	Q954H	N969K	L981F			c25000u	
	SARS-CoV-2_human_USA_CA-CDC-LC0463 33 2_021	Sin-eBank: OM0 159191	A67V	H69-	V70-	T95I	G142D	V143-	Y144-	Y145-	N211I	L212-	215ins_EPE	G339D		S371L	S373P	S375F		N440K	G446S	S477N	T478K	E484A	Q493R	G496S	Q498R	N501Y	Y505H	T547K	D614G	H655Y	N679K	P681H	N764K	D796Y	N856K	Q954H	N969K	L981F			c25000u	
	SARS-CoV-2_human_USA_MA-CDC-ASC2105 295_2021	Sin-eBank: OM0 163291	A67V	H69-	V70-	T95I	G142D	V143-	Y144-	Y145-	N211I	L212-	215ins_EPE	G339D		S371L	S373P	S375F		N440K	G446S	S477N	T478K	E484A	Q493R	G496S	Q498R	N501Y	Y505H	T547K	D614G	H655Y	N679K	P681H	N764K	D796Y	N856K	Q954H	N969K	L981F			c25000u	
	SARS-CoV-2_human_USA_MD-CDC-ASC2107 654292_202 1	Sin-eBank: OL 858801.1	A67V	H69-	V70-	T95I	G142D	V143-	Y144-	Y145-	N211I	L212-	215ins_EPE	G339D		S371L	S373P	S375F		N440K	G446S	S477N	T478K	E484A	Q493R	G496S	Q498R	N501Y	Y505H	T547K	D614G	H655Y	N679K	P681H	N764K	D796Y	N856K	Q954H	N969K	L981F			c25000u	
	SARS-CoV-2_human_USA_TX-CDC-ASC2 10629031 6_021	Sin-eBank: OL 898801.1	A67V	H69-	V70-	T95I	G142D	V143-	Y144-	Y145-	N211I	L212-	215ins_EPE	G339D		S371L	S373P	S375F	K417N		G446S	S477N	T478K	E484A	Q493R	G496S	Q498R	N501Y	Y505H	T547K	D614G	H655Y	N679K	P681H	N764K	D796Y	N856K	Q954H	N969K	L981F			c25000u	
	SARS-CoV-2_human_USA_IL-CDC-IDCC2103 5985_202 1	Sin-eBank: OM0 169371	A67V	H69-	V70-	T95I	G142D	V143-	Y144-	Y145-	N211I	L212-	215ins_EPE	G339D		S371L	S373P	S375F	K417N		G446S	S477N	T478K	E484A	Q493R	G496S	Q498R	N501Y	Y505H	T547K	D614G	H655Y	N679K	P681H	N764K	D796Y	N856K	Q954H	N969K	L981F			c25000u	
	SARS-CoV-2_human_USA_AZ-CDC-ASC2 10539359 4_021	Sin-eBank: OM0 161861	A67V	H69-	V70-	T95I	G142D	V143-	Y144-	Y145-	N211I	L212-	215ins_EPE	G339D		S371L	S373P	S375F	K417N		G446S	S477N	T478K	E484A	Q493R	G496S	Q498R	N501Y	Y505H	T547K	D614G	H655Y	N679K	P681H	N764K	D796Y	N856K	Q954H	N969K	L981F			c25000u	
	SARS-CoV-2_human_USA_AZ-CDC-ASC2 10539376 2_021	Sin-eBank: OM0 305491	A67V	H69-	V70-	T95I	G142D	V143-	Y144-	Y145-	N211I	L212-	215ins_EPE	G339D		S371L	S373P	S375F	K417N		G446S	S477N	T478K	E484A	Q493R	G496S	Q498R	N501Y	Y505H	T547K	D614G	H655Y	N679K	P681H	N764K	D796Y	N856K	Q954H	N969K	L981F			c25000u	
	SARS-CoV-2_human_USA_PA-CDC-ASC2 10626011 0_021	Sin-eBank: OM0 511711	A67V	H69-	V70-	T95I	G142D	V143-	Y144-	Y145-	N211I	L212-	215ins_EPE	G339D		S371L	S373P	S375F	K417N		G446S	S477N	T478K	E484A	Q493R	G496S	Q498R	N501Y	Y505H	T547K	D614G	H655Y	N679K	P681H	N764K	D796Y	N856K	Q954H	N969K	L981F			c25000u	
	SARS-CoV-2_human_USA_TX-CDC-ASC2 10613812 2_021	Sin-eBank: OM0 253491	A67V	H69-	V70-	T95I	G142D	V143-	Y144-	Y145-	N211I	L212-	215ins_EPE	G339D		S371L	S373P	S375F	K417N	N440K		S477N	T478K	E484A	Q493R	G496S	Q498R	N501Y	Y505H	T547K	D614G	H655Y	N679K	P681H	N764K	D796Y	N856K	Q954H	N969K	L981F			c25000u	
	SARS-CoV-2_human_USA_FL-CDC-ASC21062 9571_2021	Sin-eBank: OM0 791151	A67V	H69-	V70-	T95I	G142D	V143-	Y144-	Y145-	N211I	L212-	215ins_EPE	G339D		S371L	S373P	S375F	K417N	N440K		S477N	T478K	E484A	Q493R	G496S	Q498R	N501Y	Y505H	T547K	D614G	H655Y	N679K	P681H	N764K	D796Y	N856K	Q954H	N969K	L981F			c25000u	
	SARS-CoV-2_human_USA_IL-CDC-IDCC2103 6183_202 1	Sin-eBank: OM0 991991	A67V	H69-	V70-	T95I	G142D	V143-	Y144-	Y145-	N211I	L212-	215ins_EPE	G339D		S371L	S373P	S375F	K417N	N440K		S477N	T478K	E484A	Q493R	G496S	Q498R	N501Y	Y505H	T547K	D614G	H655Y	N679K	P681H	N764K	D796Y	N856K	Q954H	N969K	L981F			c25000u	
	SARS-CoV-2_human_USA_IL-CDC-IDCC2103 6770_202 1	Sin-eBank: OM1 34485.1	A67V	H69-	V70-	T95I	G142D	V143-	Y144-	Y145-	N211I	L212-	215ins_EPE	G339D		S371L	S373P	S375F	K417N	N440K		S477N	T478K	E484A	Q493R	G496S	Q498R	N501Y	Y505H	T547K	D614G	H655Y	N679K	P681H	N764K	D796Y	N856K	Q954H	N969K	L981F			c25000u	
	SARS-CoV-2_human_USA_NJ-CDC-ASC2 10639907 2_021	Sin-eBank: OM0 987961	A67V	H69-	V70-	T95I	G142D	V143-	Y144-	Y145-	N211I	L212-	215ins_EPE	G339D		S371L	S373P	S375F	K417N			S477N	T478K	E484A	Q493R	G496S	Q498R	N501Y	Y505H	T547K	D614G	H655Y	N679K	P681H	N764K	D796Y	N856K	Q954H	N969K	L981F			c25000u	
	SARS-CoV-2_human_USA_CA-CDPH-200 0061727_20.22	Sin-eBank: ON6 18279.1	A67V	H69-	V70-	T95I	G142D	V143-	Y144-	Y145-	N211I	L212-	215ins_EPE	G339D		S371L	S373P	S375F	K417N	N440K	G446S		T478K	E484A	Q493R	G496S	Q498R	N501Y	Y505H	T547K	D614G	H655Y	N679K	P681H	N764K	D796Y	N856K	Q954H	N969K	L981F			c25000u	
	SARS-CoV-2_human_USA_CA-CDPH-200 0061113_20.22	Sin-eBank: ON6 13939.1	A67V	H69-	V70-	T95I	G142D	V143-	Y144-	Y145-	N211I	L212-	215ins_EPE	G339D		S371L	S373P	S375F	K417N	N440K	G446S		T478K	E484A	Q493R	G496S	Q498R	N501Y	Y505H	T547K	D614G	H655Y	N679K	P681H	N764K	D796Y	N856K	Q954H	N969K	L981F			c25000u	
BA.1	SARS-CoV-2_human_USA_NY-CDC-LC0511181 1_2022	Sin-eBank: OM6 27701.1

Fig. 2 B

Variant	Definition	GenBank Accession No.	deletion[1]				deletion[2]				deletion[3]		insertion[4]	Non-synonymous																										Synonymous		
														Receptor-binding domain (RBD) 319 – 541																												
			A67V	H69-	V70-	T95I	G142D	V143-	Y144-	Y145-	N211I	L212-	215ins_EPE	G339D	R346K	S371L	S373P	S375F	K417N	N440K	G446S	S477N	T478K	E484A	Q493R	G496S	Q498R	N501Y	Y505H	T547K	D614G	H655Y	N679K	P681H	N764K	D796Y	N856K	Q954H	N969K	L981F	Others	c21595u	c25000u	Others
	SARS-CoV-2_human_PR_PR-UPRBP-54 77_2022_sq-s	Genalice's: ON695513.2		H69-	V70-	T95I	G142D	V143-	Y144-	Y145-	N211I	L212I	215ins_EPE	G339D	R346K	S371L	S373P	S375F	K417N	N440K	G446S	S477N	T478K	E484A	Q493R	G496S	Q498R	N501Y	Y505H	T547K	D614G	H655Y	N679K	P681H	N764K	D796Y	N856K	Q954H	N969K	L981F		c21595u	c25000u	
	SARS-CoV-2_human_USA_CO-CDC-MMB1140 85852_20 22.csv	Genalice's: ON969098.1		H69-	V70-	T95I	G142D	V143-	Y144-	Y145-	N211I	L212I	215ins_EPE	G339D	R346K	S371L	S373P	S375F	K417N	N440K	G446S	S477N	T478K	E484A	Q493R	G496S	Q498R	N501Y	Y505H	T547K	D614G	H655Y	N679K	P681H	N764K	D796Y	N856K	Q954H	N969K	L981F		c21595u	c25000u	
	SARS-CoV-2_human_USA_MI-CDC-IS CD1059282_20 22.csv	Genalice's: OM816934.1		H69-	V70-	T95I	G142D	V143-	Y144-	Y145-	N211I	L212I	215ins_EPE	G339D	R346K	S371L	S373P	S375F	K417N	N440K	G446S	S477N	T478K	E484A	Q493R	G496S	Q498R	N501Y	Y505H	T547K	D614G	H655Y	N679K	P681H	N764K	D796Y	N856K	Q954H	N969K	L981F		c21595u	c25000u	
	SARS-CoV-2_human_USA_TX-CDC-ASC2 1084870_20 22_sq-s	Genalice's: ON235495.2.1				T95I	G142D	V143-	Y144-	Y145-	N211I	L212I	215ins_EPE	G339D	R346K	S371L	S373P	S375F	K417N	N440K	G446S	S477N	T478K	E484A	Q493R	G496S	Q498R	N501Y	Y505H	T547K	D614G	H655Y	N679K	P681H	N764K	D796Y	N856K	Q954H	N969K	L981F		c21595u	c25000u	
	SARS-CoV-2_human_USA_VA-CDC-2-10715 11 2_022_sq-s	Genalice's: ON233414.1				T95I	G142D	V143-	Y144-	Y145-	N211I	L212I	215ins_EPE	G339D	R346K	S371L	S373P	S375F	K417N	N440K	G446S	S477N	T478K	E484A	Q493R	G496S	Q498R	N501Y	Y505H	T547K	D614G	H655Y	N679K	P681H	N764K	D796Y	N856K	Q954H	N969K	L981F			c25000u	
	SARS-CoV-2_human_JPN_Hiro C31Tc_202 2.seq	Genalice's: OP024182.1	A67V			T95I	G142D	V143-	Y144-	Y145-	N211I	L212I	215ins_EPE	G339D	R346K	S371L	S373P	S375F	K417N	N440K	G446S	S477N	T478K	E484A	Q493R	G496S	Q498R	N501Y	Y505H	T547K	D614G	H655Y	N679K	P681H	N764K	D796Y	N856K	Q954H	N969K	L981F			c25000u	
	SARS-CoV-2_human_JPN_Hiro PrO2 Tc_2022_sq-s	Genalice's: OP019732.1	A67V			T95I	G142D	V143-	Y144-	Y145-	N211I	L212I	215ins_EPE	G339D	R346K	S371L	S373P	S375F	K417N	N440K	G446S	S477N	T478K	E484A	Q493R	G496S	Q498R	N501Y	Y505H	T547K	D614G	H655Y	N679K	P681H	N764K	D796Y	N856K	Q954H	N969K	L981F			c25000u	
	SARS-CoV-2_human_USA FL-CDC-STM-0 9QQPH1P1_20 22.csv	Genalice's: MW359478.1	A67V			T95I	G142D	V143-	Y144-	Y145-	N211I	L212I	215ins_EPE	G339D	R346K	S371L	S373P	S375F	K417N	N440K	G446S	S477N	T478K	E484A	Q493R	G496S	Q498R	N501Y	Y505H	T547K	D614G	H655Y	N679K	P681H	N764K	D796Y	N856K	Q954H	N969K	L981F		c21595u	c25000u	
	SARS-CoV-2_human_USA VA-CDC-ASC2 1063491 57_2021_sq-s	Genalice's: OM999080.1	A67V	H69-	V70-		G142D	V143-	Y144-	Y145-	N211I	L212-	215ins_EPE	G339D	R346K	S371L	S373P	S375F	K417N	N440K	G446S	S477N	T478K	E484A	Q493R	G496S	Q498R	N501Y	Y505H	T547K	D614G	H655Y	N679K	P681H	N764K	D796Y	N856K	Q954H	N969K	L981F			c25000u	
	SARS-CoV-2_human_USA FL-CDC-IS CD1057222_20 21.csv	Genalice's: OM297301.1	A67V	H69-	V70-		G142D	V143-	Y144-	Y145-	N211I	L212-	215ins_EPE	G339D	R346K	S371L	S373P	S375F	K417N	N440K	G446S	S477N	T478K	E484A	Q493R	G496S	Q498R	N501Y	Y505H	T547K	D614G	H655Y	N679K	P681H	N764K	D796Y	N856K	Q954H	N969K	L981F		c21595u	c25000u	
	SARS-CoV-2_human_USA FL-CDC-IS CD1019700_20 21.csv	Genalice's: MW297438.1	A67V	H69-	V70-		G142D	V143-	Y144-	Y145-	N211I	L212-	215ins_EPE	G339D	R346K	S371L	S373P	S375F	K417N	N440K	G446S	S477N	T478K	E484A	Q493R	G496S	Q498R	N501Y	Y505H	T547K	D614G	H655Y	N679K	P681H	N764K	D796Y	N856K	Q954H	N969K	L981F			c25000u	
	SARS-CoV-2_human_USA MA-CDC-AS CD1059 5947_202 2.csv	Genalice's: OM395398.1	A67V	H69-	V70-		G142D	V143-	Y144-	Y145-	N211I	L212-	215ins_EPE	G339D	R346K	S371L	S373P	S375F	K417N	N440K	G446S	S477N	T478K	E484A	Q493R	G496S	Q498R	N501Y	Y505H	T547K	D614G	H655Y	N679K	P681H	N764K	D796Y	N856K	Q954H	N969K	L981F			c25000u	
	SARS-CoV-2_human_USA PR-CDC-IS CD1056 56_202 2.csv	Genalice's: OM395399.1	A67V	H69-	V70-		G142D	V143-	Y144-	Y145-	N211I	L212-	215ins_EPE	G339D	R346K	S371L	S373P	S375F	K417N	N440K	G446S	S477N	T478K	E484A	Q493R	G496S	Q498R	N501Y	Y505H	T547K	D614G	H655Y	N679K	P681H	N764K	D796Y	N856K	Q954H	N969K	L981F		c21595u	c25000u	
	SARS-CoV-2_human_USA FL-CDC-IS CD1029303_20 21.csv	Genalice's: MW078863.1	A67V	H69-	V70-	T95I					N211I	L212-	215ins_EPE	G339D	R346K	S371L	S373P	S375F	K417N	N440K	G446S	S477N	T478K	E484A	Q493R	G496S	Q498R	N501Y	Y505H	T547K	D614G	H655Y	N679K	P681H	N764K	D796Y	N856K	Q954H	N969K	L981F		c21595u	c25000u	
	SARS-CoV-2_human_USA GA-CDC-IS CD1063095_20 21.csv	Genalice's: MW096959.1	A67V	H69-	V70-	T95I					N211I	L212-	215ins_EPE	G339D	R346K	S371L	S373P	S375F	K417N	N440K	G446S	S477N	T478K	E484A	Q493R	G496S	Q498R	N501Y	Y505H	T547K	D614G	H655Y	N679K	P681H	N764K	D796Y	N856K	Q954H	N969K	L981F			c25000u	
	SARS-CoV-2_human_USA GA-CDC-IS CD1059 35844_20 21.csv	Genalice's: MW117135.1	A67V	H69-	V70-	T95I					N211I	L212-	215ins_EPE	G339D	R346K	S371L	S373P	S375F	K417N	N440K	G446S	S477N	T478K	E484A	Q493R	G496S	Q498R	N501Y	Y505H	T547K	D614G	H655Y	N679K	P681H	N764K	D796Y	N856K	Q954H	N969K	L981F			c25000u	
	SARS-CoV-2_human_USA TN-CDC-IS CD1063 32163_20 21.csv	Genalice's: MW133880.1	A67V	H69-	V70-	T95I					N211I	L212-	215ins_EPE	G339D	R346K	S371L	S373P	S375F	K417N	N440K	G446S	S477N	T478K	E484A	Q493R	G496S	Q498R	N501Y	Y505H	T547K	D614G	H655Y	N679K	P681H	N764K	D796Y	N856K	Q954H	N969K	L981F		c21595u	c25000u	
	SARS-CoV-2_human_USA PA-CDC-ASC2 1063312_20 21_sq-s	Genalice's: MW077358.1	A67V	H69-	V70-	T95I					N211I	L212-	215ins_EPE	G339D	R346K	S371L	S373P	S375F	K417N	N440K	G446S	S477N	T478K	E484A	Q493R	G496S	Q498R	N501Y	Y505H	T547K	D614G	H655Y	N679K	P681H	N764K	D796Y	N856K	Q954H	N969K	L981F			c25000u	
	SARS-CoV-2_human_USA FL-CDC-STM-A TMA19YUZ_2 022.seq	Genalice's: MW370205.1	A67V	H69-	V70-	T95I	G142D	V143-	Y144-	Y145-			215ins_EPE	G339D	R346K	S371L	S373P	S375F	K417N	N440K	G446S	S477N	T478K	E484A	Q493R	G496S	Q498R	N501Y	Y505H	T547K	D614G	H655Y	N679K	P681H	N764K	D796Y	N856K	Q954H	N969K	L981F			c25000u	c2 28979u
	SARS-CoV-2_human_USA IL-CDC-IS CD1060549 7_2022.seq	Genalice's: MW370362.1	A67V	H69-	V70-	T95I	G142D	V143-	Y144-	Y145-			215ins_EPE	G339D	R346K	S371L	S373P	S375F	K417N	N440K	G446S	S477N	T478K	E484A	Q493R	G496S	Q498R	N501Y	Y505H	T547K	D614G	H655Y	N679K	P681H	N764K	D796Y	N856K	Q954H	N969K	L981F			c25000u	
	SARS-CoV-2_human_USA WA-UW-22 01300 5884_2022.seq	Genalice's: MW897488.1	A67V	H69-	V70-	T95I	G142D	V143-	Y144-	Y145-			215ins_EPE	G339D	R346K	S371L	S373P	S375F	K417N	N440K	G446S	S477N	T478K	E484A	Q493R	G496S	Q498R	N501Y	Y505H	T547K	D614G	H655Y	N679K	P681H	N764K	D796Y	N856K	Q954H	N969K	L981F		c21595u	c25000u	
	SARS-CoV-2_human_USA KY-GD_02501 1_2021_sq-s	Genalice's: MW818659.1	A67V	H69-	V70-	T95I	G142D	V143-	Y144-	Y145-			215ins_EPE	G339D	R346K	S371L	S373P	S375F	K417N	N440K	G446S	S477N	T478K	E484A	Q493R	G496S	Q498R	N501Y	Y505H	T547K	D614G	H655Y	N679K	P681H	N764K	D796Y	N856K	Q954H	N969K	L981F		c21595u	c25000u	
	SARS-CoV-2_human_USA KY-GD_02804 0_2021_sq-s	Genalice's: MW818479.1	A67V	H69-	V70-	T95I	G142D	V143-	Y144-	Y145-			215ins_EPE	G339D	R346K	S371L	S373P	S375F	K417N	N440K	G446S	S477N	T478K	E484A	Q493R	G496S	Q498R	N501Y	Y505H	T547K	D614G	H655Y	N679K	P681H	N764K	D796Y	N856K	Q954H	N969K	L981F		c21595u	c25000u	
	SARS-CoV-2_human_USA CA-CDC-FG-187869_20 21.csv	Genalice's: OL897111.5	A67V	H69-	V70-	T95I	G142D	V143-	Y144-	Y145-	N211I	L212-		G339D	R346K	S371L	S373P	S375F	K417N	N440K	G446S	S477N	T478K	E484A	Q493R	G496S	Q498R	N501Y	Y505H	T547K	D614G	H655Y	N679K	P681H	N764K	D796Y	N856K	Q954H	N969K	L981F			c25000u	
	SARS-CoV-2_human_USA CA-CDC-FG-187876_20 21.csv	Genalice's: OL897114.1	A67V	H69-	V70-	T95I	G142D	V143-	Y144-	Y145-	N211I	L212-		G339D	R346K	S371L	S373P	S375F	K417N	N440K	G446S	S477N	T478K	E484A	Q493R	G496S	Q498R	N501Y	Y505H	T547K	D614G	H655Y	N679K	P681H	N764K	D796Y	N856K	Q954H	N969K	L981F			c25000u	
	SARS-CoV-2_human_USA MY-CDC-FG-192538_20 21.csv	Genalice's: OL986779.1	A67V	H69-	V70-	T95I	G142D	V143-	Y144-	Y145-	N211I	L212-		G339D	R346K	S371L	S373P	S375F	K417N	N440K	G446S	S477N	T478K	E484A	Q493R	G496S	Q498R	N501Y	Y505H	T547K	D614G	H655Y	N679K	P681H	N764K	D796Y	N856K	Q954H	N969K	L981F		c21595u	c25000u	
	SARS-CoV-2_human_USA FL-CDC-FG-192542_2 021.csv	Genalice's: OL986691.1	A67V	H69-	V70-	T95I	G142D	V143-	Y144-	Y145-	N211I	L212-		G339D	R346K	S371L	S373P	S375F	K417N	N440K	G446S	S477N	T478K	E484A	Q493R	G496S	Q498R	N501Y	Y505H	T547K	D614G	H655Y	N679K	P681H	N764K	D796Y	N856K	Q954H	N969K	L981F		c21595u	c25000u	
	SARS-CoV-2_human_USA CA-CDC-FG-192600_20 21.csv	Genalice's: OL897048.1	A67V	H69-	V70-	T95I	G142D	V143-	Y144-	Y145-	N211I	L212-		G339D	R346K	S371L	S373P	S375F	K417N	N440K	G446S	S477N	T478K	E484A	Q493R	G496S	Q498R	N501Y	Y505H	T547K	D614G	H655Y	N679K	P681H	N764K	D796Y	N856K	Q954H	N969K	L981F		c21595u	c25000u	
	SARS-CoV-2_human_USA B0114 244_2022.seq	Genalice's: ON831866.1	A67V	H69-	V70-	T95I	G142D	V143-	Y144-	Y145-	N211I	L212-	215ins_EPE	G339D	R346K	S371L	S373P	S375F	K417N	N440K	G446S	S477N	T478K	E484A	Q493R	G496S	Q498R	N501Y	Y505H	T547K	D614G	H655Y	N679K	P681H	N764K	D796Y	N856K	Q954H	N969K	L981F		c21595u	c25000u	
	SARS-CoV-2_human_USA B0114 881_2022.seq	Genalice's: MW849099.1	A67V	H69-	V70-	T95I	G142D	V143-	Y144-	Y145-	N211I	L212-	215ins_EPE	G339D	R346K	S371L	S373P	S375F	K417N	N440K	G446S	S477N	T478K	E484A	Q493R	G496S	Q498R	N501Y	Y505H	T547K	D614G	H655Y	N679K	P681H	N764K	D796Y	N856K	Q954H	N969K	L981F		c21595u	c25000u	
	SARS-CoV-2_human_USA B0117 78_2022.seq	Genalice's: ON883898.1	A67V	H69-	V70-	T95I	G142D	V143-	Y144-	Y145-	N211I	L212-	215ins_EPE	G339D	R346K	S371L	S373P	S375F	K417N	N440K	G446S	S477N	T478K	E484A	Q493R	G496S	Q498R	N501Y	Y505H	T547K	D614G	H655Y	N679K	P681H	N764K	D796Y	N856K	Q954H	N969K	L981F			c25000u	c2 28979u
	SARS-CoV-2_human_USA B0117 088_2021_sq-s	Genalice's: OP419925.1	A67V	H69-	V70-	T95I	G142D	V143-	Y144-	Y145-	N211I	L212-	215ins_EPE	G339D	R346K	S371L	S373P	S375F	K417N	N440K	G446S	S477N	T478K	E484A	Q493R	G496S	Q498R	N501Y	Y505H	T547K	D614G	H655Y	N679K	P681H	N764K	D796Y	N856K	Q954H	N969K	L981F		c21595u	c25000u	
	SARS-CoV-2_human_USA VA-CDC-IS CD1012 7_2022.seq	Genalice's: MW101672.1	A67V	H69-	V70-	T95I	G142D	V143-	Y144-	Y145-	N211I	L212-	215ins_EPE	G339D	R346K	S371L	S373P	S375F	K417N	N440K	G446S	S477N	T478K	E484A	Q493R	G496S	Q498R	N501Y	Y505H	T547K	D614G	H655Y	N679K	P681H	N764K	D796Y	N856K	Q954H	N969K	L981F		c21595u	c25000u	
	SARS-CoV-2_human_USA DC-C-DC-LC04 31855_20 21.csv	Genalice's: OM043643.1	A67V	H69-	V70-	T95I	G142D	V143-	Y144-	Y145-	N211I	L212-	215ins_EPE	G339D	R346K		S373P	S375F	K417N	N440K	G446S	S477N	T478K	E484A	Q493R	G496S	Q498R	N501Y	Y505H	T547K	D614G	H655Y	N679K	P681H	N764K	D796Y	N856K	Q954H	N969K	L981F			c25000u	c2 28979u
	SARS-CoV-2_human_USA OR-CDC-LC04 6495_2021_sq-s	Genalice's: MW761592.1	A67V	H69-	V70-	T95I	G142D	V143-	Y144-	Y145-	N211I	L212-	215ins_EPE	G339D	R346K		S373P	S375F	K417N	N440K	G446S	S477N	T478K	E484A	Q493R	G496S	Q498R	N501Y	Y505H	T547K	D614G	H655Y	N679K	P681H	N764K	D796Y	N856K	Q954H	N969K	L981F		c21595u	c25000u	
	SARS-CoV-2_human_USA IL-CDC-LC04 0537_2021_sq-s	Genalice's: MW761593.1	A67V	H69-	V70-	T95I	G142D	V143-	Y144-	Y145-	N211I	L212-	215ins_EPE	G339D	R346K		S373P	S375F	K417N	N440K	G446S	S477N	T478K	E484A	Q493R	G496S	Q498R	N501Y	Y505H	T547K	D614G	H655Y	N679K	P681H	N764K	D796Y	N856K	Q954H	N969K	L981F		c21595u	c25000u	
	SARS-CoV-2_human_USA OR-CDC-LC04 7607_2022.seq	Genalice's: MW343689.1	A67V	H69-	V70-	T95I	G142D	V143-	Y144-	Y145-	N211I	L212-	215ins_EPE	G339D	R346K		S373P	S375F	K417N	N440K	G446S	S477N	T478K	E484A	Q493R	G496S	Q498R	N501Y	Y505H	T547K	D614G	H655Y	N679K	P681H	N764K	D796Y	N856K	Q954H	N969K	L981F		c21595u	c25000u	
	SARS-CoV-2_human_USA UT-UPHL-22 0107941 0242_202 1.csv	Genalice's: MW395527.1	A67V	H69-	V70-	T95I	G142D	V143-	Y144-	Y145-	N211I	L212-	215ins_EPE	G339D	R346K		S373P	S375F	K417N	N440K	G446S	S477N	T478K	E484A	Q493R	G496S	Q498R	N501Y	Y505H	T547K	D614G	H655Y	N679K	P681H	N764K	D796Y	N856K	Q954H	N969K	L981F			c25000u	
	SARS-CoV-2_human_USA FL-CDC-MMB1140 23738_2022.seq	Genalice's: MW847073.1	A67V	H69-	V70-	T95I	G142D	V143-	Y144-	Y145-	N211I	L212-	215ins_EPE	G339D	R346K	S371L	S373P			N440K	G446S	S477N	T478K	E484A	Q493R	G496S	Q498R	N501Y	Y505H	T547K	D614G	H655Y	N679K	P681H	N764K	D796Y	N856K	Q954H	N969K	L981F			c25000u	
	SARS-CoV-2_human_USA CO-CDC-MMB1140 60760_20 22.csv	Genalice's: MW846976.1	A67V	H69-	V70-	T95I	G142D	V143-	Y144-	Y145-	N211I	L212-	215ins_EPE	G339D	R346K	S371L	S373P		K417N	N440K	G446S	S477N	T478K	E484A	Q493R	G496S	Q498R	N501Y	Y505H	T547K	D614G	H655Y	N679K	P681H	N764K	D796Y	N856K	Q954H	N969K	L981F			c25000u	
	SARS-CoV-2_human_USA CO-CDC-MMB1140 67143_20 22.csv	Genalice's: MW822024.1	A67V	H69-	V70-	T95I	G142D	V143-	Y144-	Y145-	N211I	L212-	215ins_EPE	G339D	R346K	S371L	S373P		K417N	N440K	G446S	S477N	T478K	E484A	Q493R	G496S	Q498R	N501Y	Y505H	T547K	D614G	H655Y	N679K	P681H	N764K	D796Y	N856K	Q954H	N969K	L981F		c21595u	c25000u	
	SARS-CoV-2_human_USA FL-CDC-MMB1141 42193_20 22.csv	Genalice's: MW849084.1	A67V	H69-	V70-	T95I	G142D	V143-	Y144-	Y145-	N211I	L212-	215ins_EPE	G339D	R346K	S371L	S373P		K417N	N440K	G446S	S477N	T478K	E484A	Q493R	G496S	Q498R	N501Y	Y505H	T547K	D614G	H655Y	N679K	P681H	N764K	D796Y	N856K	Q954H	N969K	L981F		c21595u	c25000u	
	SARS-CoV-2_human_USA GA-CDC-MMB1141630 98_2022.seq	Genalice's: MW906950.1	A67V	H69-	V70-	T95I	G142D	V143-	Y144-	Y145-	N211I	L212-	215ins_EPE	G339D	R346K	S371L	S373P		K417N	N440K	G446S	S477N	T478K	E484A	Q493R	G496S	Q498R	N501Y	Y505H	T547K	D614G	H655Y	N679K	P681H	N764K	D796Y	N856K	Q954H	N969K	L981F			c25000u	c2 28979u
	SARS-CoV-2_human_USA FL-CDC-IS CD1019933_2 021.csv	Genalice's: MW619933.1	A67V	H69-	V70-	T95I	G142D	V143-	Y144-	Y145-	N211I	L212-	215ins_EPE	G339D	R346K	S371L	S373P	S375F		N440K	G446S	S477N	T478K	E484A	Q493R	G496S	Q498R	N501Y	Y505H	T547K	D614G	H655Y	N679K	P681H	N764K	D796Y	N856K	Q954H	N969K	L981F		c21595u	c25000u	
	SARS-CoV-2_human_USA FL-CDC-ASC2 1053821 63_2021_sq-s	Genalice's: MW618331.1	A67V	H69-	V70-	T95I	G142D	V143-	Y144-	Y145-	N211I	L212-	215ins_EPE	G339D	R346K	S371L	S373P	S375F		N440K	G446S	S477N	T478K	E484A	Q493R	G496S	Q498R	N501Y	Y505H	T547K	D614G	H655Y	N679K	P681H	N764K	D796Y	N856K	Q954H	N969K	L981F			c25000u	
	SARS-CoV-2_human_USA FL-CDC-IS CD1016238_20 21.csv	Genalice's: MW618331.1	A67V	H69-	V70-	T95I	G142D	V143-	Y144-	Y145-	N211I	L212-	215ins_EPE	G339D	R346K	S371L	S373P	S375F		N440K	G446S	S477N	T478K	E484A	Q493R	G496S	Q498R	N501Y	Y505H	T547K	D614G	H655Y	N679K	P681H	N764K	D796Y	N856K	Q954H	N969K	L981F		c21595u	c25000u	
	SARS-CoV-2_human_USA FL-CDC-IS CD1016 24163_20 21.csv	Genalice's: MW835685.1	A67V	H69-	V70-	T95I	G142D	V143-	Y144-	Y145-	N211I	L212-	215ins_EPE	G339D	R346K	S371L	S373P	S375F		N440K	G446S	S477N	T478K	E484A	Q493R	G496S	Q498R	N501Y	Y505H	T547K	D614G	H655Y	N679K	P681H	N764K	D796Y	N856K	Q954H	N969K	L981F		c21595u	c25000u	af 40917u
	SARS-CoV-2_human_USA FL-CDC-22121 1-173_202 1.seq	Genalice's: MW835686.1	A67V	H69-	V70-	T95I	G142D	V143-	Y144-	Y145-	N211I	L212-	215ins_EPE	G339D	R346K	S371L	S373P	S375F		N440K	G446S	S477N	T478K	E484A	Q493R	G496S	Q498R	N501Y	Y505H	T547K	D614G	H655Y	N679K	P681H	N764K	D796Y	N856K	Q954H	N969K	L981F			c25000u	
	SARS-CoV-2_human_USA NC-C-DC-ASC2 1056695 12_2021_sq-s	Genalice's: MW196115.1	A67V	H69-	V70-	T95I	G142D	V143-	Y144-	Y145-	N211I	L212-	215ins_EPE	G339D	R346K	S371L	S373P	S375F			G446S	S477N	T478K	E484A	Q493R	G496S	Q498R	N501Y	Y505H	T547K	D614G	H655Y	N679K	P681H	N764K	D796Y	N856K	Q954H	N969K	L981F		c21595u	c25000u	
	SARS-CoV-2_human_USA OH-CDC-PW-0 04436_20 21.csv	Genalice's: MW196116.1	A67V	H69-	V70-	T95I	G142D	V143-	Y144-	Y145-	N211I	L212-	215ins_EPE	G339D	R346K	S371L	S373P	S375F			G446S	S477N	T478K	E484A	Q493R	G496S	Q498R	N501Y	Y505H	T547K	D614G	H655Y	N679K	P681H	N764K	D796Y	N856K	Q954H	N969K	L981F		c21595u	c25000u	
	SARS-CoV-2_human_USA OH-C-DC-ASC2 1063110 02_2021_sq-s	Genalice's: MW099560.1	A67V	H69-	V70-	T95I	G142D	V143-	Y144-	Y145-	N211I	L212-	215ins_EPE	G339D	R346K	S371L	S373P	S375F			G446S	S477N	T478K	E484A	Q493R	G496S	Q498R	N501Y	Y505H	T547K	D614G	H655Y	N679K	P681H	N764K	D796Y	N856K	Q954H	N969K	L981F		c21595u	c25000u	
	SARS-CoV-2_human_USA NJ-CDC-ASC2 1060 9354_2021_sq-s	Genalice's: MW199268.1	A67V	H69-	V70-	T95I	G142D	V143-	Y144-	Y145-	N211I	L212-	215ins_EPE	G339D	R346K	S371L	S373P	S375F			G446S	S477N	T478K	E484A	Q493R	G496S	Q498R	N501Y	Y505H	T547K	D614G	H655Y	N679K	P681H	N764K	D796Y	N856K	Q954H	N969K	L981F			c25000u	
	SARS-CoV-2_human_USA CO-CDC-STM-A YDAWMB_202 2.csv	Genalice's: MW846988.1	A67V	H69-	V70-	T95I	G142D	V143-	Y144-	Y145-	N211I	L212-	215ins_EPE	G339D	R346K	S371L	S373P	S375F			G446S	S477N	T478K	E484A	Q493R	G496S	Q498R	N501Y	Y505H	T547K	D614G	H655Y	N679K	P681H	N764K	D796Y	N856K	Q954H	N969K	L981F		c21595u	c25000u	
	SARS-CoV-2_human_USA NY-CDC-IS CD1079 2763_20 21.csv	Genalice's: MW079299.1	A67V	H69-	V70-	T95I	G142D	V143-	Y144-	Y145-	N211I	L212-	215ins_EPE	G339D	R346K	S371L	S373P	S375F	K417N	N440K		S477N	T478K	E484A	Q493R	G496S	Q498R	N501Y	Y505H	T547K	D614G	H655Y	N679K	P681H	N764K	D796Y	N856K	Q954H	N969K	L981F		c21595u	c25000u	
	SARS-CoV-2_human_USA IL-CDC-IS CD1063157 6_2021.seq	Genalice's: MW999911.1	A67V	H69-	V70-	T95I	G142D	V143-	Y144-	Y145-	N211I	L212-	215ins_EPE	G339D	R346K	S371L	S373P	S375F	K417N	N440K		S477N	T478K	E484A	Q493R	G496S	Q498R	N501Y	Y505H	T547K	D614G	H655Y	N679K	P681H	N764K	D796Y	N856K	Q954H	N969K	L981F		c21595u	c25000u	
	SARS-CoV-2_human_USA FL-CDC-ASC2 1063232 82_2021_sq-s	Genalice's: MW999912.1	A67V	H69-	V70-	T95I	G142D	V143-	Y144-	Y145-	N211I	L212-	215ins_EPE	G339D	R346K	S371L	S373P	S375F	K417N	N440K		S477N	T478K	E484A	Q493R	G496S	Q498R	N501Y	Y505H	T547K	D614G	H655Y	N679K	P681H	N764K	D796Y	N856K	Q954H	N969K	L981F		c21595u	c25000u	
	SARS-CoV-2_human_USA IL-CDC-IS CD1063521 6_2021.seq	Genalice's: MW097010.1	A67V	H69-	V70-	T95I	G142D	V143-	Y144-	Y145-	N211I	L212-	215ins_EPE	G339D	R346K	S371L	S373P	S375F	K417N	N440K		S477N	T478K	E484A	Q493R	G496S	Q498R	N501Y	Y505H	T547K	D614G	H655Y	N679K	P681H	N764K	D796Y	N856K	Q954H	N969K	L981F		c21595u	c25000u	
	SARS-CoV-2_human_USA PR-CDC-ASC2 1063979 80_2021_sq-s	Genalice's: MW173300.1	A67V	H69-	V70-	T95I	G142D	V143-	Y144-	Y145-	N211I	L212-	215ins_EPE	G339D	R346K	S371L	S373P	S375F	K417N	N440K		S477N	T478K	E484A	Q493R	G496S	Q498R	N501Y	Y505H	T547K	D614G	H655Y	N679K	P681H	N764K	D796Y	N856K	Q954H	N969K	L981F		c21595u	c25000u	
	SARS-CoV-2_human_USA IL-HEM2-5417 1 52006_20 22.csv	Genalice's: MW899061.1	A67V	H69-	V70-	T95I	G142D	V143-	Y144-	Y145-	N211I	L212-	215ins_EPE	G339D	R346K	S371L	S373P	S375F	K417N	N440K	G446S	S477N	T478K	E484A	Q493R	G496S	Q498R	N501Y	Y505H	T547K	D614G	H655Y	N679K	P681H	N764K	D796Y	N856K	Q954H	N969K	L981F			c25000u	
	SARS-CoV-2_human_USA MN-CD-C-HBXI 503827 30538_20 22.csv	Genalice's: OM883290.1	A67V	H69-	V70-	T95I	G142D	V143-	Y144-	Y145-	N211I	L212-	215ins_EPE	G339D	R346K	S371L	S373P	S375F	K417N	N440K	G446S	S477N	T478K	E484A	Q493R	G496S	Q498R	N501Y	Y505H	T547K	D614G	H655Y	N679K	P681H	N764K	D796Y	N856K	Q954H	N969K	L981F			c25000u	
	SARS-CoV-2_human_USA NJ-CDC-IBXI 24291 1012949_2022_sq-s	Genalice's: OM883285.1	A67V	H69-	V70-	T95I	G142D	V143-	Y144-	Y145-	N211I	L212-	215ins_EPE	G339D	R346K	S371L	S373P	S375F	K417N	N440K	G446S	S477N	T478K	E484A	Q493R	G496S	Q498R	N501Y	Y505H	T547K	D614G	H655Y	N679K	P681H	N764K	D796Y	N856K	Q954H	N969K	L981F		c21595u	c25000u	
	SARS-CoV-2_human_USA CA-CDC-CSPH-M 0000014_2022_sq-s	Genalice's: MW191801.1	A67V	H69-	V70-	T95I	G142D	V143-	Y144-	Y145-	N211I	L212-	215ins_EPE	G339D	R346K	S371L	S373P	S375F	K417N	N440K	G446S	S477N	T478K	E484A	Q493R	G496S	Q498R	N501Y	Y505H	T547K	D614G	H655Y	N679K	P681H	N764K	D796Y	N856K	Q954H	N969K	L981F		c21595u	c25000u	c2 38933u
	SARS-CoV-2_human_USA IN-GD-_122821-1-176_20 21.csv	Genalice's: OM846951.1	A67V	H69-	V70-	T95I	G142D	V143-	Y144-	Y145-	N211I	L212-	215ins_EPE	G339D	R346K	S371L	S373P	S375F	K417N	N440K	G446S	S477N	T478K	E484A	Q493R	G496S	Q498R	N501Y	Y505H	T547K	D614G	H655Y	N679K	P681H	N764K	D796Y	N856K	Q954H	N969K	L981F			c25000u	
	SARS-CoV-2_human_USA FL-CDC-STM-VAVNKGUR_2 2022.seq	Genalice's: MW021265.1	A67V	H69-	V70-	T95I	G142D	V143-	Y144-	Y145-	N211I	L212-	215ins_EPE	G339D	R346K	S371L	S373P	S375F	K417N	N440K	G446S	S477N		E484A	Q493R	G496S	Q498R	N501Y	Y505H	T547K	D614G	H655Y	N679K	P681H	N764K	D796Y	N856K	Q954H	N969K	L981F			c25000u	c2 44452u
	SARS-CoV-2_human_USA FL-CDC-STM-VAVNJAMB_202 2.seq	Genalice's: MW021276.1	A67V	H69-	V70-	T95I	G142D	V143-	Y144-	Y145-	N211I	L212-	215ins_EPE	G339D	R346K	S371L	S373P	S375F	K417N	N440K	G446S	S477N		E484A	Q493R	G496S	Q498R	N501Y	Y505H	T547K	D614G	H655Y	N679K	P681H	N764K	D796Y	N856K	Q954H	N969K	L981F			c25000u	c2 44452u
	SARS-CoV-2_human_USA GA-CDC-STM-NCYQTBE8S_2 022.csv	Genalice's: MW959981.1	A67V	H69-	V70-	T95I	G142D	V143-	Y144-	Y145-	N211I	L212-	215ins_EPE	G339D	R346K	S371L	S373P	S375F	K417N	N440K	G446S	S477N	T478K	E484A	Q493R	G496S	Q498R	N501Y	Y505H	T547K	D614G	H655Y	N679K	P681H	N764K	D796Y	N856K	Q954H	N969K	L981F		c21595u	c25000u	
	SARS-CoV-2_human_USA NV-CDC-IS CD1079964_20 22.csv	Genalice's: MW144127.1	A67V	H69-	V70-	T95I	G142D	V143-	Y144-	Y145-	N211I	L212-	215ins_EPE	G339D	R346K	S371L	S373P	S375F	K417N	N440K	G446S	S477N	T478K	E484A	Q493R	G496S	Q498R	N501Y	Y505H	T547K	D614G	H655Y	N679K	P681H	N764K	D796Y	N856K	Q954H	N969K	L981F		c21595u	c25000u	
BA.1.1 -0.1	SARS-CoV-2_human_USA NV-CDC-IS CD1079530_20 22.csv	Genalice's: OR437052.1	A67V	H69-	V70-	T95I	G142D	V143-	Y144-	Y145-	N211I	L212-	215ins_EPE	G339D	R346K	S371L	S373P	S375F	K417N	N440K	G446S	S477N	T478K	E484A	Q493R	G496S	Q498R	N501Y	Y505H	T547K	D614G	H655Y	N679K	P681H	N764K	D796Y	N856K	Q954H	N969K	L981F			c25000u	
	SARS-CoV-2_human_USA FL-CDC-IS CD1056 07745_20 21.csv	Genalice's: MW561641.1	A67V	H69-	V70-	T95I	G142D	V143-	Y144-	Y145-	N211I	L212-	215ins_EPE	G339D	R346K	S371L	S373P	S375F	K417N	N440K		S477N	T478K	

Fig. 3

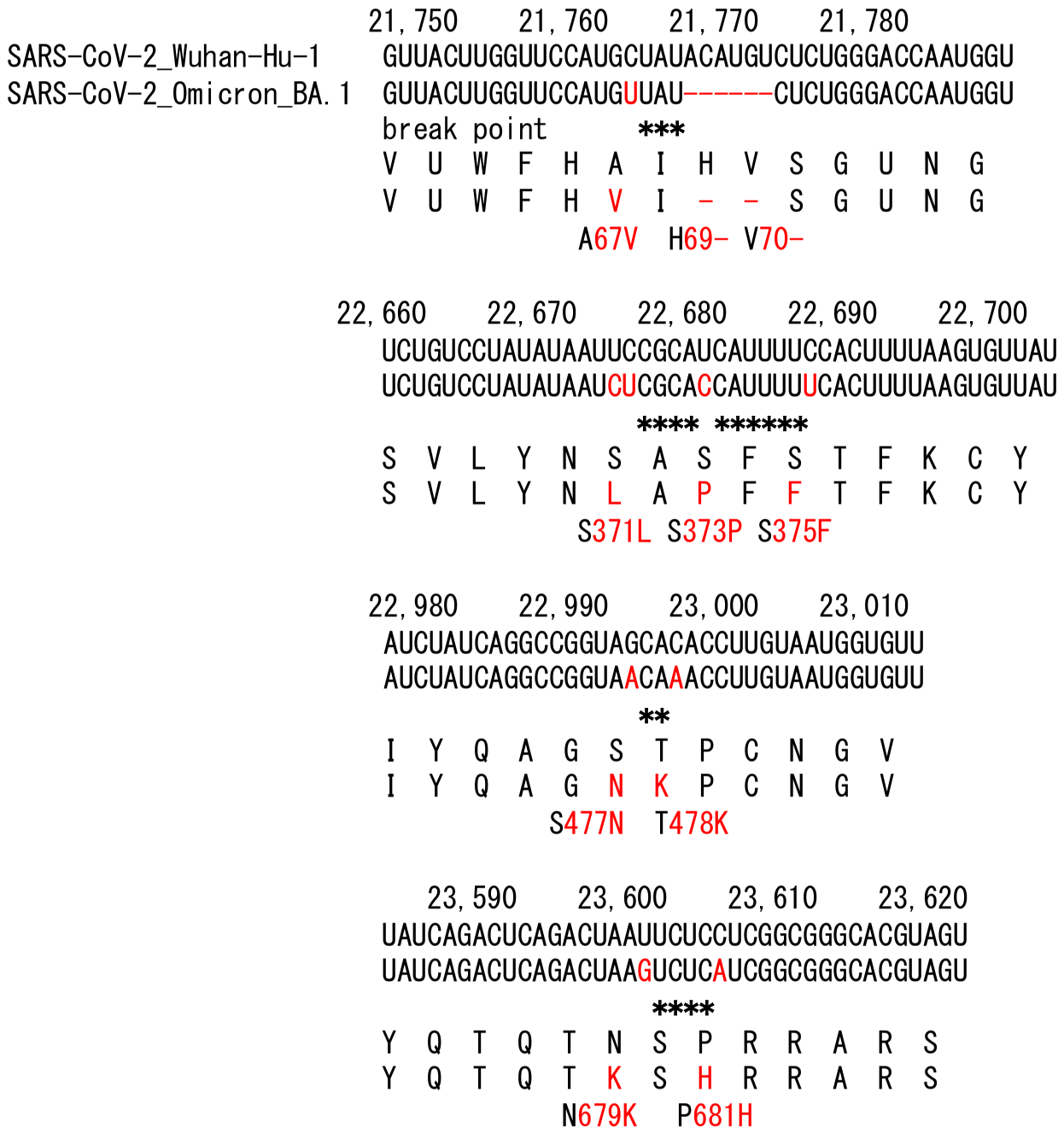
21,750 21,760 21,770 21,780
SARS-CoV-2_Wuhan-Hu-1 GUUACUUGGUUCCAUGCUAUACAUGUCUCUGGGACCAAUGGU
SARS-CoV-2_Omicron_BA.1 GUUACUUGGUUCCAUGUUAU------CUCUGGGACCAAUGGU
break point ***
V U W F H A I H V S G U N G
V U W F H V I - - S G U N G
A67V H69- V70-
22,660 22,670 22,680 22,690 22,700
UCUGUCCUAUAUAAUUCCGCAUCAUUUUCCACUUUUAAGUGUUAU
UCUGUCCUAUAUAAUCUCGCACCAUUUUUCACUUUUAAGUGUUAU
**** ******
S V L Y N S A S F S T F K C Y
S V L Y N L A P F F T F K C Y
S371L S373P S375F
22,980 22,990 23,000 23,010
AUCUAUCAGGCCGGUAGCACACCUUGUAAUGGUGUU
AUCUAUCAGGCCGGUAACAAACCUUGUAAUGGUGUU
**
I Y Q A G S T P C N G V
I Y Q A G N K P C N G V
S477N T478K
23,590 23,600 23,610 23,620
UAUCAGACUCAGACUAAUUCUCCUCGGCGGGCACGUAGU
UAUCAGACUCAGACUAAGUCUCAUCGGCGGGCACGUAGU
****
Y Q T Q T N S P R R A R S
Y Q T Q T K S H R R A R S
N679K P681H

Fig. 4 A

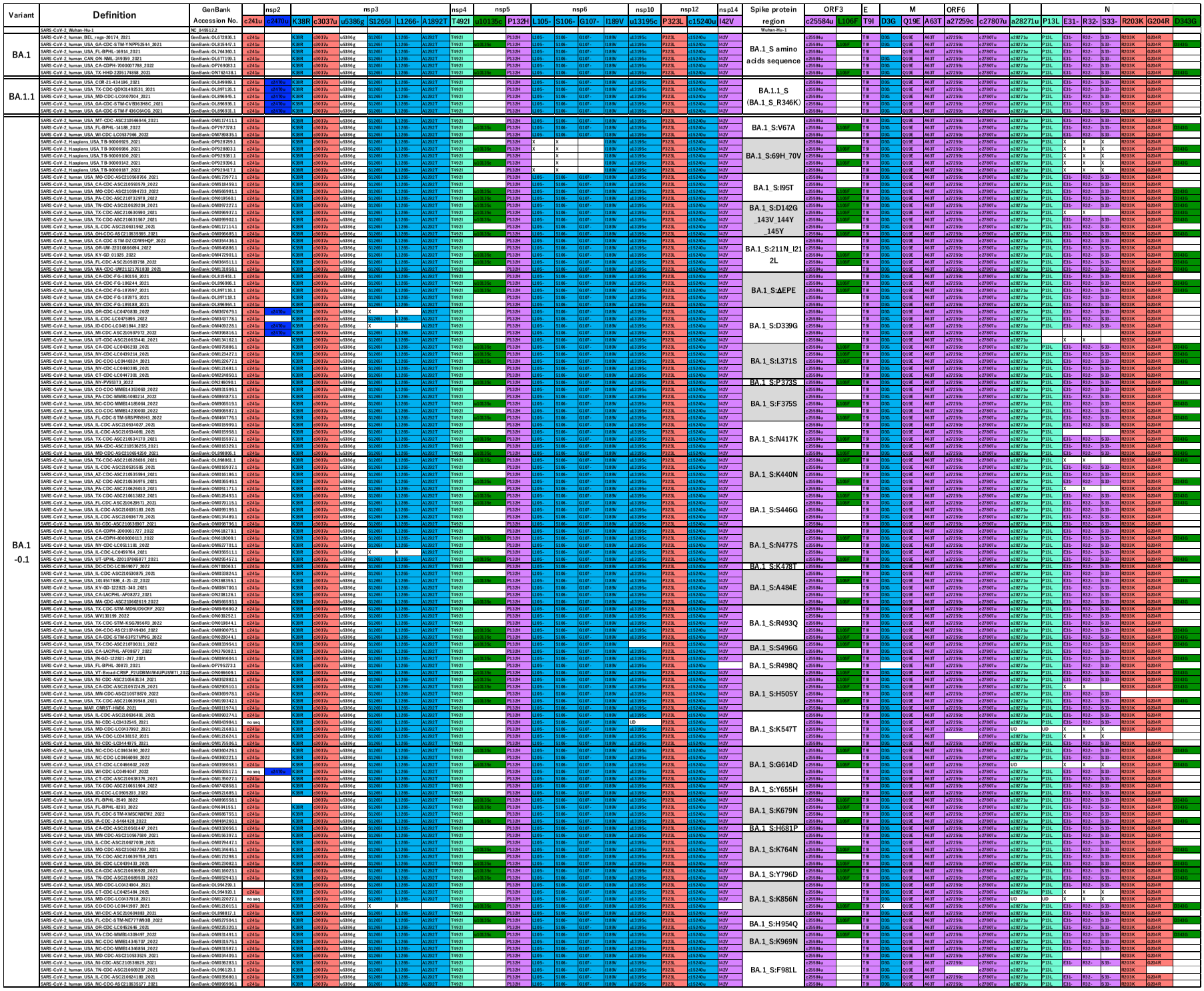

Variant	Definition	GenBank Accession No.	nsp2		nsp3					nsp4	nsp5	nsp6			nsp10	nsp12		nsp14	Spike protein region	ORF3		E	M			ORF6		N				
		NC_045512	c241u	c2470u	K38R	c3037u	u5386g	S1265I	L1266-	A1892T	T492I	u10135c	P132H	L105-	S106-	G107-	I189V	u13195c	P323L	c15240u	I42V	Wuhan-Hu-1	c25584u	L106F	T9I	D3G	Q19E	A63T	a27259c	c27807u	a28271u	P13L	E31-	R32-	S33-	R203K	G204R	D343G
BA.1	SARS-CoV-2_Wuhan-Hu-1	NC_045512																													
	SARS-CoV-2_human_BEL_rega_20174_2021	GenBank: OL672836.1	c241u		K38R	c3037u	u5386g	S1265I	L1266-	A1892T	T492I		P132H	L105-	S106-	G107-	I189V	u13195c	P323L	c15240u	I42V	BA.1_S amino acids sequence	c25584u		T9I	D3G	Q19E	A63T	a27259c	c27807u	a28271u	P13L	E31-	R32-	S33-	R203K	G204R	
	SARS-CoV-2_human_USA_GA-CDC-STM-YNPP52544_2021	GenBank: OL815447.1	c241u		K38R	c3037u	u5386g	S1265I	L1266-	A1892T	T492I	c10135t	P132H	L105-	S106-	G107-	I189V	u13195c	P323L	c15240u	I42V		c25584u	L106F	T9I	D3G	Q19E	A63T	a27259c	c27807u	a28271u	P13L	E31-	R32-	S33-	R203K	G204R	D343G
	SARS-CoV-2_human_USA_FL-BPHL-16914_2021	GenBank: OL764360.1	c241u		K38R	c3037u	u5386g	S1265I	L1266-	A1892T	T492I		P132H	L105-	S106-	G107-	I189V	u13195c	P323L	c15240u	I42V		c25584u		T9I	D3G	Q19E	A63T	a27259c	c27807u	a28271u	P13L	E31-	R32-	S33-	R203K	G204R	
	SARS-CoV-2_human_CAN_ON-NML-249359_2021	GenBank: OL677199.1	c241u		K38R	c3037u	u5386g	S1265I	L1266-	A1892T	T492I		P132H	L105-	S106-	G107-	I189V	u13195c	P323L	c15240u	I42V		c25584u		T9I	D3G	Q19E	A63T	a27259c	c27807u	a28271u	P13L	E31-	R32-	S33-	R203K	G204R	
	SARS-CoV-2_human_USA_CA-CDPH-7000007788_2022	GenBank: OP769083.1	c241u		K38R	c3037u	u5386g	S1265I	L1266-	A1892T	T492I		P132H	L105-	S106-	G107-	I189V	u13195c	P323L	c15240u	I42V		c25584u		T9I	D3G	Q19E	A63T	a27259c	c27807u	a28271u	P13L	E31-	R32-	S33-	R203K	G204R	
	SARS-CoV-2_human_USA_TX-HHD-230517488_2023	GenBank: ON762438.1	c241u		K38R	c3037u	u5386g	S1265I	L1266-	A1892T	T492I	c10135t	P132H	L105-	S106-	G107-	I189V	u13195c	P323L	c15240u	I42V		c25584u	L106F	T9I	D3G	Q19E	A63T	a27259c	c27807u	a28271u	P13L	E31-	R32-	S33-	R203K	G204R	D343G
BA.1.1	SARS-CoV-2_human_USA_COR-21-434196_2021	GenBank: OL849989.1	c241u	c2470u	K38R	c3037u	u5386g	S1265I	L1266-	A1892T	T492I		P132H	L105-	S106-	G107-	I189V	u13195c	P323L	c15240u	I42V	BA.1.1_S (BA.1_S_R346K)	c25584u		T9I	D3G	Q19E	A63T	a27259c	c27807u	a28271u	P13L	E31-	R32-	S33-	R203K	G204R	
	SARS-CoV-2_human_USA_TX-CDC-QDX149351_2021	GenBank: OL897126.1	c241u	c2470u	K38R	c3037u	u5386g	S1265I	L1266-	A1892T	T492I		P132H	L105-	S106-	G107-	I189V	u13195c	P323L	c15240u	I42V		c25584u		T9I	D3G	Q19E	A63T	a27259c	c27807u	a28271u	P13L	E31-	R32-	S33-	R203K	G204R	
	SARS-CoV-2_human_USA_MD-CDC-LC0407004_2021	GenBank: OL896945.1	c241u	c2470u	K38R	c3037u	u5386g	S1265I	L1266-	A1892T	T492I		P132H	L105-	S106-	G107-	I189V	u13195c	P323L	c15240u	I42V		c25584u		T9I	D3G	Q19E	A63T	a27259c	c27807u	a28271u	P13L	E31-	R32-	S33-	R203K	G204R	
	SARS-CoV-2_human_USA_GA-CDC-STM-CVB363H8C_2021	GenBank: OL896936.1	c241u	c2470u	K38R	c3037u	u5386g	S1265I	L1266-	A1892T	T492I		P132H	L105-	S106-	G107-	I189V	u13195c	P323L	c15240u	I42V		c25584u		T9I	D3G	Q19E	A63T	a27259c	c27807u	a28271u	P13L	E31-	R32-	S33-	R203K	G204R	
	SARS-CoV-2_human_USA_GA-CDC-STM-F416C46CG_2021	GenBank: OL896931.1	c241u	c2470u	K38R	c3037u	u5386g	S1265I	L1266-	A1892T	T492I		P132H	L105-	S106-	G107-	I189V	u13195c	P323L	c15240u	I42V		c25584u		T9I	D3G	Q19E	A63T	a27259c	c27807u	a28271u	P13L	E31-	R32-	S33-	R203K	G204R	
	SARS-CoV-2_human_USA_MT-CDC-ASC21056946_2021	GenBank: OM127411.1	c241u		K38R	c3037u	u5386g	S1265I	L1266-	A1892T	T492I		P132H	L105-	S106-	G107-	I189V	u13195c	P323L	c15240u	I42V		c25584u		T9I	D3G	Q19E	A63T	a27259c	c27807u	a28271u	P13L	E31-	R32-	S33-	R203K	G204R	
	SARS-CoV-2_human_USA_FL-BPHL-14188_2022	GenBank: OP797379.1	c241u		K38R	c3037u	u5386g	S1265I	L1266-	A1892T	T492I	c10135t	P132H	L105-	S106-	G107-	I189V	u13195c	P323L	c15240u	I42V	BA.1 S:V67A	c25584u	L106F	T9I	D3G	Q19E	A63T	a27259c	c27807u	a28271u	P13L	E31-	R32-	S33-	R203K	G204R	D343G
	SARS-CoV-2_human_USA_WI-CDC-LC0537966_2022	GenBank: OM728835.1	c241u		K38R	c3037u	u5386g	S1265I	L1266-	A1892T	T492I		P132H	L105-	S106-	G107-	I189V	u13195c	P323L	c15240u	I42V		c25584u		T9I	D3G	Q19E	A63T	a27259c	c27807u	a28271u	P13L	E31-	R32-	S33-	R203K	G204R	
	SARS-CoV-2_Hasplens_USA_TB-90006925_2021	GenBank: OP928789.1	c241u		K38R	c3037u	u5386g	S1265I	L1266-	A1892T	T492I		P132H	X	X		I189V	u13195c	P323L	c15240u	I42V	BA.1_S:69H_70V	c25584u	L106F	T9I	D3G	Q19E	A63T	a27259c	c27807u	a28271u	P13L	X	X	X	R203K	G204R	
	SARS-CoV-2_Hasplens_USA_TB-90006986_2021	GenBank: OP928803.1	c241u		K38R	c3037u	u5386g	S1265I	L1266-	A1892T	T492I	c10135t	P132H	X	X		I189V	u13195c	P323L	c15240u	I42V		c25584u	L106F	T9I	D3G	Q19E	A63T	a27259c	c27807u	a28271u	P13L	X	X	X	R203K	G204R	H245Y
	SARS-CoV-2_Hasplens_USA_TB-90009100_2021	GenBank: OP929381.1	c241u		K38R	c3037u	u5386g	S1265I	L1266-	A1892T	T492I		P132H	L105-	X		I189V	u13195c	P323L	c15240u	I42V		c25584u		T9I	D3G	Q19E	A63T	a27259c	c27807u	a28271u	P13L	X	X	X	R203K	G204R	
	SARS-CoV-2_Hasplens_USA_TB-90009142_2021	GenBank: OP929396.1	c241u		K38R	c3037u	u5386g	S1265I	L1266-	A1892T	T492I	c10135t	P132H	L105-	X		I189V	u13195c	P323L	c15240u	I42V		c25584u	L106F	T9I	D3G	Q19E	A63T	a27259c	c27807u	a28271u	P13L	X	X	X	R203K	G204R	D343G
	SARS-CoV-2_Hasplens_USA_TB-90009187_2022	GenBank: OP929417.1	c241u		K38R	c3037u	u5386g	S1265I	L1266-	A1892T	T492I		P132H	X	X		I189V	u13195c	P323L	c15240u	I42V		c25584u		T9I	D3G	Q19E	A63T	a27259c	c27807u	a28271u	P13L	X	X	X	R203K	G204R	
	SARS-CoV-2_human_USA_MO-CDC-AS-C21056876_2021	GenBank: OM173977.1	c241u		K38R	c3037u	u5386g	S1265I	L1266-	A1892T	T492I		P132H	L105-	S106-	G107-	I189V	u13195c	P323L	c15240u	I42V		c25584u		T9I	D3G	Q19E	A63T	a27259c	c27807u	a28271u	P13L	E31-	R32-	S33-	R203K	G204R	
	SARS-CoV-2_human_USA_CA-CDC-ASC21059579_2022	GenBank: OM918459.1	c241u		K38R	c3037u	u5386g	S1265I	L1266-	A1892T	T492I		P132H	L105-	S106-	G107-	I189V	u13195c	P323L	c15240u	I42V	BA.1_S:I95T	c25584u		T9I	D3G	Q19E	A63T	a27259c	c27807u	a28271u	P13L	E31-	R32-	S33-	R203K	G204R	
	SARS-CoV-2_human_USA_MO-CDC-AS-C21059733_2022	GenBank: OM918981.1	c241u		K38R	c3037u	u5386g	S1265I	L1266-	A1892T	T492I	c10135t	P132H	L105-	S106-	G107-	I189V	u13195c	P323L	c15240u	I42V		c25584u	L106F	T9I	D3G	Q19E	A63T	a27259c	c27807u	a28271u	P13L	E31-	R32-	S33-	R203K	G204R	D343G
	SARS-CoV-2_human_USA_PA-CDC-ASC21073298_2022	GenBank: ON039560.1	c241u		K38R	c3037u	u5386g	S1265I	L1266-	A1892T	T492I	c10135t	P132H	L105-	S106-	G107-	I189V	u13195c	P323L	c15240u	I42V		c25584u	L106F	T9I	D3G	Q19E	A63T	a27259c	c27807u	a28271u	P13L	E31-	R32-	S33-	R203K	G204R	D343G
	SARS-CoV-2_human_USA_TN-CDC-ASC21042920_2021	GenBank: OM097227.1	c241u		K38R	c3037u	u5386g	S1265I	L1266-	A1892T	T492I	c10135t	P132H	L105-	S106-	G107-	I189V	u13195c	P323L	c15240u	I42V	BA.1_S:D142G _143V_144Y _145Y	c25584u	L106F	T9I	D3G	Q19E	A63T	a27259c	c27807u	a28271u	P13L	E31-	R32-	S33-	R203K	G204R	D343G
	SARS-CoV-2_human_USA_TX-CDC-ASC21063090_2021	GenBank: OM098937.1	c241u		K38R	c3037u	u5386g	S1265I	L1266-	A1892T	T492I	c10135t	P132H	L105-	S106-	G107-	I189V	u13195c	P323L	c15240u	I42V		c25584u	L106F	T9I	D3G	Q19E	A63T	a27259c	c27807u	a28271u	P13L	X	X	X	R203K	G204R	D343G
	SARS-CoV-2_human_USA_TX-CDC-ASC21063139_2021	GenBank: OM098993.1	c241u		K38R	c3037u	u5386g	S1265I	L1266-	A1892T	T492I	c10135t	P132H	L105-	S106-	G107-	I189V	u13195c	P323L	c15240u	I42V		c25584u	L106F	T9I	D3G	Q19E	A63T	a27259c	c27807u	a28271u	P13L	E31-	R32-	S33-	R203K	G204R	D343G
	SARS-CoV-2_human_USA_IL-CDC-ASC21063194_2021	GenBank: OM127114.1	c241u		K38R	c3037u	u5386g	S1265I	L1266-	A1892T	T492I		P132H	L105-	S106-	G107-	I189V	u13195c	P323L	c15240u	I42V		c25584u		T9I	D3G	Q19E	A63T	a27259c	c27807u	a28271u	P13L	E31-	R32-	S33-	R203K	G204R	
	SARS-CoV-2_human_USA_OH-CDC-AS-C21053565_2021	GenBank: OM096585.1	c241u		K38R	c3037u	u5386g	S1265I	L1266-	A1892T	T492I	c10135t	P132H	L105-	S106-	G107-	I189V	u13195c	P323L	c15240u	I42V		c25584u	L106F	T9I	D3G	Q19E	A63T	a27259c	c27807u	a28271u	P13L	E31-	R32-	S33-	R203K	G204R	H245Y
	SARS-CoV-2_human_USA_CA-CDC-STM-OZCDW9HQP_2022	GenBank: OM344436.1	c241u		K38R	c3037u	u5386g	S1265I	L1266-	A1892T	T492I		P132H	L105-	S106-	G107-	I189V	u13195c	P323L	c15240u	I42V		c25584u		T9I	D3G	Q19E	A63T	a27259c	c27807u	a28271u	P13L	E31-	R32-	S33-	R203K	G204R	
	SARS-CoV-2_human_USA_UW-22-10866094_2022	GenBank: OM648986.1	c241u		K38R	c3037u	u5386g	S1265I	L1266-	A1892T	T492I		P132H	L105-	S106-	G107-	I189V	u13195c	P323L	c15240u	I42V	BA.1_S:211N_I21 2L	c25584u		T9I	D3G	Q19E	A63T	a27259c	c27807u	a28271u	P13L	E31-	R32-	S33-	R203K	G204R	
	SARS-CoV-2_human_USA_KY-GD_01925_2022	GenBank: OM479901.1	c241u		K38R	c3037u	u5386g	S1265I	L1266-	A1892T	T492I	c10135t	P132H	L105-	S106-	G107-	I189V	u13195c	P323L	c15240u	I42V		c25584u	L106F	T9I	D3G	Q19E	A63T	a27259c	c27807u	a28271u	P13L	E31-	R32-	S33-	R203K	G204R	D343G
	SARS-CoV-2_human_USA_FL-CDC-ASC21050378_2022	GenBank: OM346511.1	c241u		K38R	c3037u	u5386g	S1265I	L1266-	A1892T	T492I	c10135t	P132H	L105-	S106-	G107-	I189V	u13195c	P323L	c15240u	I42V		c25584u	L106F	T9I	D3G	Q19E	A63T	a27259c	c27807u	a28271u	P13L	E31-	R32-	S33-	R203K	G204R	D343G
	SARS-CoV-2_human_USA_WA-CDC-UW21127163030_2021	GenBank: OM131358.1	c241u		K38R	c3037u	u5386g	S1265I	L1266-	A1892T	T492I		P132H	L105-	S106-	G107-	I189V	u13195c	P323L	c15240u	I42V		c25584u		T9I	D3G	Q19E	A63T	a27259c	c27807u	a28271u	P13L	E31-	R32-	S33-	R203K	G204R	D343G
	SARS-CoV-2_human_USA_CA-CDC-FG-180156_2021	GenBank: OL810451.1	c241u		K38R	c3037u	u5386g	S1265I	L1266-	A1892T	T492I		P132H	L105-	S106-	G107-	I189V	u13195c	P323L	c15240u	I42V	BA.1_S:ΔEPE	c25584u	L106F	T9I	D3G	Q19E	A63T	a27259c	c27807u	a28271u	P13L	E31-	R32-	S33-	R203K	G204R	
	SARS-CoV-2_human_USA_CA-CDC-FG-186244_2021	GenBank: OL896986.1	c241u		K38R	c3037u	u5386g	S1265I	L1266-	A1892T	T492I	c10135t	P132H	L105-	S106-	G107-	I189V	u13195c	P323L	c15240u	I42V		c25584u	L106F	T9I	D3G	Q19E	A63T	a27259c	c27807u	a28271u	P13L	E31-	R32-	S33-	R203K	G204R	D343G
	SARS-CoV-2_human_USA_CA-CDC-FG-187697_2021	GenBank: OL897116.1	c241u		K38R	c3037u	u5386g	S1265I	L1266-	A1892T	T492I	c10135t	P132H	L105-	S106-	G107-	I189V	u13195c	P323L	c15240u	I42V		c25584u	L106F	T9I	D3G	Q19E	A63T	a27259c	c27807u	a28271u	P13L	E31-	R32-	S33-	R203K	G204R	D343G
	SARS-CoV-2_human_USA_CA-CDC-FG-187875_2021	GenBank: OL897138.1	c241u		K38R	c3037u	u5386g	S1265I	L1266-	A1892T	T492I		P132H	L105-	S106-	G107-	I189V	u13195c	P323L	c15240u	I42V		c25584u		T9I	D3G	Q19E	A63T	a27259c	c27807u	a28271u	P13L	E31-	R32-	S33-	R203K	G204R	
	SARS-CoV-2_human_USA_NY-CDC-FG-188188_2021	GenBank: OL896941.1	c241u		K38R	c3037u	u5386g	S1265I	L1266-	A1892T	T492I		P132H	L105-	S106-	G107-	I189V	u13195c	P323L	c15240u	I42V		c25584u		T9I	D3G	Q19E	A63T	a27259c	c27807u	a28271u	P13L	E31-	R32-	S33-	R203K	G204R	
	SARS-CoV-2_human_USA_OR-CDC-LC0470830_2022	GenBank: OM3476761	c241u	c2470u	K38R	c3037u	u5386g	X	X		A1892T		P132H	L105-	S106-	G107-	I189V	u13195c	P323L	c15240u	I42V		c25584u		T9I	D3G	Q19E	A63T	a27259c	c27807u	a28271u	P13L	E31-	R32-	S33-	R203K	G204R	
	SARS-CoV-2_human_USA_IL-CDC-LC0475895_2022	GenBank: OM343778.1	c241u		K38R	c3037u	u5386g	S1265I	L1266-	A1892T	T492I		P132H	L105-	S106-	G107-	I189V	u13195c	P323L	c15240u	I42V	BA.1_S:D339G	c25584u		T9I	D3G	Q19E	A63T	a27259c	c27807u	a28271u	P13L	E31-	R32-	S33-	R203K	G204R	
	SARS-CoV-2_human_USA_ID-CDC-LC0481844_2022	GenBank: OM409228.1	c241u	c2470u	K38R	c3037u	u5386g	X	X		A1892T		P132H	L105-	S106-	G107-	I189V	u13195c	P323L	c15240u	I42V		c25584u		T9I	D3G	Q19E	A63T	a27259c	c27807u	a28271u	P13L	E31-	R32-	S33-	R203K	G204R	
	SARS-CoV-2_human_USA_MI-CDC-ASC21059779_2022	GenBank: OL810491.1	c241u	c2470u	K38R	c3037u	u5386g	X	S1265I	L1266-	A1892T		P132H	L105-	S106-	G107-	I189V	u13195c	P323L	c15240u	I42V		c25584u		T9I	D3G	Q19E	A63T	a27259c	c27807u	a28271u	P13L	E31-	R32-	S33-	R203K	G204R	
	SARS-CoV-2_human_USA_UT-CDC-ASC21063141_2021	GenBank: OM131621.1	c241u		K38R	c3037u	u5386g	S1265I	L1266-	A1892T	T492I		P132H	L105-	S106-	G107-	I189V	u13195c	P323L	c15240u	I42V		c25584u		T9I	D3G	Q19E	A63T	a27259c	c27807u	a28271u		X	X		R203K	G204R	
	SARS-CoV-2_human_USA_CA-CDC-LC0436293_2021	GenBank: OM075886.1	c241u		K38R	c3037u	u5386g	S1265I	L1266-	A1892T	T492I	c10135t	P132H	L105-	S106-	G107-	I189V	u13195c	P323L	c15240u	I42V		c25584u	L106F	T9I	D3G	Q19E	A63T	a27259c	c27807u	a28271u	P13L	E31-	R32-	S33-	R203K	G204R	D343G
	SARS-CoV-2_human_USA_NY-CDC-LC0439214_2021	GenBank: OM128427.1	c241u		K38R	c3037u	u5386g	S1265I	L1266-	A1892T	T492I	c10135t	P132H	L105-	S106-	G107-	I189V	u13195c	P323L	c15240u	I42V	BA.1_S:L371S	c25584u	L106F	T9I	D3G	Q19E	A63T	a27259c	c27807u	a28271u	P13L	E31-	R32-	S33-	R203K	G204R	D343G
	SARS-CoV-2_human_USA_DC-CDC-LC0440824_2021	GenBank: OM128448.1	c241u		K38R	c3037u	u5386g	S1265I	L1266-	A1892T	T492I	c10135t	P132H	L105-	S106-	G107-	I189V	u13195c	P323L	c15240u	I42V		c25584u	L106F	T9I	D3G	Q19E	A63T	a27259c	c27807u	a28271u	P13L	E31-	R32-	S33-	R203K	G204R	D343G
	SARS-CoV-2_human_USA_NY-CDC-LC0440385_2021	GenBank: OM121681.1	c241u		K38R	c3037u	u5386g	S1265I	L1266-	A1892T	T492I		P132H	L105-	S106-	G107-	I189V	u13195c	P323L	c15240u	I42V		c25584u		T9I	D3G	Q19E	A63T	a27259c	c27807u	a28271u	P13L	E31-	R32-	S33-	R203K	G204R	
	SARS-CoV-2_human_USA_CT-CDC-LC0447301_2021	GenBank: OM228480.1	c241u		K38R	c3037u	u5386g	S1265I	L1266-	A1892T	T492I		P132H	L105-	S106-	G107-	I189V	u13195c	P323L	c15240u	I42V		c25584u		T9I	D3G	Q19E	A63T	a27259c	c27807u	a28271u	P13L	E31-	R32-	S33-	R203K	G204R	
	SARS-CoV-2_human_USA_PVS5373_2022	GenBank: ON246090.1	c241u		K38R	c3037u	u5386g	S1265I	L1266-	A1892T	T492I	c10135t	P132H	L105-	S106-	G107-	I189V	u13195c	P323L	c15240u	I42V	BA.1_S:P373S	c25584u	L106F	T9I	D3G	Q19E	A63T	a27259c	c27807u	a28271u	P13L	E31-	R32-	S33-	R203K	G204R	H245Y
	SARS-CoV-2_human_USA_CO-CDC-MMB14130090_2022	GenBank: ON931599.1	c241u		K38R	c3037u	u5386g	S1265I	L1266-	A1892T	T492I		P132H	L105-	S106-	G107-	I189V	u13195c	P323L	c15240u	I42V		c25584u		T9I	D3G	Q19E	A63T	a27259c	c27807u	a28271u	P13L	E31-	R32-	S33-	R203K	G204R	
	SARS-CoV-2_human_USA_PA-CDC-MMB14080214_2022	GenBank: OM848873.1	c241u		K38R	c3037u	u5386g	S1265I	L1266-	A1892T	T492I		P132H	L105-	S106-	G107-	I189V	u13195c	P323L	c15240u	I42V		c25584u		T9I	D3G	Q19E	A63T	a27259c	c27807u	a28271u	P13L	E31-	R32-	S33-	R203K	G204R	
	SARS-CoV-2_human_USA_NC-CDC-MMB14185064_2022	GenBank: ON990519.1	c241u		K38R	c3037u	u5386g	S1265I	L1266-	A1892T	T492I	c10135t	P132H	L105-	S106-	G107-	I189V	u13195c	P323L	c15240u	I42V	BA.1_S:F375S	c25584u	L106F	T9I	D3G	Q19E	A63T	a27259c	c27807u	a28271u	P13L	E31-	R32-	S33-	R203K	G204R	D343G
	SARS-CoV-2_human_USA_CO-CDC-MMB14230009_2022	GenBank: ON990587.1	c241u		K38R	c3037u	u5386g	S1265I	L1266-	A1892T	T492I		P132H	L105-	S106-	G107-	I189V	u13195c	P323L	c15240u	I42V		c25584u		T9I	D3G	Q19E	A63T	a27259c	c27807u	a28271u	P13L	E31-	R32-	S33-	R203K	G204R	
	SARS-CoV-2_human_USA_FL-CDC-STM-5RGPRYWH3_2022	GenBank: OM944776.1	c241u		K38R	c3037u	u5386g	S1265I	L1266-	A1892T	T492I	c10135t	P132H	L105-	S106-	G107-	I189V	u13195c	P323L	c15240u	I42V		c25584u	L106F	T9I	D3G	Q19E	A63T	a27259c	c27807u	a28271u	P13L	E31-	R32-	S33-	R203K	G204R	D343G
	SARS-CoV-2_human_USA_IL-CDC-ASC21034027_2021	GenBank: OM015947.1	c241u		K38R	c3037u	u5386g	S1265I	L1266-	A1892T	T492I		P132H	L105-	S106-	G107-	I189V	u13195c	P323L	c15240u	I42V		c25584u		T9I	D3G	Q19E	A63T	a27259c	c27807u	a28271u	P13L	E31-	R32-	S33-	R203K	G204R	
	SARS-CoV-2_human_USA_IL-CDC-ASC21034081_2021	GenBank: OM015958.1	c241u		K38R	c3037u	u5386g	S1265I	L1266-	A1892T	T492I		P132H	L105-	S106-	G107-	I189V	u13195c	P323L	c15240u	I42V		c25584u		T9I	D3G	Q19E	A63T	a27259c	c27807u	a28271u	P13L	E31-	R32-	S33-	R203K	G204R	
	SARS-CoV-2_human_USA_TX-CDC-ASC21034170_2021	GenBank: OM015597.1	c241u		K38R	c3037u	u5386g	S1265I	L1266-	A1892T	T492I	c10135t	P132H	L105-	S106-	G107-	I189V	u13195c	P323L	c15240u	I42V	BA.1_S:N417K	c25584u	L106F	T9I	D3G	Q19E	A63T	a27259c	c27807u	a28271u	P13L	E31-	R32-	S33-	R203K	G204R	D343G
	SARS-CoV-2_human_USA_MA-CDC-ASC21053255_2021	GenBank: OM016329.1	c241u		K38R	c3037u	u5386g	S1265I	L1266-	A1892T	T492I		P132H	L105-	S106-	G107-	I189V	u13195c	P323L	c15240u	I42V		c25584u		T9I	D3G	Q19E	A63T	a27259c	c27807u	a28271u	P13L	E31-	R32-	S33-	R203K	G204R	
	SARS-CoV-2_human_USA_MD-CDC-ASC21065429_2021	GenBank: OL898936.1	c241u		K38R	c3037u	u5386g	S1265I	L1266-	A1892T	T492I	c10135t	P132H	L105-	S106-	G107-	I189V	u13195c	P323L	c15240u	I42V		c25584u	L106F	T9I	D3G	Q19E	A63T	a27259c	c27807u	a28271u	P13L	E31-	R32-	S33-	R203K	G204R	D343G
	SARS-CoV-2_human_USA_TX-CDC-ASC21052836_2021	GenBank: OL898861.1	c241u		K38R	c3037u	u5386g	S1265I	L1266-	A1892T	T492I	c10135t	P132H	L105-	S106-	G107-	I189V	u13195c	P323L	c15240u	I42V		c25584u	L106F	T9I	D3G	Q19E	A63T	a27259c	c27807u	a28271u	P13L	X	X	X	R203K	G204R	D343G
	SARS-CoV-2_human_USA_IL-CDC-ASC21053585_2021	GenBank: OM016937.1	c241u		K38R	c3037u	u5386g	S1265I	L1266-	A1892T	T492I		P132H	L105-	S106-	G107-	I189V	u13195c	P323L	c15240u	I42V	BA.1_S:K440N	c25584u		T9I	D3G	Q19E	A63T	a27259c	c27807u	a28271u	P13L	E31-	R32-	S33-	R203K	G204R	
	SARS-CoV-2_human_USA_AZ-CDC-ASC21053594_2021	GenBank: OM016186.1	c241u		K38R	c3037u	u5386g	S1265I	L1266-	A1892T	T492I		P132H	L105-	S106-	G107-	I189V	u13195c	P323L	c15240u	I42V		c25584u		T9I	D3G	Q19E	A63T	a27259c	c27807u	a28271u	P13L	E31-	R32-	S33-	R203K	G204R	
	SARS-CoV-2_human_USA_AZ-CDC-ASC21053649_2021	GenBank: OM016449.1	c241u		K38R	c3037u	u5386g	S1265I	L1266-	A1892T	T492I	c10135t	P132H	L105-	S106-	G107-	I189V	u13195c	P323L	c15240u	I42V		c25584u	L106F	T9I	D3G	Q19E	A63T	a27259c	c27807u	a28271u	P13L	E31-	R32-	S33-	R203K	G204R	D343G
	SARS-CoV-2_human_USA_PA-CDC-ASC21052601_2021	GenBank: OM015171.1	c241u		K38R	c3037u	u5386g	S1265I	L1266-	A1892T	T492I		P132H	L105-	S106-	G107-	I189V	u13195c	P323L	c15240u	I42V		c25584u		T9I	D3G	Q19E	A63T	a27259c	c27807u	a28271u	P13L	X	X		R203K	G204R	
	SARS-CoV-2_human_USA_TX-CDC-ASC21063832_2021	GenBank: OM126493.1	c241u		K38R	c3037u	u5386g	S1265I	L1266-	A1892T	T492I	c10135t	P132H	L105-	S106-	G107-	I189V	u13195c	P323L	c15240u	I42V		c25584u	L106F	T9I	D3G	Q19E	A63T	a27259c	c27807u	a28271u	P13L	E31-	R32-	S33-	R203K	G204R	D343G
	SARS-CoV-2_human_USA_FL-CDC-ASC21062957_2021	GenBank: OM079115.1	c241u		K38R	c3037u	u5386g	S1265I	L1266-	A1892T	T492I	c10135t	P132H	L105-	S106-	G107-	I189V	u13195c	P323L	c15240u	I42V	BA.1_S:S446G	c25584u	L106F	T9I	D3G	Q19E	A63T	a27259c	c27807u	a28271u	P13L	E31-	R32-	S33-	R203K	G204R	D343G
	SARS-CoV-2_human_USA_IL-CDC-ASC21063185_2021	GenBank: OM134893.1	c241u		K38R	c3037u	u5386g	S1265I	L1266-	A1892T	T492I		P132H	L105-	S106-	G107-	I189V	u13195c	P323L	c15240u	I42V		c25584u		T9I	D3G	Q19E	A63T	a27259c	c27807u	a28271u	P13L	E31-	R32-	S33-	R203K	G204R	
	SARS-CoV-2_human_USA_IL-CDC-ASC21063670_2021	GenBank: OM134489.1	c241u		K38R	c3037u	u5386g	S1265I	L1266-	A1892T	T492I		P132H	L105-	S106-	G107-	I189V	u13195c	P323L	c15240u	I42V		c25584u		T9I	D3G	Q19E	A63T	a27259c	c27807u	a28271u	P13L	E31-	R32-	S33-	R203K	G204R	
	SARS-CoV-2_human_USA_NJ-CDC-ASC21063807_2021	GenBank: OM098796.1	c241u		K38R	c3037u	u5386g	S1265I	L1266-	A1892T	T492I		P132H	L105-	S106-	G107-	I189V	u13195c	P323L	c15240u	I42V		c25584u		T9I	D3G	Q19E	A63T	a27259c	c27807u	a28271u	P13L	E31-	R32-	S33-	R203K	G204R	
	SARS-CoV-2_human_USA_CA-CDPH-2000061727_2022	GenBank: ON638279.1	c241u		K38R	c3037u	u5386g	S1265I	L1266-	A1892T	T492I		P132H	L105-	S106-	G107-	I189V	u13195c	P323L	c15240u	I42V		c25584u		T9I	D3G	Q19E	A63T	a27259c	c27807u	a28271u	P13L	E31-	R32-	S33-	R203K	G204R	
BA.1 -0.1	SARS-CoV-2_human_USA_CA-CDPH-8000000112_2022	GenBank: ON618926.1	c241u		K38R	c3037u	u5386g	S1265I	L1266-	A1892T	T492I	c10135t	P132H	L105-	S106-	G107-	I189V	u13195c	P323L	c15240u	I42V	BA.1_S:N477S	c25584u	L106F	T9I	D3G	Q19E	A63T	a27259c	c27807u	a28271u	P13L	E31-	R32-	S33-	R203K	G204R	D343G
	SARS-CoV-2_human_USA_NY-CDC-LC0511181_2022	GenBank: OM627701.1	c241u		K38R	c3037u	u5386g	S1265I	L1266-	A1892T	T492I		P132H	L105-	S106-	G107-	I189V	u13195c	P323L	c15240u	I42V		c25584u		T9I	D3G	Q19E	A63T	a27259c	c27807u	a28271u	P13L	E31-	R32-	S33-	R203K	G204R	
	SARS-CoV-2_human_USA_IL-CDC-LC0459764_2021	GenBank: OM396511.1	c241u		K38R	c3037u	u5386g	X	X		A1892T		P132H	L105-	S106-	G107-	I189V	u13195c	P323L	c15240u	I42V		c25584u		T9I	D3G	Q19E	A63T	a27259c	c27807u	a28271u	P13L	E31-	R32-	S33-	R203K	G204R	
	SARS-CoV-2_human_USA_UT-UPHL-22010786877_2021	GenBank: OM295457.1	c241u		K38R	c3037u	u5386g	S1265I	L1266-	A1892T	T492I	c10135t	P132H	L105-	S106-	G107-	I189V	u13195c	P323L	c15240u	I42V		c25584u	L106F	T9I	D3G	Q19E	A63T	a27259c	c27807u	a28271u	P13L	E31-	R32-	S33-	R203K	G204R	D343G
	SARS-CoV-2_human_USA_DC-CDC-LC0461877_2021	GenBank: OM700211.1	c241u		K38R	c3037u	u5386g	S1265I	L1266-	A1892T	T492I		P132H	L105-	S106-	G107-	I189V	u13195c	P323L	c15240u	I42V	BA.1_S:K478T	c25584u		T9I	D3G	Q19E	A63T	a27259c	c27807u	a28271u	P13L	E31-	R32-	S33-	R203K	G204R	
	SARS-CoV-2_human_USA_IL-CDC-ASC21053075_2021	GenBank: OM033824.1	c241u		K38R	c3037u	u5386g	S1265I	L1266-	A1892T	T492I		P132H	L105-	S106-	G107-	I189V	u13195c	P323L	c15240u	I42V		c25584u		T9I	D3G	Q19E	A63T	a27259c	c27807u	a28271u	P13L	E31-	R32-	S33-	R203K	G204R	
	SARS-CoV-2_human_USA_10147547886_4-21-22_2022	GenBank: ON368355.1	c241u		K38R	c3037u	u5386g	S1265I	L1266-	A1892T	T492I	c10135t	P132H	L105-	S106-	G107-	I189V	u13195c	P323L	c15240u	I42V	BA.1_S:A484E	c25584u	L106F	T9I	D3G	Q19E	A63T	a27259c	c27807u	a28271u	P13L	E31-	R32-	S33-	R203K	G204R	D343G
	SARS-CoV-2_human_USA_KY-GD-122821-340_2021	GenBank: ON084700.1	c241u		K38R	c3037u	u5386g	S1265I	L1266-	A1892T	T492I		P132H	L105-	S106-	G107-	I189V	u13195c	P323L	c15240u	I42V		c25584u		T9I	D3G	Q19E	A63T	a27259c	c27807u	a28271u	P13L	E31-	R32-	S33-	R203K	G204R	
	SARS-CoV-2_human_USA_CA-LACPHL-AF08272_2021	GenBank: OM126126.1	c241u		K38R	c3037u	u5386g	S1265I	L1266-	A1892T	T492I		P132H	L105-	S106-	G107-	I189V	u13195c	P323L	c15240u	I42V		c25584u		T9I	D3G	Q19E	A63T	a27259c	c27807u	a28271u	P13L	E31-	R32-	S33-	R203K	G204R	
	SARS-CoV-2_human_USA_MA-CDC-ASC21062619_2022	GenBank: OM546593.1	c241u		K38R	c3037u	u5386g	S1265I	L1266-	A1892T	T492I	c10135t	P132H	L105-	S106-	G107-	I189V	u13195c	P323L	c15240u

Fig. 4 B

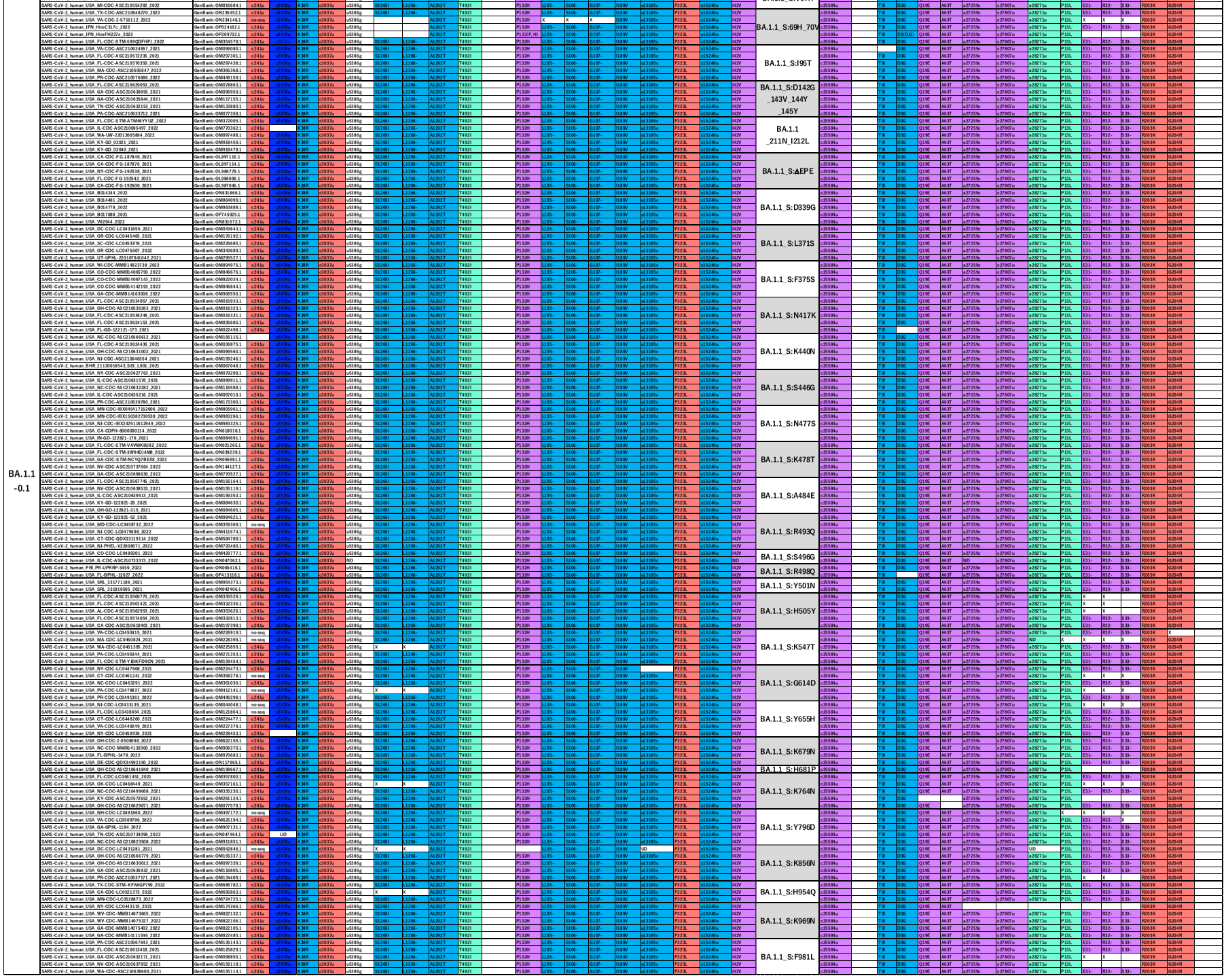

Variant	Definition	GenBank Accession No.	nsp2		nsp3						nsp4	nsp5	nsp6			nsp10	nsp12		nsp14	Spike protein region	ORF3		E	M			ORF6			N			
			c241u	c2470u	K38R	c3037u	u5386g	S1265l	L1266-	A1892T	T492I	u10135c	P132H	L105-	S106-	G107-	I189V	u13195c	P323L	c15240u	I42V		c25584u	L106F	T9I	D3G	Q19E	A63T	a27259c	c27807u	a28271u	P13L	E31-	R32-	S33-	R203K	G204R	D343G
	SARS-CoV-2_human_PR_PR-UPR1RP-5477_2022	GenBank:ON085532.1	c241u	c2470u	K38R	c3037u	u5386g	S1265l	L1266-	A1892T	T492I		P132H	L105-	S106-	G107-	I189V	u13195c	P323L	c15240u	I42V		c25584u		T9I		Q19E	A63T	a27259c	c27807u	a28271u	P13L	E31-	R32-	S33-	R203K	G204R		
	SARS-CoV-2_human_USA_CO-CDC-MMB14406852_2022	GenBank:ON980898.1	c241u	c2470u	K38R	c3037u	u5386g	S1265l	L1266-	A1892T	T492I		P132H	L105-	S106-	G107-	I189V	u13195c	P323L	c15240u	I42V	BA.1.1_S:V67A	c25584u		T9I	D3G	Q19E	A63T	a27259c	c27807u	a28271u	P13L	E31-	R32-	S33-	R203K	G204R		
	SARS-CoV-2_human_USA_MI-CDC-MMB14406842_2022	GenBank:ON818604.1	c241u	c2470u	K38R	c3037u	u5386g	S1265l	L1266-	A1892T	T492I		P132H	L105-	S106-	G107-	I189V	u13195c	P323L	c15240u	I42V		c25584u		T9I	D3G	Q19E	A63T	a27259c	c27807u	a28271u	P13L	E31-	R32-	S33-	R203K	G204R		
	SARS-CoV-2_human_USA_TX-CDC-MMB14406842_2022	GenBank:ON238452.1	c241u	c2470u	K38R	c3037u	u5386g	S1265l	L1266-	A1892T	T492I		P132H	L105-	S106-	G107-	I189V	u13195c	P323L	c15240u	I42V		c25584u		T9I	D3G	Q19E	A63T	a27259c	c27807u	a28271u	P13L	E31-	R32-	S33-	R203K	G204R		
	SARS-CoV-2_human_USA_VA-CDC-2-5715112_2022	GenBank:ON334146.1	no seq	c2470u	K38R	c3037u	u5386g			A1892T	T492I		P132H	x	x	x	I189V	u13195c	P323L	c15240u	I42V	BA.1.1_S:69H_70V	c25584u		T9I	D3G	Q19E	A63T	a27259c	c27807u	a28271u	P13L	x	x	x	R203K	G204R		
	SARS-CoV-2_human_IPN_HinC317c_2022	GenBank:OP024182.1	c241u	c2470u	K38R	c3037u	u5386g			A1892T	T492I		P132H	L105-	S106-	G107-	I189V	u13195c	P323L	c15240u	I42V		c25584u		T9I	D3G	Q19E	A63T	a27259c	c27807u	a28271u	P13L	E31-	R32-	S33-	R203K	G204R		
	SARS-CoV-2_human_IPN_HinP1272c_2022	GenBank:OP269701.1	c241u	c2470u	K38R	c3037u	u5386g			A1892T	T492I		P132(P,H)	L105-	S106-	G107-	I189V	u13195c	P323L	c15240u	I42V		c25584u		T9I	D3G(D,G)	Q19E	A63T	a27259c	c27807u	a28271u	P13L	E31-	R32-	S33-	R203K	G204R		
	SARS-CoV-2_human_USA_FL-CDC-STM-598QDFHPJ_2022	GenBank:OM3545781	c241u	c2470u	K38R	c3037u	u5386g	S1265l	L1266-	A1892T	T492I		P132H	L105-	S106-	G107-	I189V	u13195c	P323L	c15240u	I42V		c25584u		T9I	D3G	Q19E	A63T	a27259c	c27807u	a28271u	P13L	E31-	R32-	S33-	R203K	G204R		
	SARS-CoV-2_human_USA_VA-CDC-SC2106349657_2021	GenBank:OM090980.1	c241u	c2470u	K38R	c3037u	u5386g	S1265l	L1266-	A1892T	T492I		P132H	L105-	S106-	G107-	I189V	u13195c	P323L	c15240u	I42V		c25584u			D3G	Q19E	A63T	a27259c	c27807u	a28271u	P13L	E31-	R32-	S33-	R203K	G204R		
	SARS-CoV-2_human_USA_FL-CDC-ASC21057223S_2021	GenBank:OM297301.1	c241u	c2470u	K38R	c3037u	u5386g	S1265l	L1266-	A1892T	T492I		P132H	L105-	S106-	G107-	I189V	u13195c	P323L	c15240u	I42V	BA.1.1_S:I95T	c25584u		T9I	D3G	Q19E	A63T	a27259c	c27807u	a28271u	P13L	E31-	R32-	S33-	R203K	G204R		
	SARS-CoV-2_human_USA_FL-CDC-ASC21076310_2021	GenBank:OM297438.1	c241u	c2470u	K38R	c3037u	u5386g	S1265l	L1266-	A1892T	T492I		P132H	L105-	S106-	G107-	I189V	u13195c	P323L	c15240u	I42V		c25584u		T9I	D3G	Q19E	A63T	a27259c	c27807u	a28271u	P13L	E31-	R32-	S33-	R203K	G204R		
	SARS-CoV-2_human_USA_MA-CDC-ASC21050847_2022	GenBank:OM385368.1	c241u	c2470u	K38R	c3037u	u5386g	S1265l	L1266-	A1892T	T492I		P132H	L105-	S106-	G107-	I189V	u13195c	P323L	c15240u	I42V		c25584u		T9I	D3G	Q19E	A63T	a27259c	c27807u	a28271u	P13L	E31-	R32-	S33-	R203K	G204R		
	SARS-CoV-2_human_USA_PR-CDC-ASC21057686_2022	GenBank:OM449159.1	c241u	c2470u	K38R	c3037u	u5386g	S1265l	L1266-	A1892T	T492I		P132H	L105-	S106-	G107-	I189V	u13195c	P323L	c15240u	I42V		c25584u		T9I	D3G	Q19E	A63T	a27259c	c27807u	a28271u	P13L	E31-	R32-	S33-	R203K	G204R		
	SARS-CoV-2_human_USA_FL-CDC-ASC21062053_2021	GenBank:OM078363.1	c241u	c2470u	K38R	c3037u	u5386g	S1265l	L1266-	A1892T	T492I		P132H	L105-	S106-	G107-	I189V	u13195c	P323L	c15240u	I42V	BA.1.1_S:D142G _143V_144Y _145Y	c25584u		T9I	D3G	Q19E	A63T	a27259c	c27807u	a28271u	P13L	E31-	R32-	S33-	R203K	G204R		
	SARS-CoV-2_human_USA_GA-CDC-ASC21063049_2021	GenBank:OM098959.1	c241u	c2470u	K38R	c3037u	u5386g	S1265l	L1266-	A1892T	T492I		P132H	L105-	S106-	G107-	I189V	u13195c	P323L	c15240u	I42V		c25584u		T9I	D3G	Q19E	A63T	a27259c	c27807u	a28271u	P13L	E31-	R32-	S33-	R203K	G204R		
	SARS-CoV-2_human_USA_GA-CDC-ASC21063844_2021	GenBank:OM117155.1	c241u	c2470u	K38R	c3037u	u5386g	S1265l	L1266-	A1892T	T492I		P132H	L105-	S106-	G107-	I189V	u13195c	P323L	c15240u	I42V		c25584u		T9I	D3G	Q19E	A63T	a27259c	c27807u	a28271u	P13L	E31-	R32-	S33-	R203K	G204R		
	SARS-CoV-2_human_USA_TN-CDC-ASC21063213_2021	GenBank:OM133880.1	c241u	c2470u	K38R	c3037u	u5386g	S1265l	L1266-	A1892T	T492I		P132H	L105-	S106-	G107-	I189V	u13195c	P323L	c15240u	I42V		c25584u		T9I	D3G	Q19E	A63T	a27259c	c27807u	a28271u	P13L	E31-	R32-	S33-	R203K	G204R		
	SARS-CoV-2_human_USA_PA-CDC-ASC21063172_2021	GenBank:OM077358.1	c241u	c2470u	K38R	c3037u	u5386g	S1265l	L1266-	A1892T	T492I		P132H	L105-	S106-	G107-	I189V	u13195c	P323L	c15240u	I42V		c25584u		T9I	D3G	Q19E	A63T	a27259c	c27807u	a28271u	P13L	E31-	R32-	S33-	R203K	G204R		
	SARS-CoV-2_human_USA_CA-STM-A-TM4617_2022	GenBank:OM372065.1	c241u	c2470u	K38R	c3037u	u5386g	S1265l	L1266-	A1892T	T492I		P132H	L105-	S106-	G107-	I189V	u13195c	P323L	c15240u	I42V		c25584u		T9I	D3G	Q19E	A63T	a27259c	c27807u	a28271u	P13L	E31-	R32-	S33-	R203K	G204R		
	SARS-CoV-2_human_USA_IL-CDC-ASC21069597_2022	GenBank:OM770362.1	c241u		K38R	c3037u	u5386g	S1265l	L1266-	A1892T	T492I		P132H	L105-	S106-	G107-	I189V	u13195c	P323L	c15240u	I42V	BA.1.1 _211N_I212L	c25584u		T9I	D3G	Q19E	A63T	a27259c	c27807u	a28271u	P13L	E31-	R32-	S33-	R203K	G204R		
	SARS-CoV-2_human_USA_WA-LW-22013005884_2022	GenBank:OM897488.1	c241u	c2470u	K38R	c3037u	u5386g	S1265l	L1266-	A1892T	T492I		P132H	L105-	S106-	G107-	I189V	u13195c	P323L	c15240u	I42V		c25584u		T9I	D3G	Q19E	A63T	a27259c	c27807u	a28271u	P13L	E31-	R32-	S33-	R203K	G204R		
	SARS-CoV-2_human_USA_KY-GD_02021_2021	GenBank:OM918459.1	c241u	c2470u	K38R	c3037u	u5386g	S1265l	L1266-	A1892T	T492I		P132H	L105-	S106-	G107-	I189V	u13195c	P323L	c15240u	I42V		c25584u		T9I	D3G	Q19E	A63T	a27259c	c27807u	a28271u	P13L	E31-	R32-	S33-	R203K	G204R		
	SARS-CoV-2_human_USA_KY-GD_02040_2021	GenBank:OM918478.1	c241u	c2470u	K38R	c3037u	u5386g	S1265l	L1266-	A1892T	T492I		P132H	L105-	S106-	G107-	I189V	u13195c	P323L	c15240u	I42V		c25584u		T9I	D3G	Q19E	A63T	a27259c	c27807u	a28271u	P13L	E31-	R32-	S33-	R203K	G204R		
	SARS-CoV-2_human_USA_CA-CDC-FG-187849_2021	GenBank:OL897135.1	c241u	c2470u	K38R	c3037u	u5386g	S1265l	L1266-	A1892T	T492I		P132H	L105-	S106-	G107-	I189V	u13195c	P323L	c15240u	I42V		c25584u		T9I	D3G	Q19E	A63T	a27259c	c27807u	a28271u	P13L	E31-	R32-	S33-	R203K	G204R		
	SARS-CoV-2_human_USA_CA-CDC-FG-187876_2021	GenBank:OL897114.1	c241u	c2470u	K38R	c3037u	u5386g	S1265l	L1266-	A1892T	T492I		P132H	L105-	S106-	G107-	I189V	u13195c	P323L	c15240u	I42V		c25584u		T9I	D3G	Q19E	A63T	a27259c	c27807u	a28271u	P13L	E31-	R32-	S33-	R203K	G204R		
	SARS-CoV-2_human_USA_NY-CDC-FG-192538_2021	GenBank:OL908779.1	c241u	c2470u	K38R	c3037u	u5386g	S1265l	L1266-	A1892T	T492I		P132H	L105-	S106-	G107-	I189V	u13195c	P323L	c15240u	I42V	BA.1.1_S:ΔEPE	c25584u		T9I	D3G	Q19E	A63T	a27259c	c27807u	a28271u	P13L	E31-	R32-	S33-	R203K	G204R		
	SARS-CoV-2_human_USA_FL-CDC-FG-192542_2021	GenBank:OL908698.1	c241u	c2470u	K38R	c3037u	u5386g	S1265l	L1266-	A1892T	T492I		P132H	L105-	S106-	G107-	I189V	u13195c	P323L	c15240u	I42V		c25584u		T9I	D3G	Q19E	A63T	a27259c	c27807u	a28271u	P13L	E31-	R32-	S33-	R203K	G204R		
	SARS-CoV-2_human_USA_CA-CDC-FG-192600_2021	GenBank:OL907046.1	c241u	c2470u	K38R	c3037u	u5386g	S1265l	L1266-	A1892T	T492I		P132H	L105-	S106-	G107-	I189V	u13195c	P323L	c15240u	I42V		c25584u		T9I	D3G	Q19E	A63T	a27259c	c27807u	a28271u	P13L	E31-	R32-	S33-	R203K	G204R		
	SARS-CoV-2_human_USA_B01424_2022	GenBank:ON831866.1	c241u	c2470u	K38R	c3037u	u5386g	S1265l	L1266-	A1892T	T492I		P132H	L105-	S106-	G107-	I189V	u13195c	P323L	c15240u	I42V		c25584u		T9I	D3G	Q19E	A63T	a27259c	c27807u	a28271u	P13L	E31-	R32-	S33-	R203K	G204R		
	SARS-CoV-2_human_USA_B01481_2022	GenBank:ON844099.1	c241u	c2470u	K38R	c3037u	u5386g	S1265l	L1266-	A1892T	T492I		P132H	L105-	S106-	G107-	I189V	u13195c	P323L	c15240u	I42V		c25584u		T9I	D3G	Q19E	A63T	a27259c	c27807u	a28271u	P13L	E31-	R32-	S33-	R203K	G204R		
	SARS-CoV-2_human_USA_B01477_2022	GenBank:ON860888.1	c241u	c2470u	K38R	c3037u	u5386g	S1265l	L1266-	A1892T	T492I		P132H	L105-	S106-	G107-	I189V	u13195c	P323L	c15240u	I42V	BA.1.1_S:D339G	c25584u		T9I	D3G	Q19E	A63T	a27259c	c27807u	a28271u	P13L	E31-	R32-	S33-	R203K	G204R		
	SARS-CoV-2_human_USA_B01788_2021	GenBank:OM745971.1	no seq	c2470u	K38R	c3037u	u5386g	S1265l	L1266-	A1892T	T492I		P132H	L105-	S106-	G107-	I189V	u13195c	P323L	c15240u	I42V		c25584u		T9I	D3G	Q19E	A63T	a27259c	c27807u	a28271u	P13L	E31-	R32-	S33-	R203K	G204R		
	SARS-CoV-2_human_USA_V02944_2022	GenBank:ON831672.1	c241u	c2470u	K38R	c3037u	u5386g	S1265l	L1266-	A1892T	T492I		P132H	L105-	S106-	G107-	I189V	u13195c	P323L	c15240u	I42V		c25584u		T9I	D3G	Q19E	A63T	a27259c	c27807u	a28271u	P13L	E31-	R32-	S33-	R203K	G204R		
	SARS-CoV-2_human_USA_DC-CDC-LC0431655_2021	GenBank:OM043643.1	c241u	c2470u	K38R	c3037u	u5386g	S1265l	L1266-	A1892T	T492I		P132H	L105-	S106-	G107-	I189V	u13195c	P323L	c15240u	I42V		c25584u		T9I	D3G	Q19E	A63T	a27259c	c27807u	a28271u	P13L	E31-	R32-	S33-	R203K	G204R		
	SARS-CoV-2_human_USA_OR-CDC-LC0445460_2021	GenBank:OM176192.1	c241u	c2470u	K38R	c3037u	u5386g	S1265l	L1266-	A1892T	T492I		P132H	L105-	S106-	G107-	I189V	u13195c	P323L	c15240u	I42V		c25584u		T9I	D3G	Q19E	A63T	a27259c	c27807u	a28271u	P13L	E31-	R32-	S33-	R203K	G204R		
	SARS-CoV-2_human_USA_SC-CDC-LC0496388_2021	GenBank:OM043649.1	c241u	c2470u	K38R	c3037u	u5386g	S1265l	L1266-	A1892T	T492I		P132H	L105-	S106-	G107-	I189V	u13195c	P323L	c15240u	I42V	BA.1.1_S:L371S	c25584u		T9I	D3G	Q19E	A63T	a27259c	c27807u	a28271u	P13L	E31-	R32-	S33-	R203K	G204R		
	SARS-CoV-2_human_USA_OR-CDC-LC0475607_2022	GenBank:OM343689.1	c241u	c2470u	K38R	c3037u	u5386g	S1265l	L1266-	A1892T	T492I		P132H	L105-	S106-	G107-	I189V	u13195c	P323L	c15240u	I42V		c25584u		T9I	D3G	Q19E	A63T	a27259c	c27807u	a28271u	P13L	E31-	R32-	S33-	R203K	G204R		
	SARS-CoV-2_human_USA_UT-UPHL_22010794104Z_2021	GenBank:OM295527.1	c241u	c2470u	K38R	c3037u	u5386g	S1265l	L1266-	A1892T	T492I		P132H	L105-	S106-	G107-	I189V	u13195c	P323L	c15240u	I42V		c25584u		T9I	D3G	Q19E	A63T	a27259c	c27807u	a28271u	P13L	E31-	R32-	S33-	R203K	G204R		
	SARS-CoV-2_human_USA_WI-CDC-MMB14023738_2022	GenBank:OM894975.1	c241u	c2470u	K38R	c3037u	u5386g	S1265l	L1266-	A1892T	T492I		P132H	L105-	S106-	G107-	I189V	u13195c	P323L	c15240u	I42V		c25584u		T9I	D3G	Q19E	A63T	a27259c	c27807u	a28271u	P13L	E31-	R32-	S33-	R203K	G204R		
	SARS-CoV-2_human_USA_CDC-MMB14068790_2022	GenBank:OM894984.1	c241u	c2470u	K38R	c3037u	u5386g	S1265l	L1266-	A1892T	T492I		P132H	L105-	S106-	G107-	I189V	u13195c	P323L	c15240u	I42V		c25584u		T9I	D3G	Q19E	A63T	a27259c	c27807u	a28271u	P13L	E31-	R32-	S33-	R203K	G204R		
	SARS-CoV-2_human_USA_CO-CDC-MMB14067143_2022	GenBank:OM822024.1	c241u	c2470u	K38R	c3037u	u5386g	S1265l	L1266-	A1892T	T492I		P132H	L105-	S106-	G107-	I189V	u13195c	P323L	c15240u	I42V	BA.1.1_S:F375S	c25584u		T9I	D3G	Q19E	A63T	a27259c	c27807u	a28271u	P13L	E31-	R32-	S33-	R203K	G204R		
	SARS-CoV-2_human_USA_CO-CDC-MMB14142193_2022	GenBank:OM846844.1	c241u	c2470u	K38R	c3037u	u5386g	S1265l	L1266-	A1892T	T492I		P132H	L105-	S106-	G107-	I189V	u13195c	P323L	c15240u	I42V		c25584u		T9I	D3G	Q19E	A63T	a27259c	c27807u	a28271u	P13L	E31-	R32-	S33-	R203K	G204R		
	SARS-CoV-2_human_USA_GA-CDC-MMB14163308_2022	GenBank:OM906550.1	c241u	c2470u	K38R	c3037u	u5386g	S1265l	L1266-	A1892T	T492I		P132H	L105-	S106-	G107-	I189V	u13195c	P323L	c15240u	I42V		c25584u		T9I	D3G	Q19E	A63T	a27259c	c27807u	a28271u	P13L	E31-	R32-	S33-	R203K	G204R		
	SARS-CoV-2_human_USA_FL-CDC-ASC21053409_2021	GenBank:OM032933.1	c241u	c2470u	K38R	c3037u	u5386g	S1265l	L1266-	A1892T	T492I		P132H	L105-	S106-	G107-	I189V	u13195c	P323L	c15240u	I42V		c25584u		T9I	D3G	Q19E	A63T	a27259c	c27807u	a28271u	P13L	E31-	R32-	S33-	R203K	G204R		
	SARS-CoV-2_human_USA_OH-CDC-ASC21053263_2021	GenBank:OM036323.1	c241u	c2470u	K38R	c3037u	u5386g	S1265l	L1266-	A1892T	T492I		P132H	L105-	S106-	G107-	I189V	u13195c	P323L	c15240u	I42V		c25584u		T9I	D3G	Q19E	A63T	a27259c	c27807u	a28271u	P13L	E31-	R32-	S33-	R203K	G204R		
	SARS-CoV-2_human_USA_FL-CDC-ASC21053624_2021	GenBank:OM036331.1	c241u	c2470u	K38R	c3037u	u5386g	S1265l	L1266-	A1892T	T492I		P132H	L105-	S106-	G107-	I189V	u13195c	P323L	c15240u	I42V	BA.1.1_S:N417K	c25584u		T9I	D3G	Q19E	A63T	a27259c	c27807u	a28271u	P13L	E31-	R32-	S33-	R203K	G204R		
	SARS-CoV-2_human_USA_FL-CDC-ASC21062413_2021	GenBank:OM036585.1	c241u	c2470u	K38R	c3037u	u5386g	S1265l	L1266-	A1892T	T492I		P132H	L105-	S106-	G107-	I189V	u13195c	P323L	c15240u	I42V		c25584u		T9I	D3G	Q19E	A63T	a27259c	c27807u	a28271u	P13L	E31-	R32-	S33-	R203K	G204R		
	SARS-CoV-2_human_USA_FL-GD-122121-173_2021	GenBank:OM082327.1	c241u	c2470u	K38R	c3037u	u5386g	S1265l	L1266-	A1892T	T492I		P132H	L105-	S106-	G107-	I189V	u13195c	P323L	c15240u	I42V		c25584u		T9I	D3G	Q19E	A63T	a27259c	c27807u	a28271u	P13L	E31-	R32-	S33-	R203K	G204R		
	SARS-CoV-2_human_USA_NC-CDC-ASC21066612_2021	GenBank:OM196115.1		c2470u	K38R	c3037u	u5386g	S1265l	L1266-	A1892T	T492I		P132H	L105-	S106-	G107-	I189V	u13195c	P323L	c15240u	I42V		c25584u		T9I	D3G	Q19E	A63T	a27259c	c27807u	a28271u	P13L	E31-	R32-	S33-	R203K	G204R		
	SARS-CoV-2_human_USA_FL-CDC-ASC21062436_2021	GenBank:OM036875.1	c241u	c2470u	K38R	c3037u	u5386g	S1265l	L1266-	A1892T	T492I		P132H	L105-	S106-	G107-	I189V	u13195c	P323L	c15240u	I42V	BA.1.1_S:K440N	c25584u		T9I	D3G	Q19E	A63T	a27259c	c27807u	a28271u	P13L	E31-	R32-	S33-	R203K	G204R		
	SARS-CoV-2_human_USA_OH-CDC-ASC21063102_2021	GenBank:OM099560.1	c241u	c2470u	K38R	c3037u	u5386g	S1265l	L1266-	A1892T	T492I		P132H	L105-	S106-	G107-	I189V	u13195c	P323L	c15240u	I42V		c25584u		T9I	D3G	Q19E	A63T	a27259c	c27807u	a28271u	P13L	E31-	R32-	S33-	R203K	G204R		
	SARS-CoV-2_human_USA_NJ-CDC-ASC21064018_2021	GenBank:OM102746.1	c241u	c2470u	K38R	c3037u	u5386g	S1265l	L1266-	A1892T	T492I		P132H	L105-	S106-	G107-	I189V	u13195c	P323L	c15240u	I42V		c25584u		T9I	D3G	Q19E	A63T	a27259c	c27807u	a28271u	P13L	E31-	R32-	S33-	R203K	G204R		
	SARS-CoV-2_human_BHR_21120016543_S81_L001_2021	GenBank:OM047048.1	c241u	c2470u	K38R	c3037u	u5386g	S1265l	L1266-	A1892T	T492I		P132H	L105-	S106-	G107-	I189V	u13195c	P323L	c15240u	I42V		c25584u		T9I	D3G	Q19E	A63T	a27259c	c27807u	a28271u	P13L	E31-	R32-	S33-	R203K	G204R		
	SARS-CoV-2_human_USA_NY-CDC-ASC21062763_2021	GenBank:OM079299.1	c241u	c2470u	K38R	c3037u	u5386g	S1265l	L1266-	A1892T	T492I		P132H	L105-	S106-	G107-	I189V	u13195c	P323L	c15240u	I42V		c25584u		T9I	D3G	Q19E	A63T	a27259c	c27807u	a28271u	P13L	E31-	R32-	S33-	R203K	G204R		
	SARS-CoV-2_human_USA_IL-CDC-ASC21063176_2021	GenBank:OM099911.1	c241u	c2470u	K38R	c3037u	u5386g	S1265l	L1266-	A1892T	T492I		P132H	L105-	S106-	G107-	I189V	u13195c	P323L	c15240u	I42V	BA.1.1_S:S446G	c25584u		T9I	D3G	Q19E	A63T	a27259c	c27807u	a28271u	P13L	E31-	R32-	S33-	R203K	G204R		
	SARS-CoV-2_human_USA_CDC-ASC21063282_2021	GenBank:OM099398.1	c241u	c2470u	K38R	c3037u	u5386g	S1265l	L1266-	A1892T	T492I		P132H	L105-	S106-	G107-	I189V	u13195c	P323L	c15240u	I42V		c25584u		T9I	D3G	Q19E	A63T	a27259c	c27807u	a28271u	P13L	E31-	R32-	S33-	R203K	G204R		
	SARS-CoV-2_human_USA_IL-CDC-ASC21065216_2021	GenBank:OM097010.1	c241u	c2470u	K38R	c3037u	u5386g	S1265l	L1266-	A1892T	T492I		P132H	L105-	S106-	G107-	I189V	u13195c	P323L	c15240u	I42V		c25584u		T9I	D3G	Q19E	A63T	a27259c	c27807u	a28271u	P13L	E31-	R32-	S33-	R203K	G204R		
	SARS-CoV-2_human_USA_PR-CDC-ASC21063978O_2021	GenBank:OM173300.1	c241u	c2470u	K38R	c3037u	u5386g	S1265l	L1266-	A1892T	T492I		P132H	L105-	S106-	G107-	I189V	u13195c	P323L	c15240u	I42V		c25584u		T9I	D3G	Q19E	A63T	a27259c	c27807u	a28271u	P13L	E31-	R32-	S33-	R203K	G204R		
	SARS-CoV-2_human_USA_MIN-CDC-IB-10458173152606_2022	GenBank:OM809961.1	c241u	c2470u	K38R	c3037u	u5386g	S1265l	L1266-	A1892T	T492I		P132H	L105-	S106-	G107-	I189V	u13195c	P323L	c15240u	I42V		c25584u		T9I	D3G	Q19E	A63T	a27259c	c27807u	a28271u	P13L	E31-	R32-	S33-	R203K	G204R		
	SARS-CoV-2_human_USA_MIN-CDC-IB-K150827370S8_2022	GenBank:OM809970.1	c241u	c2470u	K38R	c3037u	u5386g	S1265l	L1266-	A1892T	T492I		P132H	L105-	S106-	G107-	I189V	u13195c	P323L	c15240u	I42V		c25584u		T9I	D3G	Q19E	A63T	a27259c	c27807u	a28271u	P13L	E31-	R32-	S33-	R203K	G204R		
	SARS-CoV-2_human_USA_NJ-CDC-IB-K249131612949_2022	GenBank:OM983325.1	c241u	c2470u	K38R	c3037u	u5386g	S1265l	L1266-	A1892T	T492I		P132H	L105-	S106-	G107-	I189V	u13195c	P323L	c15240u	I42V	BA.1.1_S:N477S	c25584u		T9I	D3G	Q19E	A63T	a27259c	c27807u	a28271u	P13L	E31-	R32-	S33-	R203K	G204R		
	SARS-CoV-2_human_USA_CA_CDPH-8000000114_2022	GenBank:ON618010.1	c241u	c2470u	K38R	c3037u	u5386g	S1265l	L1266-	A1892T	T492I		P132H	L105-	S106-	G107-	I189V	u13195c	P323L	c15240u	I42V		c25584u		T9I	D3G	Q19E	A63T	a27259c	c27807u	a28271u	P13L	E31-	R32-	S33-	R203K	G204R		
	SARS-CoV-2_human_USA_IN-GD-122821-176_2021	GenBank:OM094691.1	c241u	c2470u	K38R	c3037u	u5386g	S1265l	L1266-	A1892T	T492I		P132H	L105-	S106-	G107-	I189V	u13195c	P323L	c15240u	I42V		c25584u		T9I	D3G	Q19E	A63T	a27259c	c27807u	a28271u	P13L	E31-	R32-	S33-	R203K	G204R		
	SARS-CoV-2_human_USA_FL-CDC-STM-VAVMKB0Y2_2022	GenBank:ON021265.1	c241u	c2470u	K38R	c3037u	u5386g	S1265l	L1266-	A1892T	T492I		P132H	L105-	S106-	G107-	I189V	u13195c	P323L	c15240u	I42V		c25584u		T9I	D3G	Q19E	A63T	a27259c	c27807u	a28271u	P13L	E31-	R32-	S33-	R203K	G204R		
	SARS-CoV-2_human_USA_FL-CDC-STM-3WN4DJ4MB_2022	GenBank:ON078219.1	c241u	c2470u	K38R	c3037u	u5386g	S1265l	L1266-	A1892T	T492I		P132H	L105-	S106-	G107-	I189V	u13195c	P323L	c15240u	I42V		c25584u		T9I	D3G	Q19E	A63T	a27259c	c27807u	a28271u	P13L	E31-	R32-	S33-	R203K	G204R		
	SARS-CoV-2_human_USA_GA-CDC-STM-NCVQ7BEX8_2022	GenBank:ON096988.1	c241u	c2470u	K38R	c3037u	u5386g	S1265l	L1266-	A1892T	T492I		P132H	L105-	S106-	G107-	I189V	u13195c	P323L	c15240u	I42V	BA.1.1_S:K478T	c25584u		T9I	D3G	Q19E	A63T	a27259c	c27807u	a28271u	P13L	E31-	R32-	S33-	R203K	G204R		
BA.1.1 -0.1	SARS-CoV-2_human_USA_NV-CDC-ASC21073764_2022	GenBank:ON144127.1	c241u	c2470u	K38R	c3037u	u5386g	S1265l	L1266-	A1892T	T492I		P132H	L105-	S106-	G107-	I189V	u13195c	P323L	c15240u	I42V		c25584u		T9I	D3G	Q19E	A63T	a27259c	c27807u	a28271u	P13L	E31-	R32-	S33-	R203K	G204R		
	SARS-CoV-2_human_USA_GA-CDC-ASC21049663_2022	GenBank:OM730527.1	c241u	c2470u	K38R	c3037u	u5386g	S1265l	L1266-	A1892T	T492I		P132H	L105-	S106-	G107-	I189V	u13195c	P323L	c15240u	I42V		c25584u		T9I	D3G	Q19E	A63T	a27259c	c27807u	a28271u	P13L	E31-	R32-	S33-	R203K	G204R		
	SARS-CoV-2_human_USA_CA-CDC-LC0459774_2021	GenBank:OM385284.1	c241u	c2470u	K38R	c3037u	u5386g	S1265l	L1266-	A1892T	T492I		P132H	L105-	S106-	G107-	I189V	u13195c	P323L	c15240u	I42V		c25584u		T9I	D3G	Q19E	A63T	a27259c	c27807u	a28271u	P13L	E31-	R32-	S33-	R203K	G204R		
	SARS-CoV-2_human_USA_NV-CDC-ASC21063853S_2021	GenBank:OM195119.1	c241u	c2470u	K38R	c3037u	u5386g	S1265l	L1266-	A1892T	T492I		P132H	L105-	S106-	G107-	I189V	u13195c	P323L	c15240u	I42V	BA.1.1_S:A484E	c25584u		T9I	D3G	Q19E	A63T	a27259c	c27807u	a28271u	P13L	E31-	R32-	S33-	R203K	G204R		
	SARS-CoV-2_human_USA_IL-CDC-ASC21063953_2021	GenBank:OM199353.1	c241u	c2470u	K38R	c3037u	u5386g	S1265l	L1266-	A1892T	T492I		P132H	L105-	S106-	G107-	I189V	u13195c	P323L	c15240u	I42V		c25584u		T9I	D3G	Q19E	A63T	a27259c	c27807u	a28271u	P13L	E31-	R32-	S33-	R203K	G204R		
	SARS-CoV-2_human_USA_KY-GD-122821-26_2021	GenBank:OM084630.1	c241u	c2470u	K38R	c3037u	u5386g	S1265l	L1266-	A1892T	T492I		P132H	L105-	S106-	G107-	I189V	u13195c	P323L	c15240u	I42V		c25584u		T9I	D3G	Q19E	A63T	a27259c	c27807u	a28271u	P13L	E31-	R32-	S33-	R203K	G204R		
	SARS-CoV-2_human_USA_OH-GD-122821-315_2021	GenBank:OM084605.1	c241u	c2470u	K38R	c3037u	u5386g	S1265l	L1266-	A1892T	T492I		P132H	L105-	S106-	G107-	I189V	u13195c	P323L	c15240u	I42V		c25584u		T9I	D3G	Q19E	A63T	a27259c	c27807u	a28271u	P13L	E31-	R32-	S33-	R203K	G204R		
	SARS-CoV-2_human_USA_KY-GD-122821-52_2021	GenBank:OM094621.1	c241u	c2470u	K38R	c3037u	u5386g	S1265l	L1266-	A1892T	T492I		P132H	L105-	S106-	G107-	I189V	u13195c	P323L	c15240u	I42V		c25584u		T9I	D3G	Q19E	A63T	a27259c	c27807u	a28271u	P13L	E31-	R32-	S33-	R203K	G204R		
	SARS-CoV-2_human_USA_MID-CDC-LC0458732_2022	GenBank:OM399369.1	no seq	c2470u	K38R	c3037u	u5386g	S1265l	L1266-	A1892T	T492I		P132H	L105-	S106-	G107-	I189V	u13195c	P323L	c15240u	I42V		c25584u		T9I	D3G	Q19E	A63T	a27259c	c27807u	a28271u	P13L	E31-	R32-	S33-	R203K	G204R		
	SARS-CoV-2_human_USA_NJ-CDC-LC0479598_2022	GenBank:OM411574.1	c241u	c2470u	K38R	c3037u	u5386g	S1265l	L1266-	A1892T	T492I		P132H	L105-	S106-	G107-	I189V	u13195c	P323L	c15240u	I42V	BA.1.1_S:R493Q	c25584u		T9I	D3G	Q19E	A63T	a27259c	c27807u	a28271u	P13L	E31-	R32-	S33-	R203K	G204R		
	SARS-CoV-2_human_USA_CT-CDC-QDX31191141_2022	GenBank:OM591311.1	c241u	c2470u	K38R	c3037u	u5386g	S1265l	L1266-	A1892T	T492I		P132H	L105-	S106-	G107-	I189V	u13195c	P323L	c15240u	I42V		c25584u		T9I	D3G	Q19E	A63T	a27259c	c27807u	a28271u	P13L	E31-	R32-	S33-	R203K	G204R		
	SARS-CoV-2_human_USA_NJ-PHEL-V22008671_2022	GenBank:OM720486.1	c241u	c2470u	K38R	c3037u	u5386g	S1265l	L1266-	A1892T	T492I		P132H	L105-	S106-	G107-	I189V	u13195c	P323L	c15240u	I42V		c25584u		T9I	D3G	Q19E	A63T	a27259c	c27807u	a28271u	P13L	E31-	R32-	S33-	R203K	G204R		
	SARS-CoV-2_human_USA_CO-CDC-LC0489301_2022	GenBank:OM429777.1	c241u	c2470u	K38R	c3037u	u5386g			A1892T	T492I		P132H	L105-	S106-	G107-	I189V	u13195c	P323L	c15240u	I42V	BA.1.1_S:S496G	c25584u		T9I	D3G	Q19E	A63T	a27259c	c27807u	a28271u	P13L	E31-	R32-	S33-	R203K	G204R		
	SARS-CoV-2_human_USA_IL-CDC-ASC21073373_2022	GenBank:ON047062.1	c241u	c2470u	K38R	c3037u	ND	S1265l	L1266-	A1892T	T492I		P

Fig. 5

A

SARS-CoV-2_Omicron_BA1-BA2 recombinant (BA1/2)

Variant	Definition	GenBank Accession No.	deletion[5]						deletion[1]				deletion[2]			deletion[3]			insertion[4]	Non-synonymous: Receptor-binding domain (RBD) 319 – 541																															Synonymous			
								A67V	H69-	V70-	T95I	G142D	V143-	Y144-	Y145-	N211I	L212-		215ins. EPE	G339D	R346K	S371L	S373P	S375F				K417N	N440K	G446S	S477N	T478K	E484A	Q493R	G496S	Q498R	N501Y	Y505H	T547K	D614G	H655Y	N679K	P681H	N764K	D796Y	N856K	Q954H	N969K	L981F	Others*	c21595u*	c22792u*	c25000u	Others*
			T19I	L24-	P25-	P26-	A27S					G142D						V213G		G339D		S371F	S373P	S375F	T376A	D405N	R408S	K417N	N440K		S477N	T478K	E484A	Q493R		Q498R	N501Y	Y505H		D614G	H655Y	N679K	P681H	N764K	D796Y		Q954H	N969K						
BA1.1	SARS-CoV-2_human_USA_TX-CDC-QDX31492531_2021	GenBank: OL897126.1						A67V	H69-	V70-	T95I	G142D	V143-	Y144-	Y145-	N211I	L212-		215ins. EPE	G339D	R346K	S371L	S373P	S375F				K417N	N440K	G446S	S477N	T478K	E484A	Q493R	G496S	Q498R	N501Y	Y505H	T547K	D614G	H655Y	N679K	P681H	N764K	D796Y	N856K	Q954H	N969K	L981F				c25000u	
BA2	SARS-CoV-2_human_USA_CA-CDC-FG-229617_2021	GenBank: OM233931.1	T19I	L24-	P25-	P26-	A27S					G142D						V213G		G339D		S371F	S373P	S375F	T376A	D405N	R408S	K417N	N440K		S477N	T478K	E484A	Q493R		Q498R	N501Y	Y505H		D614G	H655Y	N679K	P681H	N764K	D796Y		Q954H	N969K					c25000u	
BA1/2	SARS-CoV-2_human_USA_VA-CDC-LC0464413_2022	GenBank: OM360636.1	T19I					A67V	H69-	V70-	T95I	G142D	V143-	Y144-	Y145-	N211I	L212-		215ins. EPE	G339D		S371L	S373P	S375F				K417N	N440K	G446S	S477N	T478K	E484A	Q493R	G496S	Q498R	N501Y	Y505H	T547K	D614G	H655Y	N679K	P681H	N764K	D796Y	N856K	Q954H	N969K	L981F				c25000u	
	SARS-CoV-2_human_USA_NY-CDC-LC0476274_2022	GenBank: OM410816.1	T19I					A67V	H69-	V70-	T95I	G142D	V143-	Y144-	Y145-	N211I	L212-		215ins. EPE	G339D		S371L	S373P	S375F				K417N	N440K	G446S	S477N	T478K	E484A	Q493R	G496S	Q498R	N501Y	Y505H	T547K	D614G	H655Y	N679K	P681H	N764K	D796Y	N856K	Q954H	N969K	L981F				c25000u	
	SARS-CoV-2_human_USA_AZ-CDC-LC0488280_2022	GenBank: OM429902.1	T19I					A67V	H69-	V70-	T95I	G142D	V143-	Y144-	Y145-	N211I	L212-		215ins. EPE	G339D		S371L	S373P	S375F				K417N	N440K	G446S	S477N	T478K	E484A	Q493R	G496S	Q498R	N501Y	Y505H	T547K	D614G	H655Y	N679K	P681H	N764K	D796Y	N856K	Q954H	N969K	L981F				c25000u	
	SARS-CoV-2_human_USA_WA-CDC-LC0499478_2022	GenBank: OM497964.1	T19I					A67V	H69-	V70-	T95I	G142D	V143-	Y144-	Y145-	N211I	L212-		215ins. EPE	G339D		S371L	S373P	S375F				K417N	N440K	G446S	S477N	T478K	E484A	Q493R	G496S	Q498R	N501Y	Y505H	T547K	D614G	H655Y	N679K	P681H	N764K	D796Y	N856K	Q954H	N969K	L981F				c25000u	c25117u
	SARS-CoV-2_human_USA_MS-CDC-ASC210602041_2022	GenBank: OM565587.1	T19I					A67V	H69-	V70-	T95I	G142D	V143-	Y144-	Y145-	N211I	L212-		215ins. EPE	G339D		S371L	S373P	S375F				K417N	N440K	G446S	S477N	T478K	E484A	Q493R	G496S	Q498R	N501Y	Y505H	T547K	D614G	H655Y	N679K	P681H	N764K	D796Y	N856K	Q954H	N969K	L981F				c25000u	
	SARS-CoV-2_human_USA_NJ-CDC-LC0510764_2022	GenBank: OM628132.1	T19I					A67V	H69-	V70-	T95I	G142D	V143-	Y144-	Y145-	N211I	L212-		215ins. EPE	G339D		S371L	S373P	S375F		D405N	R408S	K417N	N440K	G446S	S477N	T478K	E484A	Q493R	G496S	Q498R	N501Y	Y505H	T547K	D614G	H655Y	N679K	P681H	N764K	D796Y		Q954H	N969K	L981F				c25000u	
	SARS-CoV-2_human_USA_MP-CDC-2-5772902_2022	GenBank: ON549899.1	T19I	L24-	P25-	P26-	A27S	A67V	H69-	V70-	T95I	G142D	V143-	Y144-	Y145-	N211I	L212-		215ins. EPE	G339D	R346K	S371L	S373P	S375F				K417N	N440K	G446S	S477N	T478K	E484A	Q493R	G496S	Q498R	N501Y	Y505H		D614G	H655Y	N679K	P681H	N764K	D796Y	N856K	Q954H	N969K	L981F				c25000u	
	SARS-CoV-2_human_USA_NJ-CDC-LC0592441_2022	GenBank: ON449685.1	T19I	L24-	P25-	P26-	A27S	A67V	H69-	V70-	T95I	G142D	V143-	Y144-	Y145-	N211I	L212-		215ins. EPE	G339D		S371L	S373P	S375F		D405N		K417N	N440K	G446S	S477N	T478K	E484A	Q493R	G496S	Q498R	N501Y	Y505H		D614G	H655Y	N679K	P681H	N764K	D796Y		Q954H	N969K					c25000u	
	SARS-CoV-2_human_USA_FL-CDC-QDX35136213_2022	GenBank: ON176765.1	T19I	L24-	P25-	P26-	A27S	A67V	H69-	V70-		G142D	V143-	Y144-	Y145-	N211I	L212-		215ins. EPE	G339D	R346K	S371L	S373P	S375F			R408S	K417N	N440K		S477N	T478K	E484A	Q493R	G496S	Q498R	N501Y	Y505H		D614G	H655Y	N679K	P681H	N764K	D796Y	N856K	Q954H	N969K	L981F				c25000u	
	SARS-CoV-2_human_USA_PA-CDC-LC0510661_2022	GenBank: OM628094.1	T19I	L24-	P25-	P26-	A27S	A67V	H69-	V70-	T95I	G142D	V143-	Y144-	Y145-	N211I	L212-		215ins. EPE	G339D		S371L	S373P	S375F	T376A	D405N	R408S	K417N	N440K		S477N	T478K	E484A	Q493R	G496S	Q498R	N501Y	Y505H		D614G	H655Y	N679K	P681H	N764K	D796Y		Q954H	N969K					c25000u	
	SARS-CoV-2_human_MWI_MLW000918_2022	GenBank: ON099844.1	T19I	L24-	P25-	P26-	A27S	A67V	H69-	V70-	T95I	G142D	V143-	Y144-	Y145-	N211I	L212-		215ins. EPE	G339D		S371F	S373P	S375F	T376A	D405N	R408S	K417N	N440K		S477N	T478K	E484A	Q493R		Q498R	N501Y	Y505H		D614G	H655Y	N679K	P681H	N764K	D796Y		Q954H	N969K					c25000u	
	SARS-CoV-2_human_USA_MD-CDC-LC0548614_2022	GenBank: OM942313.1	T19I	L24-	P25-	P26-	A27S					G142D	V143-	Y144-	Y145-	N211I	L212-		215ins. EPE	G339D		S371F	S373P	S375F	T376A	D405N	R408S	K417N	N440K		S477N	T478K	E484A	Q493R		Q498R	N501Y	Y505H	T547K	D614G	H655Y	N679K	P681H	N764K	D796Y		Q954H	N969K	L981F				c25000u	
	SARS-CoV-2_human_USA_VT-CDC-LC0584068_2022	GenBank: ON395480.1	T19I	L24-	P25-	P26-	A27S	A67V	H69-	V70-	T95I	G142D	V143-	Y144-	Y145-	N211I	L212-		215ins. EPE	G339D		S371F	S373P	S375F	T376A	D405N	R408S	K417N	N440K		S477N	T478K	E484A	Q493R		Q498R	N501Y	Y505H	T547K	D614G	H655Y	N679K	P681H	N764K	D796Y		Q954H	N969K					c25000u	g25126a
	SARS-CoV-2_human_BHR_22020050752_2022	GenBank: ON171854.1						A67V	H69-	V70-	T95I	G142D	V143-	Y144-	Y145-	N211I	L212-		215ins. EPE	G339D		S371F	S373P	S375F	T376A			K417N	N440K	G446S	S477N	T478K	E484A	Q493R	G496S	Q498R	N501Y	Y505H	T547K	D614G	H655Y	N679K	P681H	N764K	D796Y	N856K	Q954H	N969K	L981F				c25000u	
	SARS-CoV-2_human_BHR_22020083147_2022	GenBank: ON172005.1						A67V	H69-	V70-	T95I	G142D	V143-	Y144-	Y145-	N211I	L212-		215ins. EPE	G339D		S371F	S373P	S375F	T376A			K417N	N440K	G446S	S477N	T478K	E484A	Q493R	G496S	Q498R	N501Y	Y505H	T547K	D614G	H655Y	N679K	P681H	N764K	D796Y	N856K	Q954H	N969K	L981F				c25000u	
	SARS-CoV-2_human_BHR_R45902244162_2022	GenBank: ON076710.1						A67VI108:I1	H69-	V70-	T95I	G142D	V143-	Y144-	Y145-	N211I	L212-		215ins. EPE	G339D		S371F	S373P	S375F	T376A	D405N	R408S	K417N		G446S	S477N	T478K	E484A	Q493R	G496S	Q498R	N501Y	Y505H	T547K	D614G	H655Y	N679K	P681H	N764K	D796Y	N856K	Q954H	N969K	L981F	N81K			c25000u	
	SARS-CoV-2_human_PRI_PR-UPRRP-582_2020	GenBank: ON928946.1						A67V	H69-	V70-	T95I	G142D	V143-	Y144-	Y145-	N211I	L212-		215ins. EPE	G339D		S371F	S373P	S375F	T376A	D405N	R408S	K417N	N440K		S477N	T478K	E484A	Q493R		Q498R	N501Y	Y505H	T547K	D614G	H655Y	N679K	P681H	N764K	D796Y	N856K	Q954H	N969K	L981F				c25000u	
	SARS-CoV-2_human_USA_CO-CDPHE-2102746580_2022	GenBank: OM932113.1						A67V	H69-	V70-	T95I	G142D	V143-	Y144-	Y145-	N211I	L212-	V213G	215ins. EPE	G339D	R346K	S371L	S373P	S375F				K417N	N440K	G446S	S477N	T478K	E484A	Q493R	G496S	Q498R	N501Y	Y505H	T547K	D614G	H655Y	N679K	P681H	N764K	D796Y	N856K	Q954H	N969K	L981F		c21595u		c25000u	
	SARS-CoV-2_human_USA_NC-CDC-LC0549417_2022	GenBank: OM942438.1						A67V	H69-	V70-	T95I	G142D	V143-	Y144-	Y145-	N211I	L212-	V213G	215ins. EPE	G339D	R346K	S371L	S373P	S375F				K417N	N440K	G446S	S477N	T478K	E484A	Q493R	G496S	Q498R	N501Y	Y505H	T547K	D614G	H655Y	N679K	P681H	N764K	D796Y	N856K	Q954H	N969K	L981F				c25000u	a23146g
	SARS-CoV-2_human_USA_NC-CDC-LC0558337_2022	GenBank: OM989528.1						A67V	H69-	V70-	T95I	G142D	V143-	Y144-	Y145-	N211I	L212-	V213G	215ins. EPE	G339D	R346K	S371L	S373P	S375F				K417N	N440K	G446S	S477N	T478K	E484A	Q493R	G496S	Q498R	N501Y	Y505H	T547K	D614G	H655Y	N679K	P681H	N764K	D796Y	N856K	Q954H	N969K	L981F				c25000u	a23146g
	SARS-CoV-2_human_USA_VA-CDC-LC0495278_2022	GenBank: OM499181.1						A67V	H69-	V70-	T95I	G142D	V143-	Y144-	Y145-	N211I	L212-	V213G	215ins. EPE	G339D		S371F	S373P	S375F	T376A	D405N	R408S	K417N	N440K		S477N	T478K	E484A	Q493R		Q498R	N501Y	Y505H		D614G	H655Y	N679K	P681H	N764K	D796Y	N856K	Q954H	N969K	L981F				c25000u	
	SARS-CoV-2_human_USA_NJ-CDC-LC0589728_2022	GenBank: ON414822.1						A67V	H69-	V70-	T95I	G142D	V143-	Y144-	Y145-	N211I	L212-		215ins. EPE	G339D		S371F	S373P	S375F	T376A	D405N	R408S	K417N	N440K		S477N	T478K	E484A	Q493R	G496S	Q498R	N501Y	Y505H	T547K	D614G	H655Y	N679K	P681H	N764K	D796Y	N856K	Q954H	N969K	L981F				c25000u	
	SARS-CoV-2_human_USA_CA-CDC-FG-280689_2022	GenBank: OM878325.1						A67V	H69-	V70-	T95I	G142D	V143-	Y144-	Y145-	N211I	L212-		215ins. EPE	G339D		S371F	S373P	S375F	T376A	D405N	R408S	K417N	N440K	G446S	S477N	T478K	E484A	Q493R	G496S	Q498R	N501Y	Y505H	T547K	D614G	H655Y	N679K	P681H	N764K	D796Y	N856K	Q954H	N969K	L981F			c22792u	c25000u	
	SARS-CoV-2_human_BHR_22970089376_2022	GenBank: ON103067.1						A67V	H69-	V70-	T95I	G142D	V143-	Y144-	Y145-	N211I	L212-		215ins. EPE	G339D	R346K	S371F	S373P	S375F	T376A	D405N	R408S	K417N	N440K	G446S	S477N	T478K	E484A	Q493R	G496S	Q498R	N501Y	Y505H	T547K	D614G	H655Y	N679K	P681H	N764K	D796Y	N856K	Q954H	N969K	L981F				c25000u	
	SARS-CoV-2_human_BHR_22970088641_2022	GenBank: ON103153.1						A67V	H69-	V70-	T95I	G142D	V143-	Y144-	Y145-	N211I	L212-		215ins. EPE	G339D	R346K	S371F	S373P	S375F	T376A	D405N	R408S	K417N	N440K	G446S	S477N	T478K	E484A	Q493R	G496S	Q498R	N501Y	Y505H	T547K	D614G	H655Y	N679K	P681H	N764K	D796Y	N856K	Q954H	N969K	L981F				c25000u	
	SARS-CoV-2_human_BHR_22970059078_2022	GenBank: ON419036.1						A67V	H69-	V70-	T95I	G142D	V143-	Y144-	Y145-	N211I	L212-		215ins. EPE	G339D	R346K	S371F	S373P	S375F	T376A	D405N	R408S	K417N	N440K	G446S	S477N	T478K	E484A	Q493R	G496S	Q498R	N501Y	Y505H	T547K	D614G	H655Y	N679K	P681H	N764K	D796Y	N856K	Q954H	N969K	L981F				c25000u	
	SARS-CoV-2_human_PRI_PR-UPRRP-5813_2022	GenBank: ON928719.1						A67V	H69-	V70-	T95I	G142D	V143-	Y144-	Y145-	N211I	L212-		215ins. EPE	G339D	R346K	S371F	S373P	S375F	T376A	D405N	R408S	K417N	N440K	G446S	S477N	T478K	E484A	Q493R	G496S	Q498R	N501Y	Y505H	T547K	D614G	H655Y	N679K	P681H	N764K	D796Y	N856K	Q954H	N969K	L981F		c21595u	c22792u	c25000u	
	SARS-CoV-2_human_USA_MA-MGB-04990_2022	GenBank: ON337887.1						A67V	H69-	V70-	T95I	G142D	V143-	Y144-	Y145-	N211I	L212-		215ins. EPE	G339D		S371F	S373P	S375F	T376A	D405N	R408S	K417N		G446S	S477N	T478K	E484A	Q493R	G496S	Q498R	N501Y	Y505H	T547K	D614G	H655Y	N679K	P681H	N764K	D796Y	N856K	Q954H	N969K	L981F		c21595u			
	SARS-CoV-2_human_BHR_22020079101_2022	GenBank: ON420444.1						A67V	H69-	V70-	T95I	G142D	V143-	Y144-	Y145-	N211I	L212-		215ins. EPE	G339D		S371F	S373P	S375F	T376A	D405N	R408S	K417N		G446S	S477N	T478K	E484A	Q493R	G496S	Q498R	N501Y	Y505H	T547K	D614G	H655Y	N679K	P681H	N764K	D796Y	N856K	Q954H	N969K	L981F				c25000u	
	SARS-CoV-2_human_BHR_22020048762_2022	GenBank: ON146520.1						A67V	H69-	V70-	T95I	G142D	V143-	Y144-	Y145-	N211I	L212-		215ins. EPE	G339D	R346K	S371F	S373P	S375F	T376A			K417N	N440K	G446S	S477N	T478K	E484A	Q493R	G496S	Q498R	N501Y	Y505H	T547K	D614G	H655Y	N679K	P681H	N764K	D796Y	N856K	Q954H	N969K	L981F				c25000u	
	SARS-CoV-2_human_USA_TX-CDC-QDX32791919_2022	GenBank: OM469541.1						A67V	H69-	V70-	T95I	G142D	V143-	Y144-	Y145-	N211I	L212-		215ins. EPE	G339D		S371L	S373P	S375F	T376A			K417N	N440K	G446S	S477N	T478K	E484A	Q493R	G496S	Q498R	N501Y	Y505H	T547K	D614G	H655Y	N679K	P681H	N764K	D796Y	N856K	Q954H	N969K	L981F				c25000u	
	SARS-CoV-2_human_USA_CT-CDC-QDX33920786_2022	GenBank: OM904085.1						A67V	H69-	V70-	T95I	G142D	V143-	Y144-	Y145-	N211I	L212-		215ins. EPE	G339D		S371L	S373P	S375F	T376A			K417N	N440K	G446S	S477N	T478K	E484A	Q493R	G496S	Q498R	N501Y	Y505H	T547K	D614G	H655Y	N679K	P681H	N764K	D796Y	N856K	Q954H	N969K	L981F				c25000u	
	SARS-CoV-2_human_USA_TX-DSHS-18056_2022	GenBank: ON254531.1						A67V	H69-	V70-	T95I	G142D	V143-	Y144-	Y145-	N211I	L212-		215ins. EPE	G339D		S371L	S373P	S375F	T376A			K417N	N440K	G446S	S477N	T478K	E484A	Q493R	G496S	Q498R	N501Y	Y505H	T547K	D614G	H655Y	N679K	P681H	N764K	D796Y	N856K	Q954H	N969K	L981F				c25000u	g21724a,a23416T
	SARS-CoV-2_human_USA_CA-CDC-FG-283967_2022	GenBank: OM881098.1						A67V	H69-	V70-	T95I	G142D	V143-	Y144-	Y145-	N211I	L212-		215ins. EPE	G339D		S371L	S373P	S375F		D405N	R408S	K417N	N440K	G446S	S477N	T478K	E484A	Q493R	G496S	Q498R	N501Y	Y505H	T547K	D614G	H655Y	N679K	P681H	N764K	D796Y	N856K	Q954H	N969K	L981F				c25000u	
	SARS-CoV-2_human_USA_IL-CDC-LC0582943_2022	GenBank: ON373310.1						A67V	H69-	V70-	T95I	G142D	V143-	Y144-	Y145-	N211I	L212-		215ins. EPE	G339D	R346K	S371L	S373P	S375F		D405N	R408S	K417N	N440K	G446S	S477N	T478K	E484A	Q493R	G496S	Q498R	N501Y	Y505H	T547K	D614G	H655Y	N679K	P681H	N764K	D796Y	N856K	Q954H	N969K					c25000u	c25006u

B

SARS-CoV-2_isolated in Puerto Rico in 2020

Variant	Definition	GenBank Accession No.	T19I	L24-	P25-	P26-	A27S	A67V	H69-	V70-	T95I	G142D	V143-	Y144-	Y145-	N211I	L212-	V213G	215ins. EPE	G339D	R346K	S371L/S371F	S373P	S375F	T376A	D405N	R408S	K417N	N440K	G446S	S477N	T478K	E484A	Q493R	G496S	Q498R	N501Y	Y505H	T547K	D614G	H655Y	N679K	P681H	N764K	D796Y	N856K	Q954H	N969K	L981F	Others*	c21595u*	c22792u*	c25000u	Others*
BA.1.1	SARS-CoV-2_human_PRI_PR-UPRRP-477_2020	GenBank: ON928761.1						A67V	H69-	V70-	T95I	G142D	V143-	Y144-	Y145-	N211I	L212-		215ins. EPE	G339D	R346K	S371L	S373P	S375F				K417N	N440K	G446S	S477N	T478K	E484A	Q493R	G496S	Q498R	N501Y	Y505H	T547K	D614G	H655Y	N679K	P681H	N764K	D796Y	N856K	Q954H	N969K	L981F	V83L	c21595u		c25000u	
	SARS-CoV-2_human_PRI_PR-UPRRP-483_2020	GenBank: ON928660.1						A67V	H69-	V70-	T95I	G142D	V143-	Y144-	Y145-	N211I	L212-		215ins. EPE	G339D	R346K	S371L	S373P	S375F				K417N	N440K	G446S	S477N	T478K	E484A	Q493R	G496S	Q498R	N501Y	Y505H	T547K	D614G	H655Y	N679K	P681H	N764K	D796Y	N856K	Q954H	N969K	L981F		c21595u		c25000u	
	SARS-CoV-2_human_PRI_PR-UPRRP-484_2020	GenBank: ON928794.1						A67V	H69-	V70-	T95I	G142D	V143-	Y144-	Y145-	N211I	L212-		215ins. EPE	G339D	R346K	S371L	S373P	S375F				K417N	N440K	G446S	S477N	T478K	E484A	Q493R	G496S	Q498R	N501Y	Y505H	T547K	D614G	H655Y	N679K	P681H	N764K	D796Y	N856K	Q954H	N969K	L981F		c21595u		c25000u	
	SARS-CoV-2_human_PRI_PR-UPRRP-485_2020	GenBank: ON928762.1						A67V	H69-	V70-	T95I	G142D	V143-	Y144-	Y145-	N211I	L212-		215ins. EPE	G339D	R346K	S371L	S373P	S375F				K417N	N440K	G446S	S477N	T478K	E484A	Q493R	G496S	Q498R	N501Y	Y505H	T547K	D614G	H655Y	N679K	P681H	N764K	D796Y	N856K	Q954H	N969K	L981F		c21595u		c25000u	
	SARS-CoV-2_human_PRI_PR-UPRRP-492_2020	GenBank: ON928848.1						A67V	H69-	V70-	T95I	G142D	V143-	Y144-	Y145-	N211I	L212-		215ins. EPE	G339D	R346K	S371L	S373P	S375F				K417N	N440K	G446S	S477N	T478K	E484A	Q493R	G496S	Q498R	N501Y	Y505H	T547K	D614G	H655Y	N679K	P681H	N764K	D796Y	N856K	Q954H	N969K	L981F		c21595u		c25000u	
	SARS-CoV-2_human_PRI_PR-UPRRP-493_2020	GenBank: ON928741.1						A67V	H69-	V70-	T95I	G142D	V143-	Y144-	Y145-	N211I	L212-		215ins. EPE	G339D	R346K	S371L	S373P	S375F				K417N	N440K	G446S	S477N	T478K	E484A	Q493R	G496S	Q498R	N501Y	Y505H	T547K	D614G	H655Y	N679K	P681H	N764K	D796Y	N856K	Q954H	N969K	L981F		c21595u		c25000u	
	SARS-CoV-2_human_PRI_PR-UPRRP-499_2020	GenBank: ON928918.1						A67V	H69-	V70-	T95I	G142D	V143-	Y144-	Y145-	N211I	L212-		215ins. EPE	G339D	R346K	S371L	S373P	S375F				K417N	N440K	G446S	S477N	T478K	E484A	Q493R	G496S	Q498R	N501Y	Y505H	T547K	D614G	H655Y	N679K	P681H	N764K	D796Y	N856K	Q954H	N969K	L981F		c21595u		c25000u	
	SARS-CoV-2_human_PRI_PR-UPRRP-500_2020	GenBank: ON928680.1						A67V	H69-	V70-	T95I	G142D	V143-	Y144-	Y145-	N211I	L212-		215ins. EPE	G339D	R346K	S371L	S373P	S375F				K417N	N440K	G446S	S477N	T478K	E484A	Q493R	G496S	Q498R	N501Y	Y505H	T547K	D614G	H655Y	N679K	P681H	N764K	D796Y	N856K	Q954H	N969K	L981F		c21595u		c25000u	
	SARS-CoV-2_human_PRI_PR-UPRRP-501_2020	GenBank: ON928975.1						A67V	H69-	V70-	T95I	G142D	V143-	Y144-	Y145-	N211I	L212-		215ins. EPE	G339D	R346K	S371L	S373P	S375F				K417N	N440K	G446S	S477N	T478K	E484A	Q493R	G496S	Q498R	N501Y	Y505H	T547K	D614G	H655Y	N679K	P681H	N764K	D796Y	N856K	Q954H	N969K	L981F		c21595u		c25000u	
	SARS-CoV-2_human_PRI_PR-UPRRP-508_2020	GenBank: ON928949.1						A67V	H69-	V70-	T95I	G142D	V143-	Y144-	Y145-	N211I	L212-		215ins. EPE	G339D	R346K	S371L	S373P	S375F				K417N	N440K	G446S	S477N	T478K	E484A	Q493R	G496S	Q498R	N501Y	Y505H	T547K	D614G	H655Y	N679K	P681H	N764K	D796Y	N856K	Q954H	N969K	L981F		c21595u		c25000u	
	SARS-CoV-2_human_PRI_PR-UPRRP-509_2020	GenBank: ON928673.1						A67V	H69-	V70-	T95I	G142D	V143-	Y144-	Y145-	N211I	L212-		215ins. EPE	G339D	R346K	S371L	S373P	S375F				K417N	N440K	G446S	S477N	T478K	E484A	Q493R	G496S	Q498R	N501Y	Y505H	T547K	D614G	H655Y	N679K	P681H	N764K	D796Y	N856K	Q954H	N969K	L981F		c21595u		c25000u	
	SARS-CoV-2_human_PRI_PR-UPRRP-515_2020	GenBank: ON928865.1						A67V	H69-	V70-	T95I	G142D	V143-	Y144-	Y145-	N211I	L212-		215ins. EPE	G339D	R346K	S371L	S373P	S375F				K417N	N440K	G446S	S477N	T478X	E484A	Q493R	G496S	Q498R	N501Y	Y505H	T547K	D614G	H655Y	N679K	P681H	N764K	D796Y	N856K	Q954H	N969K	L981F		c21595u		c25000u	
	SARS-CoV-2_human_PRI_PR-UPRRP-517_2020	GenBank: ON928716.1						A67V	H69-	V70-	T95I	G142D	V143-	Y144-	Y145-	N211I	L212-		215ins. EPE	G339D	R346K	S371L	S373P	S375F				K417N	N440K	G446S	S477N	T478K	E484A	Q493R	G496S	Q498R	N501Y	Y505H	T547K	D614G	H655Y	N679K	P681H	N764K	D796Y	N856K	Q954H	N969K	L981F		c21595u		c25000u	
	SARS-CoV-2_human_PRI_PR-UPRRP-524_2020	GenBank: ON928663.1						A67V	H69-	V70-	T95I	G142D	V143-	Y144-	Y145-	N211I	L212-		215ins. EPE	G339D	R346K	S371L	S373P	S375F				K417N	N440K	G446S	S477N	T478K	E484A	Q493R	G496S	Q498R	N501Y	Y505H	T547K	D614G	H655Y	N679K	P681H	N764K	D796Y	N856K	Q954H	N969K	L981F				c25000u	
	SARS-CoV-2_human_PRI_PR-UPRRP-525_2020	GenBank: ON928779.1						A67V	H69-	V70-	T95I	G142D	V143-	Y144-	Y145-	N211I	L212-		215ins. EPE	G339D	R346K	S371L	S373P	S375F				K417N	N440K	G446S	S477N	T478K	E484A	Q493R	G496S	Q498R	N501Y	Y505H	T547K	D614G	H655Y	N679K	P681H	N764K	D796Y	N856K	Q954H	N969K	L981F		c21595u		c25000u	
	SARS-CoV-2_human_PRI_PR-UPRRP-532_2020	GenBank: ON928896.1						A67V	H69-	V70-	T95I	G142D	V143-	Y144-	Y145-	N211I	L212-		215ins. EPE	G339D	R346K	S371L	S373P	S375F				K417N	N440K	G446S	S477N	T478K	E484A	Q493R	G496S	Q498R	N501Y	Y505H	T547K	D614G	H655Y	N679K	P681H	N764K	D796Y	N856K	Q954H	N969K	L981F		c21595u		c25000u	
BA.1/2	SARS-CoV-2_human_PRI_PR-UPRRP-582_2020	GenBank: ON928946.1						A67V	H69-	V70-	T95I	G142D	V143-	Y144-	Y145-	N211I	L212-		215ins. EPE	G339D		S371F	S373P	S375F	T376A	D405N	R408S	K417N	N440K		S477N	T478K	E484A	Q493R		Q498R	N501Y	Y505H	T547K	D614G	H655Y	N679K	P681H	N764K	D796Y	N856K	Q954H	N969K	L981F				c25000u	
BA.2 & BA.2-0.1 (K440N)	SARS-CoV-2_human_PRI_PR-UPRRP-278_2020	GenBank: ON928912.1	T19I	L24-	P25-	P26-	A27S					G142D						V213G		G339D		S371F	S373P	S375F	T376A	D405N	R408S	K417N			S477N	T478K	E484A	Q493R		Q498R	N501Y	Y505H		D614G	H655Y	N679K	P681H	N764K	D796Y		Q954H	N969K				c22792u	c25000u	
	SARS-CoV-2_human_PRI_PR-UPRRP-574_2020	GenBank: ON928704.1	T19I	L24-	P25-	P26-	A27S					G142D						V213G		G339D		S371F	S373P	S375F	T376A	D405N	R408S	K417N			S477N	T478K	E484A	Q493R		Q498R	N501Y	Y505H		D614G	H655Y	N679K	P681H	N764K	D796Y		Q954H	N969K		F79S			c25000u	
	SARS-CoV-2_human_PRI_PR-UPRRP-575_2020	GenBank: ON928873.1	T19I	L24-	P25-	P26-	A27S					G142D						V213G		G339D		S371F	S373P	S375F	T376A	D405N	R408S	K417N	N440K		S477N	T478K	E484A	Q493R		Q498R	N501Y	Y505H		D614G	H655Y	N679K	P681H	N764K	D796Y		Q954H	N969K				c22792u	c25000u	
	SARS-CoV-2_human_PRI_PR-UPRRP-576_2020	GenBank: ON928813.1	T19I	L24-	P25-	P26-	A27S					G142D						V213G		G339D		S371F	S373P	S375F	T376A	D405N	R408S	K417N	N440K		S477N	T478K	E484A	Q493R		Q498R	N501Y	Y505H		D614G	H655Y	N679K	P681H	N764K	D796Y		Q954H	N969K					c25000u	
	SARS-CoV-2_human_PRI_PR-UPRRP-579_2020	GenBank: ON928898.1	T19I	L24-	P25-	P26-	A27S					G142D						V213G		G339D		S371F	S373P	S375F	T376A	D405N	R408S	K417N	N440K		S477N	T478K	E484A	Q493R		Q498R	N501Y	Y505H		D614G	H655Y	N679K	P681H	N764K	D796Y		Q954H	N969K					c25000u	
	SARS-CoV-2_human_PRI_PR-UPRRP-581_2020	GenBank: ON928765.1	T19I	L24-	P25-	P26-	A27S					G142D						V213G		G339D		S371F	S373P	S375F	T376A	D405N	R408S	K417N	N440K		S477N	T478K	E484A	Q493R		Q498R	N501Y	Y505H		D614G	H655Y	N679K	P681H	N764K	D796Y		Q954H	N969K					c25000u	c21811u
	SARS-CoV-2_human_PRI_PR-UPRRP-583_2020	GenBank: ON928883.1	T19I	L24-	P25-	P26-	A27S					G142D						V213G		G339D		S371F	S373P	S375F	T376A	D405N	R408S	K417N			S477N	T478K	E484A	Q493R		Q498R	N501Y	Y505H		D614G	H655Y	N679K	P681H	N764K	D796Y		Q954H	N969K				c22792u	c25000u	
	SARS-CoV-2_human_PRI_PR-UPRRP-584_2020	GenBank: ON928957.1	T19I	L24-	P25-	P26-	A27S					G142D						V213G		G339D		S371F	S373P	S375F	T376A	D405N	R408S	K417N			S477N	T478K	E484A	Q493R		Q498R	N501Y	Y505H		D614G	H655Y	N679K	P681H	N764K	D796Y		Q954H	N969K					c25000u	
	SARS-CoV-2_human_PRI_PR-UPRRP-588_2020	GenBank: ON928880.1	T19I	L24-	P25-	P26-	A27S					G142D						V213G		G339D		S371F	S373P	S375F	T376A	D405N	R408S	K417N			S477N	T478K	E484A	Q493R		Q498R	N501Y	Y505H		D614G	H655Y	N679K	P681H	N764K	D796Y		Q954H	N969K					c25000u	c22267u
	SARS-CoV-2_human_PRI_PR-UPRRP-589_2020	GenBank: ON928699.1	T19I	L24-	P25-	P26-	A27S					G142D						V213G		G339D		S371F	S373P	S375F	T376A	D405N	R408S	K417N			S477N	T478K	E484A	Q493R		Q498R	N501Y	Y505H		D614G	H655Y	N679K	P681H	N764K	D796Y		Q954H	N969K		Q613H		c22792u	c25000u	a23767g
	SARS-CoV-2_human_PRI_PR-UPRRP-590_2020	GenBank: ON928724.1	T19I	L24-	P25-	P26-	A27S					G142D					L212S	V213G		G339D		S371F	S373P	S375F	T376A	D405N	R408S	K417N			S477N	T478K	E484A	Q493R		Q498R	N501Y	Y505H		D614G	H655Y	N679K	P681H	N764K	D796Y		Q954H	N969K		L212S, D215E		c22792u	c25000u	c21658u,c24865u
	SARS-CoV-2_human_PRI_PR-UPRRP-591_2020	GenBank: ON928941.1	T19I	L24-	P25-	P26-	A27S					G142D					L212S	V213G		G339D		S371F	S373P	S375F	T376A	D405N	R408S	K417N			S477N	T478K	E484A	Q493R		Q498R	N501Y	Y505H		D614G	H655Y	N679K	P681H	N764K	D796Y		Q954H	N969K		L212S,			c25000u	

Supplemental Figure 1

A

B

Supplemental Figure 2

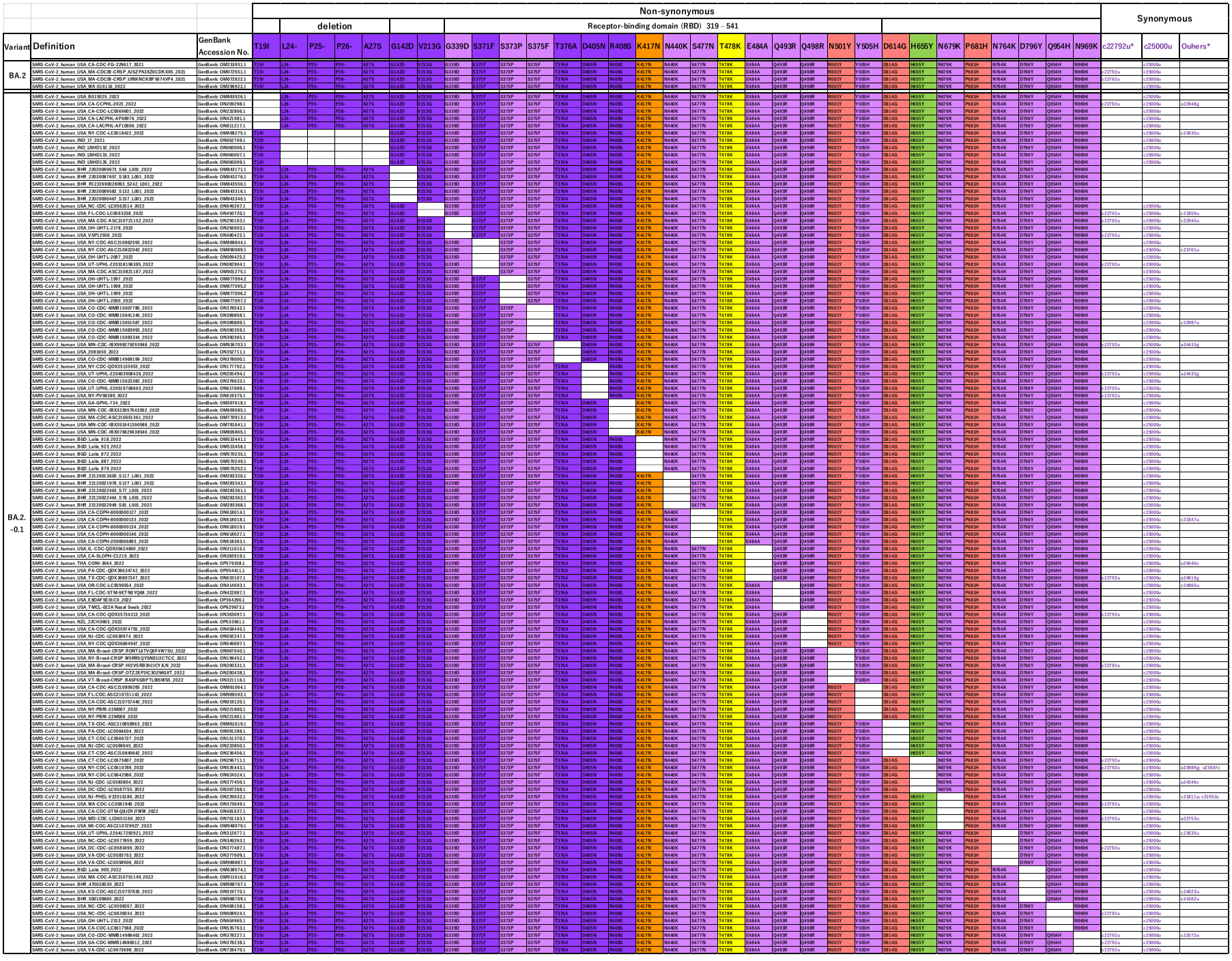

Variant	Definition	GenBank Accession No.	Non-synonymous: deletion T19I	L24-	P25-	P26-	A27S	Receptor-binding domain (RBD) 319 – 541: G142D	V213G	G339D	S371F	S373P	S375F	T376A	D405N	R408S	K417N	N440K	S477N	T478K	E484A	Q493R	Q498R	N501Y	Y505H	Non-synonymous: D614G	H655Y	N679K	P681H	N764K	D796Y	Q954H	N969K	Synonymous c22792u*	c25000u	Ouhers*
BA.2	SARS-CoV-2_human_USA_CA-CDC-FG-229617_2021	GenBank OM233931.1	T19I	L24-	P25-	P26-	A27S	G142D	V213G	G339D	S371F	S373P	S375F	T376A	D405N	R408S	K417N	N440K	S477N	T478K	E484A	Q493R	Q498R	N501Y	Y505H	D614G	H655Y	N679K	P681H	N764K	D796Y	Q954H	N969K		c25000u	
	SARS-CoV-2_human_USA_MA-CDCBI-CRSP_AJSZPA3X2K6CDKXX6_2021	GenBank OM072551.1	T19I	L24-	P25-	P26-	A27S	G142D	V213G	G339D	S371F	S373P	S375F	T376A	D405N	R408S	K417N	N440K	S477N	T478K	E484A	Q493R	Q498R	N501Y	Y505H	D614G	H655Y	N679K	P681H	N764K	D796Y	Q954H	N969K	c22792u	c25000u	
	SARS-CoV-2_human_USA_MA-CDCBI-CRSP_URBKNCKBF9674VF4_2021	GenBank OM072822.1	T19I	L24-	P25-	P26-	A27S	G142D	V213G	G339D	S371F	S373P	S375F	T376A	D405N	R408S	K417N	N440K	S477N	T478K	E484A	Q493R	Q498R	N501Y	Y505H	D614G	H655Y	N679K	P681H	N764K	D796Y	Q954H	N969K	c22792u	c25000u	
	SARS-CoV-2_human_USA_WA-SLH136_2022	GenBank OM296222.1	T19I	L24-	P25-	P26-	A27S	G142D	V213G	G339D	S371F	S373P	S375F	T376A	D405N	R408S	K417N	N440K	S477N	T478K	E484A	Q493R	Q498R	N501Y	Y505H	D614G	H655Y	N679K	P681H	N764K	D796Y	Q954H	N969K		c25000u	
BA.2.-0.1	SARS-CoV-2_human_USA_B019025_2022	GenBank OM043926.1		L24-	P25-	P26-	A27S	G142D	V213G	G339D	S371F	S373P	S375F	T376A	D405N	R408S	K417N	N440K	S477N	T478K	E484A	Q493R	Q498R	N501Y	Y505H	D614G	H655Y	N679K	P681H	N764K	D796Y	Q954H	N969K		c25000u	
	SARS-CoV-2_human_USA_CA-CCPHL-2023_2022	GenBank ON209298.1		L24-	P25-	P26-	A27S	G142D	V213G	G339D	S371F	S373P	S375F	T376A	D405N	R408S	K417N	N440K	S477N	T478K	E484A	Q493R	Q498R	N501Y	Y505H	D614G	H655Y	N679K	P681H	N764K	D796Y	Q954H	N969K	c22792u	c25000u	a22948g
	SARS-CoV-2_human_USA_CA-CDC-LC0569601_2022	GenBank ON232806.1		L24-	P25-	P26-	A27S	G142D	V213G	G339D	S371F	S373P	S375F	T376A	D405N	R408S	K417N	N440K	S477N	T478K	E484A	Q493R	Q498R	N501Y	Y505H	D614G	H655Y	N679K	P681H	N764K	D796Y	Q954H	N969K		c25000u	
	SARS-CoV-2_human_USA_CA-LACPHL-AF08676_2022	GenBank ON421981.1		L24-	P25-	P26-	A27S	G142D	V213G	G339D	S371F	S373P	S375F	T376A	D405N	R408S	K417N	N440K	S477N	T478K	E484A	Q493R	Q498R	N501Y	Y505H	D614G	H655Y	N679K	P681H	N764K	D796Y	Q954H	N969K		c25000u	
	SARS-CoV-2_human_USA_CA-LACPHL-AF10606_2022	GenBank ON811217.1		L24-	P25-	P26-	A27S	G142D	V213G	G339D	S371F	S373P	S375F	T376A	D405N	R408S	K417N	N440K	S477N	T478K	E484A	Q493R	Q498R	N501Y	Y505H	D614G	H655Y	N679K	P681H	N764K	D796Y	Q954H	N969K		c25000u	
	SARS-CoV-2_human_USA_NC-CDC-LC0562514_2022	GenBank ON049267.1	T19I	L24-	P25-	P26-	A27S	G142D		G339D	S371F	S373P	S375F	T376A	D405N	R408S	K417N	N440K	S477N	T478K	E484A	Q493R	Q498R	N501Y	Y505H	D614G	H655Y	N679K	P681H	N764K	D796Y	Q954H	N969K		c25000u	
	SARS-CoV-2_human_USA_FL-CDC-LC0593238_2022	GenBank ON407201.1	T19I	L24-	P25-	P26-	A27S	G142D		G339D	S371F	S373P	S375F	T376A	D405N	R408S	K417N	N440K	S477N	T478K	E484A	Q493R	Q498R	N501Y	Y505H	D614G	H655Y	N679K	P681H	N764K	D796Y	Q954H	N969K	c22792u	c25000u	c23859u
	SARS-CoV-2_human_USA_MA-CDC-ASC210721152_2022	GenBank ON291163.1	T19I	L24-	P25-	P26-	A27S	G142D	V213G		S371F	S373P	S375F	T376A	D405N	R408S	K417N	N440K	S477N	T478K	E484A	Q493R	Q498R	N501Y	Y505H	D614G	H655Y	N679K	P681H	N764K	D796Y	Q954H	N969K	c22792u	c25000u	c23945u
	SARS-CoV-2_human_USA_OH-UHTL-2178_2022	GenBank ON256603.1	T19I	L24-	P25-	P26-	A27S	G142D	V213G		S371F	S373P	S375F	T376A	D405N	R408S	K417N	N440K	S477N	T478K	E484A	Q493R	Q498R	N501Y	Y505H	D614G	H655Y	N679K	P681H	N764K	D796Y	Q954H	N969K		c25000u	
	SARS-CoV-2_human_USA_VSP12938_2022	GenBank ON480422.1	T19I	L24-	P25-	P26-	A27S	G142D	V213G		S371F	S373P	S375F	T376A	D405N	R408S	K417N	N440K	S477N	T478K	E484A	Q493R	Q498R	N501Y	Y505H	D614G	H655Y	N679K	P681H	N764K	D796Y	Q954H	N969K	c22792u	c25000u	
	SARS-CoV-2_human_USA_NY-CDC-ASC210862593_2022	GenBank OM888844.1	T19I	L24-	P25-	P26-	A27S	G142D	V213G	G339D		S373P	S375F	T376A	D405N	R408S	K417N	N440K	S477N	T478K	E484A	Q493R	Q498R	N501Y	Y505H	D614G	H655Y	N679K	P681H	N764K	D796Y	Q954H	N969K		c25000u	
	SARS-CoV-2_human_USA_NY-CDC-ASC210882042_2022	GenBank OM902694.1	T19I	L24-	P25-	P26-	A27S	G142D	V213G	G339D		S373P	S375F	T376A	D405N	R408S	K417N	N440K	S477N	T478K	E484A	Q493R	Q498R	N501Y	Y505H	D614G	H655Y	N679K	P681H	N764K	D796Y	Q954H	N969K		c25000u	c23701u
	SARS-CoV-2_human_USA_OH-UHTL-2187_2022	GenBank ON000425.2	T19I	L24-	P25-	P26-	A27S	G142D	V213G	G339D		S373P	S375F	T376A	D405N	R408S	K417N	N440K	S477N	T478K	E484A	Q493R	Q498R	N501Y	Y505H	D614G	H655Y	N679K	P681H	N764K	D796Y	Q954H	N969K		c25000u	
	SARS-CoV-2_human_USA_UT-UPHL-220318196385_2022	GenBank ON082904.1	T19I	L24-	P25-	P26-	A27S	G142D	V213G	G339D		S373P	S375F	T376A	D405N	R408S	K417N	N440K	S477N	T478K	E484A	Q493R	Q498R	N501Y	Y505H	D614G	H655Y	N679K	P681H	N764K	D796Y	Q954H	N969K	c22792u	c25000u	
	SARS-CoV-2_human_USA_MA-CDC-ASC210821187_2022	GenBank OM901275.1	T19I	L24-	P25-	P26-	A27S	G142D	V213G	G339D		S373P	S375F	T376A	D405N	R408S	K417N	N440K	S477N	T478K	E484A	Q493R	Q498R	N501Y	Y505H	D614G	H655Y	N679K	P681H	N764K	D796Y	Q954H	N969K		c25000u	
	SARS-CoV-2_human_USA_OH-UHTL-1997_2022	GenBank OM877094.2	T19I	L24-	P25-	P26-	A27S	G142D	V213G	G339D	S371F		S375F	T376A	D405N	R408S	K417N	N440K	S477N	T478K	E484A	Q493R	Q498R	N501Y	Y505H	D614G	H655Y	N679K	P681H	N764K	D796Y	Q954H	N969K		c25000u	
	SARS-CoV-2_human_USA_OH-UHTL-1998_2022	GenBank OM877095.2	T19I	L24-	P25-	P26-	A27S	G142D	V213G	G339D	S371F		S375F	T376A	D405N	R408S	K417N	N440K	S477N	T478K	E484A	Q493R	Q498R	N501Y	Y505H	D614G	H655Y	N679K	P681H	N764K	D796Y	Q954H	N969K		c25000u	
	SARS-CoV-2_human_USA_OH-UHTL-1999_2022	GenBank OM877096.2	T19I	L24-	P25-	P26-	A27S	G142D	V213G	G339D	S371F		S375F	T376A	D405N	R408S	K417N	N440K	S477N	T478K	E484A	Q493R	Q498R	N501Y	Y505H	D614G	H655Y	N679K	P681H	N764K	D796Y	Q954H	N969K		c25000u	
	SARS-CoV-2_human_USA_OH-UHTL-2000_2022	GenBank OM877097.2	T19I	L24-	P25-	P26-	A27S	G142D	V213G	G339D	S371F		S375F	T376A	D405N	R408S	K417N	N440K	S477N	T478K	E484A	Q493R	Q498R	N501Y	Y505H	D614G	H655Y	N679K	P681H	N764K	D796Y	Q954H	N969K		c25000u	
	SARS-CoV-2_human_USA_CO-CDC-MMB15007786_2022	GenBank ON378542.1	T19I	L24-	P25-	P26-	A27S	G142D	V213G	G339D	S371F	S373P		T376A	D405N	R408S	K417N	N440K	S477N	T478K	E484A	Q493R	Q498R	N501Y	Y505H	D614G	H655Y	N679K	P681H	N764K	D796Y	Q954H	N969K		c25000u	
	SARS-CoV-2_human_USA_CO-CDC-MMB15041240_2022	GenBank ON396740.1	T19I	L24-	P25-	P26-	A27S	G142D	V213G	G339D	S371F	S373P		T376A	D405N	R408S	K417N	N440K	S477N	T478K	E484A	Q493R	Q498R	N501Y	Y505H	D614G	H655Y	N679K	P681H	N764K	D796Y	Q954H	N969K		c25000u	
	SARS-CoV-2_human_USA_CO-CDC-MMB15051587_2022	GenBank ON389889.1	T19I	L24-	P25-	P26-	A27S	G142D	V213G	G339D	S371F	S373P		T376A	D405N	R408S	K417N	N440K	S477N	T478K	E484A	Q493R	Q498R	N501Y	Y505H	D614G	H655Y	N679K	P681H	N764K	D796Y	Q954H	N969K		c25000u	c22087u
	SARS-CoV-2_human_USA_CO-CDC-MMB15083993_2022	GenBank ON390359.1	T19I	L24-	P25-	P26-	A27S	G142D	V213G	G339D	S371F	S373P		T376A	D405N	R408S	K417N	N440K	S477N	T478K	E484A	Q493R	Q498R	N501Y	Y505H	D614G	H655Y	N679K	P681H	N764K	D796Y	Q954H	N969K		c25000u	
	SARS-CoV-2_human_USA_CO-CDC-MMB15083344_2022	GenBank ON390365.1	T19I	L24-	P25-	P26-	A27S	G142D	V213G	G339D	S371F	S373P		T376A	D405N	R408S	K417N	N440K	S477N	T478K	E484A	Q493R	Q498R	N501Y	Y505H	D614G	H655Y	N679K	P681H	N764K	D796Y	Q954H	N969K		c25000u	
	SARS-CoV-2_human_USA_MN-CDC-MXX997873_2022	GenBank ON390703.1	T19I	L24-	P25-	P26-	A27S	G142D	V213G	G339D	S371F	S373P	S375F		D405N	R408S	K417N	N440K	S477N	T478K	E484A	Q493R	Q498R	N501Y	Y505H	D614G	H655Y	N679K	P681H	N764K	D796Y	Q954H	N969K	c22792u	c25000u	a24433g
	SARS-CoV-2_human_USA_2081650_2022	GenBank ON352711.1	T19I	L24-	P25-	P26-	A27S	G142D	V213G	G339D	S371F	S373P	S375F		D405N	R408S	K417N	N440K	S477N	T478K	E484A	Q493R	Q498R	N501Y	Y505H	D614G	H655Y	N679K	P681H	N764K	D796Y	Q954H	N969K		c25000u	
	SARS-CoV-2_human_USA_CO-CDC-MMB14989199_2022	GenBank ON378000.1	T19I	L24-	P25-	P26-	A27S	G142D	V213G	G339D	S371F	S373P	S375F		D405N	R408S	K417N	N440K	S477N	T478K	E484A	Q493R	Q498R	N501Y	Y505H	D614G	H655Y	N679K	P681H	N764K	D796Y	Q954H	N969K		c25000u	
	SARS-CoV-2_human_USA_NY-CDC-QDX35135993_2022	GenBank ON177702.1	T19I	L24-	P25-	P26-	A27S	G142D	V213G	G339D	S371F	S373P	S375F	T376A		R408S	K417N	N440K	S477N	T478K	E484A	Q493R	Q498R	N501Y	Y505H	D614G	H655Y	N679K	P681H	N764K	D796Y	Q954H	N969K		c25000u	
	SARS-CoV-2_human_USA_UPHL-220403908426_2022	GenBank ON205451.1	T19I	L24-	P25-	P26-	A27S	G142D	V213G	G339D	S371F	S373P	S375F	T376A		R408S	K417N	N440K	S477N	T478K	E484A	Q493R	Q498R	N501Y	Y505H	D614G	H655Y	N679K	P681H	N764K	D796Y	Q954H	N969K	c22792u	c25000u	a24433g
	SARS-CoV-2_human_USA_CO-CDC-MMB15023382_2022	GenBank ON378633.1	T19I	L24-	P25-	P26-	A27S	G142D	V213G	G339D	S371F	S373P	S375F	T376A		R408S	K417N	N440K	S477N	T478K	E484A	Q493R	Q498R	N501Y	Y505H	D614G	H655Y	N679K	P681H	N764K	D796Y	Q954H	N969K		c25000u	
	SARS-CoV-2_human_USA_UT-UPHL-220519708663_2022	GenBank ON617689.1	T19I	L24-	P25-	P26-	A27S	G142D	V213G	G339D	S371F	S373P	S375F	T376A		R408S	K417N	N440K	S477N	T478K	E484A	Q493R	Q498R	N501Y	Y505H	D614G	H655Y	N679K	P681H	N764K	D796Y	Q954H	N969K	c22792u	c25000u	
	SARS-CoV-2_human_USA_NY-PVS8389_2022	GenBank ON619375.1	T19I	L24-	P25-	P26-	A27S	G142D	V213G	G339D	S371F	S373P	S375F	T376A		R408S	K417N	N440K	S477N	T478K	E484A	Q493R	Q498R	N501Y	Y505H	D614G	H655Y	N679K	P681H	N764K	D796Y	Q954H	N969K	c22792u	c25000u	
	SARS-CoV-2_human_USA_GA-GPHL-734_2022	GenBank OM567618.1	T19I	L24-	P25-	P26-	A27S	G142D	V213G	G339D	S371F	S373P	S375F	T376A	D405N		K417N	N440K	S477N	T478K	E484A	Q493R	Q498R	N501Y	Y505H	D614G	H655Y	N679K	P681H	N764K	D796Y	Q954H	N969K		c25000u	
	SARS-CoV-2_human_USA_MN-CDC-IBX32657642052_2022	GenBank OM395513.1	T19I	L24-	P25-	P26-	A27S	G142D	V213G	G339D	S371F	S373P	S375F	T376A	D405N		K417N	N440K	S477N	T478K	E484A	Q493R	Q498R	N501Y	Y505H	D614G	H655Y	N679K	P681H	N764K	D796Y	Q954H	N969K		c25000u	
	SARS-CoV-2_human_USA_MA-CDC-ASC210651361_2022	GenBank OM709113.1	T19I	L24-	P25-	P26-	A27S	G142D	V213G	G339D	S371F	S373P	S375F	T376A	D405N		K417N	N440K	S477N	T478K	E484A	Q493R	Q498R	N501Y	Y505H	D614G	H655Y	N679K	P681H	N764K	D796Y	Q954H	N969K		c25000u	
	SARS-CoV-2_human_USA_MN-CDC-IBX91341390588_2022	GenBank OM781641.1	T19I	L24-	P25-	P26-	A27S	G142D	V213G	G339D	S371F	S373P	S375F	T376A	D405N		K417N	N440K	S477N	T478K	E484A	Q493R	Q498R	N501Y	Y505H	D614G	H655Y	N679K	P681H	N764K	D796Y	Q954H	N969K		c25000u	
	SARS-CoV-2_human_USA_MN-CDC-IBX07882943540_2022	GenBank OM808865.1	T19I	L24-	P25-	P26-	A27S	G142D	V213G	G339D	S371F	S373P	S375F	T376A	D405N		K417N	N440K	S477N	T478K	E484A	Q493R	Q498R	N501Y	Y505H	D614G	H655Y	N679K	P681H	N764K	D796Y	Q954H	N969K		c25000u	
	SARS-CoV-2_BGD_Laib_318_2022	GenBank OM533441.1	T19I	L24-	P25-	P26-	A27S	G142D	V213G	G339D	S371F	S373P	S375F	T376A	D405N	R408S		N440K	S477N	T478K	E484A	Q493R	Q498R	N501Y	Y505H	D614G	H655Y	N679K	P681H	N764K	D796Y	Q954H	N969K		c25000u	
	SARS-CoV-2_BGD_Laib_923_2022	GenBank OM534581.1	T19I	L24-	P25-	P26-	A27S	G142D	V213G	G339D	S371F	S373P	S375F	T376A	D405N	R408S		N440K	S477N	T478K	E484A	Q493R	Q498R	N501Y	Y505H	D614G	H655Y	N679K	P681H	N764K	D796Y	Q954H	N969K		c25000u	
	SARS-CoV-2_BGD_Laib_872_2022	GenBank OM570235.1	T19I	L24-	P25-	P26-	A27S	G142D	V213G	G339D	S371F	S373P	S375F	T376A	D405N	R408S		N440K	S477N	T478K	E484A	Q493R	Q498R	N501Y	Y505H	D614G	H655Y	N679K	P681H	N764K	D796Y	Q954H	N969K		c25000u	
	SARS-CoV-2_BGD_Laib_887_2022	GenBank OM570249.1	T19I	L24-	P25-	P26-	A27S	G142D	V213G	G339D	S371F	S373P	S375F	T376A	D405N	R408S		N440K	S477N	T478K	E484A	Q493R	Q498R	N501Y	Y505H	D614G	H655Y	N679K	P681H	N764K	D796Y	Q954H	N969K		c25000u	
	SARS-CoV-2_BGD_Laib_879_2022	GenBank OM570252.1	T19I	L24-	P25-	P26-	A27S	G142D	V213G	G339D	S371F	S373P	S375F	T376A	D405N	R408S		N440K	S477N	T478K	E484A	Q493R	Q498R	N501Y	Y505H	D614G	H655Y	N679K	P681H	N764K	D796Y	Q954H	N969K		c25000u	
	SARS-CoV-2_human_BHR_2212003600_S117_L001_2022	GenBank OM283320.1	T19I	L24-	P25-	P26-	A27S	G142D	V213G	G339D	S371F	S373P	S375F	T376A	D405N	R408S	K417N		S477N	T478K	E484A	Q493R	Q498R	N501Y	Y505H	D614G	H655Y	N679K	P681H	N764K	D796Y	Q954H	N969K		c25000u	
	SARS-CoV-2_human_BHR_2212002978_S127_L001_2022	GenBank OM283343.1	T19I	L24-	P25-	P26-	A27S	G142D	V213G	G339D	S371F	S373P	S375F	T376A	D405N	R408S	K417N		S477N	T478K	E484A	Q493R	Q498R	N501Y	Y505H	D614G	H655Y	N679K	P681H	N764K	D796Y	Q954H	N969K		c25000u	
	SARS-CoV-2_human_BHR_2212002463_S77_L001_2022	GenBank OM283361.1	T19I	L24-	P25-	P26-	A27S	G142D	V213G	G339D	S371F	S373P	S375F	T376A	D405N	R408S	K417N		S477N	T478K	E484A	Q493R	Q498R	N501Y	Y505H	D614G	H655Y	N679K	P681H	N764K	D796Y	Q954H	N969K		c25000u	
	SARS-CoV-2_human_BHR_2212002446_S78_L001_2022	GenBank OM283377.1	T19I	L24-	P25-	P26-	A27S	G142D	V213G	G339D	S371F	S373P	S375F	T376A	D405N	R408S	K417N		S477N	T478K	E484A	Q493R	Q498R	N501Y	Y505H	D614G	H655Y	N679K	P681H	N764K	D796Y	Q954H	N969K		c25000u	
	SARS-CoV-2_human_BHR_2212002949_S81_L001_2022	GenBank OM283368.1	T19I	L24-	P25-	P26-	A27S	G142D	V213G	G339D	S371F	S373P	S375F	T376A	D405N	R408S	K417N		S477N	T478K	E484A	Q493R	Q498R	N501Y	Y505H	D614G	H655Y	N679K	P681H	N764K	D796Y	Q954H	N969K		c25000u	
	SARS-CoV-2_human_USA_CA-CDPH-8000000127_2022	GenBank ON618014.1	T19I	L24-	P25-	P26-	A27S	G142D	V213G	G339D	S371F	S373P	S375F	T376A	D405N	R408S	K417N	N440K		T478K	E484A	Q493R	Q498R	N501Y	Y505H	D614G	H655Y	N679K	P681H	N764K	D796Y	Q954H	N969K		c25000u	
	SARS-CoV-2_human_USA_CA-CDPH-8000000133_2022	GenBank ON618018.1	T19I	L24-	P25-	P26-	A27S	G142D	V213G	G339D	S371F	S373P	S375F	T376A	D405N	R408S	K417N	N440K		T478K	E484A	Q493R	Q498R	N501Y	Y505H	D614G	H655Y	N679K	P681H	N764K	D796Y	Q954H	N969K		c25000u	c23347u
	SARS-CoV-2_human_USA_CA-CDPH-8000000139_2022	GenBank ON618022.1	T19I	L24-	P25-	P26-	A27S	G142D	V213G	G339D	S371F	S373P	S375F	T376A	D405N	R408S	K417N	N440K		T478K	E484A	Q493R	Q498R	N501Y	Y505H	D614G	H655Y	N679K	P681H	N764K	D796Y	Q954H	N969K		c25000u	
	SARS-CoV-2_human_USA_CA-CDPH-8000000146_2022	GenBank ON618027.1	T19I	L24-	P25-	P26-	A27S	G142D	V213G	G339D	S371F	S373P	S375F	T376A	D405N	R408S	K417N	N440K		T478K	E484A	Q493R	Q498R	N501Y	Y505H	D614G	H655Y	N679K	P681H	N764K	D796Y	Q954H	N969K		c25000u	
	SARS-CoV-2_human_USA_CA-CDPH-20000661893_2022	GenBank ON618363.1	T19I	L24-	P25-	P26-	A27S	G142D	V213G	G339D	S371F	S373P	S375F	T376A	D405N	R408S	K417N	N440K		T478K	E484A	Q493R	Q498R	N501Y	Y505H	D614G	H655Y	N679K	P681H	N764K	D796Y	Q954H	N969K		c25000u	
	SARS-CoV-2_human_USA_IL-CDC-QDX59624490_2022	GenBank ON311615.1	T19I	L24-	P25-	P26-	A27S	G142D	V213G	G339D	S371F	S373P	S375F	T376A	D405N	R408S	K417N	N440K	S477N	T478K			Q493R	N501Y	Y505H	D614G	H655Y	N679K	P681H	N764K	D796Y	Q954H	N969K		c25000u	
	SARS-CoV-2_human_USA_CA-SLOPH-C1219_2022	GenBank ON383919.1	T19I	L24-	P25-	P26-	A27S	G142D	V213G	G339D	S371F	S373P	S375F	T376A	D405N	R408S	K417N	N440K	S477N	T478K			Q493R	N501Y	Y505H	D614G	H655Y	N679K	P681H	N764K	D796Y	Q954H	N969K		c25000u	
	SARS-CoV-2_THA-MHIDL-1644_2022	GenBank ON677938.1	T19I	L24-	P25-	P26-	A27S	G142D	V213G	G339D	S371F	S373P	S375F	T376A	D405N	R408S	K417N	N440K	S477N	T478K			Q493R	N501Y	Y505H	D614G	H655Y	N679K	P681H	N764K	D796Y	Q954H	N969K		c25000u	a24640c
	SARS-CoV-2_human_USA_PA-CDC-QDX36634742_2022	GenBank OP054411.1	T19I	L24-	P25-	P26-	A27S	G142D	V213G	G339D	S371F	S373P	S375F	T376A	D405N	R408S	K417N	N440K	S477N	T478K			Q493R	N501Y	Y505H	D614G	H655Y	N679K	P681H	N764K	D796Y	Q954H	N969K		c25000u	
	SARS-CoV-2_human_USA_TX-CDC-QDX36807347_2022	GenBank ON631707.1	T19I	L24-	P25-	P26-	A27S	G142D	V213G	G339D	S371F	S373P	S375F	T376A	D405N	R408S	K417N	N440K	S477N	T478K			Q493R	N501Y	Y505H	D614G	H655Y	N679K	P681H	N764K	D796Y	Q954H	N969K	c22792u	c25000u	a24619g
	SARS-CoV-2_human_USA_OR-CDC-LC0590954_2022	GenBank ON341693.1	T19I	L24-	P25-	P26-	A27S	G142D	V213G	G339D	S371F	S373P	S375F	T376A	D405N	R408S	K417N	N440K	S477N	T478K	E484A		Q498R	N501Y	Y505H	D614G	H655Y	N679K	P681H	N764K	D796Y	Q954H	N969K		c25000u	c24665u
	SARS-CoV-2_human_USA_OHD-STM-WETNLYQ68_2022	GenBank ON422881.1	T19I	L24-	P25-	P26-	A27S	G142D	V213G	G339D	S371F	S373P	S375F	T376A	D405N	R408S	K417N	N440K	S477N	T478K	E484A		Q498R	N501Y	Y505H	D614G	H655Y	N679K	P681H	N764K	D796Y	Q954H	N969K		c25000u	
	SARS-CoV-2_human_USA_E8DAF5E01C9_2022	GenBank OP364296.1	T19I	L24-	P25-	P26-	A27S	G142D	V213G	G339D	S371F	S373P	S375F	T376A	D405N	R408S	K417N	N440K	S477N	T478K	E484A		Q498R	N501Y	Y505H	D614G	H655Y	N679K	P681H	N764K	D796Y	Q954H	N969K		c25000u	
	SARS-CoV-2_human_USA_TMCL-022A Nasal Swab_2022	GenBank OP629673.1	T19I	L24-	P25-	P26-	A27S	G142D	V213G	G339D	S371F	S373P	S375F	T376A	D405N	R408S	K417N	N440K	S477N	T478K	E484A		Q498R	N501Y	Y505H	D614G	H655Y	N679K	P681H	N764K	D796Y	Q954H	N969K		c25000u	
	SARS-CoV-2_human_USA_CA-CDC-QDX35734313_2022	GenBank ON630971.1	T19I	L24-	P25-	P26-	A27S	G142D	V213G	G339D	S371F	S373P	S375F	T376A	D405N	R408S	K417N	N440K	S477N	T478K	E484A	Q493R		N501Y	Y505H	D614G	H655Y	N679K	P681H	N764K	D796Y	Q954H	N969K	c22792u	c25000u	
	SARS-CoV-2_human_USA_CA-CDC-LC0577702_2022	GenBank ON630977.1	T19I	L24-	P25-	P26-	A27S	G142D	V213G	G339D	S371F	S373P	S375F	T376A	D405N	R408S	K417N	N440K	S477N	T478K	E484A	Q493R		N501Y	Y505H	D614G	H655Y	N679K	P681H	N764K	D796Y	Q954H	N969K		c25000u	
	SARS-CoV-2_human_USA_CA-CDC-QDX35974735_2022	GenBank ON584451.1	T19I	L24-	P25-	P26-	A27S	G142D	V213G	G339D	S371F	S373P	S375F	T376A	D405N	R408S	K417N	N440K	S477N	T478K	E484A	Q493R		N501Y	Y505H	D614G	H655Y	N679K	P681H	N764K	D796Y	Q954H	N969K		c25000u	
	SARS-CoV-2_human_USA_NJ-CDC-LC0630974_2022	GenBank ON592247.1	T19I	L24-	P25-	P26-	A27S	G142D	V213G	G339D	S371F	S373P	S375F	T376A	D405N	R408S	K417N	N440K	S477N	T478K	E484A	Q493R		N501Y	Y505H	D614G	H655Y	N679K	P681H	N764K	D796Y	Q954H	N969K		c25000u	
	SARS-CoV-2_human_USA_NY-CDC-QDX36404947_2022	GenBank ON594687.1	T19I	L24-	P25-	P26-	A27S	G142D	V213G	G339D	S371F	S373P	S375F	T376A	D405N	R408S	K417N	N440K	S477N	T478K	E484A	Q493R		N501Y	Y505H	D614G	H655Y	N679K	P681H	N764K	D796Y	Q954H	N969K		c25000u	
	SARS-CoV-2_human_USA_MA-Broad-CRSP_MGNT1ATVQ6F4W7SU_2022	GenBank ON602780	T19I	L24-	P25-	P26-	A27S	G142D	V213G	G339D	S371F	S373P	S375F	T376A	D405N	R408S	K417N	N440K	S477N	T478K	E484A	Q493R	Q498R		Y505H	D614G	H655Y	N679K	P681H	N764K	D796Y	Q954H	N969K		c25000u	
	SARS-CoV-2_human_USA_NY-Broad-CRSP_WSRRSQYSNEUZCTCC_2022	GenBank ON194952.1	T19I	L24-	P25-	P26-	A27S	G142D	V213G	G339D	S371F	S373P	S375F	T376A	D405N	R408S	K417N	N440K	S477N	T478K	E484A	Q493R	Q498R		Y505H	D614G	H655Y	N679K	P681H	N764K	D796Y	Q954H	N969K		c25000u	
	SARS-CoV-2_human_USA_MA-Broad-CRSP_HI2V5RB3HJJCYJLN_2022	GenBank ON200331.1	T19I	L24-	P25-	P26-	A27S	G142D	V213G	G339D	S371F	S373P	S375F	T376A	D405N	R408S	K417N	N440K	S477N	T478K	E484A	Q493R	Q498R		Y505H	D614G	H655Y	N679K	P681H	N764K	D796Y	Q954H	N969K	c22792u	c25000u	
	SARS-CoV-2_human_USA_MA-Broad-CRSP_OTZZKP3IC3O2MGXT_2022	GenBank ON200438.1	T19I	L24-	P25-	P26-	A27S	G142D	V213G	G339D	S371F	S373P	S375F	T376A	D405N	R408S	K417N	N440K	S477N	T478K	E484A	Q493R	Q498R		Y505H	D614G	H655Y	N679K	P681H	N764K	D796Y	Q954H	N969K		c25000u	
	SARS-CoV-2_human_USA_VT-Broad-CRSP_BA5F6B9TLB5WS5_2022	GenBank ON321116.1	T19I	L24-	P25-	P26-	A27S	G142D	V213G	G339D	S371F	S373P	S375F	T376A	D405N	R408S	K417N	N440K	S477N	T478K	E484A	Q493R	Q498R		Y505H	D614G	H655Y	N679K	P681H	N764K	D796Y	Q954H	N969K		c25000u	
	SARS-CoV-2_human_USA_NC-CDC-LC0581989_2022	GenBank ON672089.1	T19I	L24-	P25-	P26-	A27S	G142D	V213G	G339D	S371F	S373P	S375F	T376A	D405N	R408S	K417N	N440K	S477N	T478K			Q493R	N501Y		D614G	H655Y	N679K	P681H	N764K	D796Y	Q954H	N969K		c25000u	
	SARS-CoV-2_human_USA_FL-CDC-ASC210731143_2022	GenBank OM969592.1	T19I	L24-	P25-	P26-	A27S	G142D	V213G	G339D	S371F	S373P	S375F	T376A	D405N	R408S	K417N	N440K	S477N	T478K	E484A	Q493R	Q498R	N501Y		D614G	H655Y	N679K	P681H	N764K	D796Y	Q954H	N969K		c25000u	
	SARS-CoV-2_human_USA_CA-CDC-ASC210797440_2022	GenBank ON391210.1	T19I	L24-	P25-	P26-	A27S	G142D	V213G	G339D	S371F	S373P	S375F	T376A	D405N	R408S	K417N	N440K	S477N	T478K	E484A	Q493R	Q498R	N501Y		D614G	H655Y	N679K	P681H	N764K	D796Y	Q954H	N969K		c25000u	
	SARS-CoV-2_human_USA_NY-PIBR-22M007_2022	GenBank ON221860.1	T19I	L24-	P25-	P26-	A27S	G142D	V213G	G339D	S371F	S373P	S375F	T376A	D405N	R408S	K417N	N440K	S477N	T478K	E484A	Q493R	Q498R	N501Y		D614G	H655Y	N679K	P681H	N764K	D796Y	Q954H	N969K		c25000u	
	SARS-CoV-2_human_USA_NY-PIBR-22M008_2022	GenBank ON221866.1	T19I	L24-	P25-	P26-	A27S	G142D	V213G	G339D	S371F	S373P	S375F	T376A	D405N	R408S	K417N	N440K	S477N	T478K	E484A	Q493R	Q498R	N501Y		D614G	H655Y	N679K	P681H	N764K	D796Y	Q954H	N969K		c25000u	
	SARS-CoV-2_human_USA_TX-CDC-ASC210858963_2022	GenBank OM861619.1	T19I	L24-	P25-	P26-	A27S	G142D	V213G	G339D	S371F	S373P	S375F	T376A	D405N	R408S	K417N	N440K	S477N	T478K	E484A	Q493R	Q498R	N501Y	Y505H		H655Y	N679K	P681H	N764K	D796Y	Q954H	N969K		c25000u	
	SARS-CoV-2_human_USA_PA-CDC-LC0564604_2022	GenBank ON691288.1	T19I	L24-	P25-	P26-	A27S	G142D	V213G	G339D	S371F	S373P	S375F	T376A	D405N	R408S	K417N	N440K	S477N	T478K	E484A	Q493R	Q498R	N501Y	Y505H		H655Y	N679K	P681H	N764K	D796Y	Q954H	N969K		c25000u	
	SARS-CoV-2_human_USA_CT-CDC-LC0566727_2022	GenBank ON513701.1	T19I	L24-	P25-	P26-	A27S	G142D	V213G	G339D	S371F	S373P	S375F	T376A	D405N	R408S	K417N	N440K	S477N	T478K	E484A	Q493R	Q498R	N501Y	Y505H		H655Y	N679K	P681H	N764K	D796Y	Q954H	N969K		c25000u	
	SARS-CoV-2_human_USA_NY-CDC-LC0589045_2022	GenBank ON623981.1	T19I	L24-	P25-	P26-	A27S	G142D	V213G	G339D	S371F	S373P	S375F	T376A	D405N	R408S	K417N	N440K	S477N	T478K	E484A	Q493R	Q498R	N501Y	Y505H		H655Y	N679K	P681H	N764K	D796Y	Q954H	N969K		c25000u	
	SARS-CoV-2_human_USA_CT-CDC-ASC210849642_2022	GenBank ON236456.1	T19I	L24-	P25-	P26-	A27S	G142D	V213G	G339D	S371F	S373P	S375F	T376A	D405N	R408S	K417N	N440K	S477N	T478K	E484A	Q493R	Q498R	N501Y	Y505H		H655Y	N679K	P681H	N764K	D796Y	Q954H	N969K		c25000u	
	SARS-CoV-2_human_USA_CT-CDC-LC0575807_2022	GenBank ON296711.1	T19I	L24-	P25-	P26-	A27S	G142

Supplemental Figure 3

A

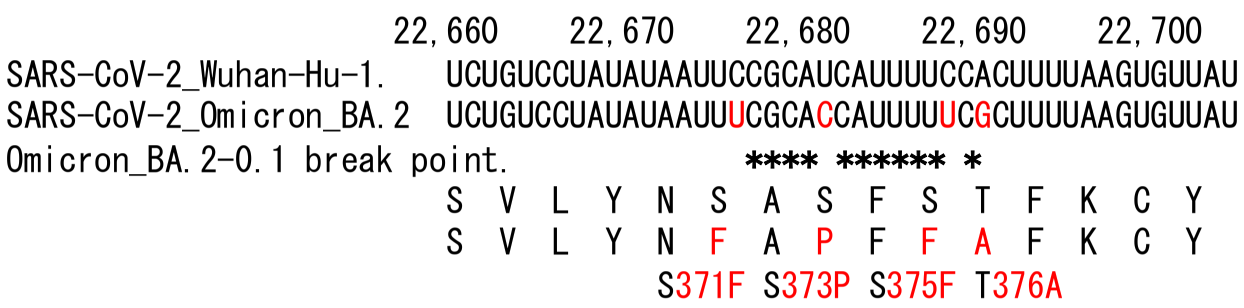

B